Atomic Energy Control Board
P.O. Box 1046
Ottawa, Canada
K1P 5S9

Commission de contrôle de l'énergie atomique
C.P. 1046
Ottawa, Canada
K1P 5S9

INFO-0254-2

CRACK PROPAGATION IN TOUGH DUCTILE MATERIALS (PHASE II)

by

R.D. Venter, A.N. Sinclair
and
D. McCammond
University of Toronto

A research report prepared for the
Atomic Energy Control Board
Ottawa, Canada

Project No. 2.105.1

June 1989

Canada

Research report

90-06865/

CRACK PROPAGATION IN TOUGH DUCTILE MATERIALS (Phase II)

A report prepared by R.D. Venter, A.N. Sinclair and D. McCammond, Structural Integrity, Fracture and Fatigue Research Laboratory (SIFFRL), Department of Mechanical Engineering, University of Toronto, under contract to the Atomic Energy Control Board.

SUMMARY

This report comprises the second phase of the work initiated in "Crack Propagation in Tough Ductile Materials (Phase 1)", AECB report INFO-0254-1, November, 1987.

The thrust of this work was to investigate the J material resistance and stress-strain data which have been published and which are applicable to the understanding of crack propagation in tough ductile steels, particularly SA 106 Grade B pipe steel. This data has been assembled from PIFRAC, AECB report INFO-0254-1 and Ontario Hydro sources and is presented in Appendix B, C and D respectively. The data has been uniformly formatted and presented to facilitate comparison and assessment. While the data is in many aspects incomplete it has enabled an evaluation of the influence of temperature, specimen thickness and specimen orientation to be made in the context of the experimental J-R curves so determined. Comparisons of the stress-strain data within the Ramburg-Osgood formulation are also considered.

A further component of this report addresses the development of the required software to utilise what is referred to as the 'engineering approach to elasto-plastic analysis' to investigate the load carrying capacity of selected cracked pipe geometries which are representative of applied crack propagation studies associated with piping systems in the nuclear industry. Three specific geometries and loading situations, identified as Condition A, B and C have been evaluated; the results are presented and illustrate the variation in applied load as a function of an initial and final crack extension leading to instability.

RESUME

Le présent rapport traite de la deuxième étape du projet intitulé "Crack Propagation in Tough Ductile Materials (Phase I)" [Propagation des fissures dans les matières ductiles (1 étape)], publié comme rapport INFO-0254-1 de la CCEA en novembre 1987.

Les travaux avaient pour but d'étudier la résistance des matériaux J et les données sur les contraintes et la résistance qui ont déjà été publiées et qui peuvent servir à mieux comprendre la propagation des fissures dan les aciers ductiles, particulièrement les conduites d'acier SA 106 de type B. Ces données ont été recueillies à partir de PIFRAC, du rapport INFO-0254-1 de la CCEA et de sources d'Ontario Hydro; elles figurent à l'annexe B, C et D respectivement. Les données ont été disposées uniformément et présentées de façon à en faciliter la comparaison et l'évaluation. Bien que les données soient incomplètes à plusieurs égards, elles ont quand même permis d'évaluer l'influence des températures, de l'épaisseur des échantillons et de leur orientation dans le contexte des courbes expérimentales J-R ainsi déterminées. Le rapport traite aussi des comparaisons des données sur les contraintes et la résistance à la lumière de la formulation de Ramburg-Osgood.

Le rapport aborde aussi la question du perfectionnement du logiciel nécessaire à utiliser comme <<approche d'ingénierie aux analyses élastoplastiques>> pour étudier la capacité de chargement de certaines configurations géométriques de certains systèmes de conduites fissurées qui sont représentatives des études appliquées sur la propagation des fissures associées aux systèmes de conduites dans l'industrie nucléaire. Trois configurations géométriques et leur situation de chargement correspondante, désignées comme condition A, B et C, sont évaluées; les résultats sont présentés et illustrent la variation des chargements appliqués comme une fonction de l'extension de la fissure originale et finale provoquant

l'instabilité.

DISCLAIMER

The Atomic Energy Control Board is not responsible for the accuracy of the statements made or opinions expressed in this publication and neither the Board nor the authors assume liability with respect to any damage or loss incurred as a result of the use made of the information contained in this publication.

ACKNOWLEDGEMENT

The authors wish to acknowledge the considerable contributions made by Messers. K. Gilbert and J. Drossis of the Structural Integrity, Fracture and Fatigue Research Laboratory in the Department of Mechanical Engineering. Their involvement in the preparation, compilation and assessment of the material presented in this report was invaluable.

TABLE OF CONTENTS

A. INTRODUCTION 1

B. J-RESISTANCE CURVE DATA 2

1. General 2

2. Observations from J-R Curves 2

2.1 Influence of Temperature on the J-R Curve 2

2.2 Influence of Orientation of Specimen on the J-R Curve 2

2.3 Influence of Specimen Thickness of the J-R Curve 3

C. STRESS-STRAIN DATA 11

1. General 11

2. Assessment of Curve Fitting 11

D. ENGINEERING APPROACH TO ELASTO-PLASTIC ANALYSIS 20

1. General 20

2. Geometric and Loading Conditions A, B and C 20

E. ASSESSMENT OF RESULTS AND CONCLUSIONS 34

REFERENCES 35

APPENDICES

PIFRAC Data Sheets ..... APPENDIX A

Tabulation of Data and Graphical Results ..... APPENDIX B

Test Data from AECB INFO-025401 ..... APPENDIX C

Ontario Hydro Data ..... APPENDIX D

Development of Software for Engineering Approach to ..... APPENDIX E

Elasto-Plastic Analysis

A. INTRODUCTION

In October 1985, a comprehensive study into the understanding of crack and fracture behaviour in tough ductile materials was completed. This study entitled "Crack and Fracture Behaviour in Tough Ductile Materials" and documented as AECB INFO-0169, [Ref. 1] described the fundamental fracture mechanics concepts, their extension to include elasto-plastic considerations and the preferred options available for the development of appropriate design methodologies. A second study entitled "Crack Propagation in Tough Ductile Materials (Phase I), AECB INFO-0254-1, [Ref. 2] was completed in November 1987. This particular study focused on the evaluation of J-resistance curves for SA 106 Grade B pipe. The significant results from this work was to emphasize the considerable difference in J-R curves experimentally obtained for the L-C and C-L orientations for compact tension tests, and to assess the influence of specimen thickness for cracks propagating in each of these directions.

The present study, Phase II, is directed to a compilation of J-resistance curve data on SA 106 Grade B material and an assessment of this data in relation to the J-controlled growth definition to develop an understanding of SA 106 Grade B material crack behaviour. The base data for these comparisons has been obtained from three sources, namely

i) PIFRAC. Piping Fracture Mechanics Data Base made available through AECB on floppy diskettes, see Appendix A.

ii) The test data reported in "Crack Propagation in Tough Ductile Materials- Phase I" AECB, INFO-0254-1, and

iii) Test results made available through Ontario Hydro Research and summarized in Reference 3.

The presentation of this data, in standard format, in which J is plotted as a function of the crack extension for each of the data sources identified as i), ii) and iii) above are presented in Appendices B, C and D respectively together with the true stress- true strain material properties as appropriate. The presentation of this data from each of the individual sources has purposely been categorized into separate appendices for independant assessment; the reason is simply that while a large amount of data exists, the wide range of potentially unifying parameters is such as to make precise comparisons between the test data awkward at best. A assessment of these results, trends and comparisons are presented in the following sections.

A second component of the present undertaking relates to an investigation into the potential use of these experimental J-resistance curves and J-driving curves for three specific pipe geometrics and loading conditions. This aspect of the work must be regarded as exploratory and has been directed to the following conditions only

Condition A: An internally pressurized cylinder (pipe) with an axial crack

Condition B: A cylinder (pipe) with an internal circumferential crack under remote tension, and

Condition C: A through wall flaw under remote tension.

It must be emphasized that the evaluation of the 'crack extension' for each of these conditions is grossly oversimplified and is based on what is termed "an engineering approach to elasto-plastic analysis" [Ref. 4, 5].

Utilizing the finite element based results [Ref. 4, 5] requires the appropriate interpolation of the graphical data obtained from these methods to investigate each of the conditions A, B and C. The stable crack extension determined by this approach must not and can not be interpreted as one in which the real behaviour of the resistance by the material has been incorporated in extending the flaw (crack) from an initial size a_i to some limiting value a_f. In this analysis the material behaviour is only represented by the J-R curve and the J-driving curve is determined for various values of crack length for a defined loading condition. Details of the procedure are presented in Appendix E. The true value of the procedure and the results so obtained is simply to provide a qualitative assessment of the magnitude of loads and geometry of the crack which might be tolerated prior to an instability.

B. J-RESISTANCE CURVE DATA

1. General

A series of J-resistance curves are presented in Appendices B, C and D. The reader is referred to each Appendix for the specific details of each test condition and other relevant information. A few key points are briefly summarized:

i) all test data was derived from compact tension specimens

ii) the constants in the power law relationship, $J=H(\Delta a)^n$, which is used to characterize the J-resistance curve were determined as follows: For all PIFRAC data the constants were derived from a minimization of the error (least squares) as fitted to the power law. This result is distinctly different from the fit which would result from a "linearization" of the power law. For all test data in Appendix C a similar approach was used; here the extent of crack extension was small as a result of load control being employed. The J-R curves shown are simply an extrapolation of the curve determined from the data points shown for small crack extensions. In the case of the data from Ontario Hydro the exponent and the constant for each of the J-R curves shown was provided by Ontario Hydro. The details as to how these constants were determined is therefore unknown to the authors.

2. Observations from J-R Curves

A brief summary of some of the key trends indicated by the J-R curves, presented in Appendices B, C and D is provided. For simplicity, selected J-R curves contained within these appendices are reproduced and superimposed upon one another to assess and illustrate the influence of particular variables, which include temperature, orientation of the specimen, specimen thickness, etc., on the shift and profile of the expermentally determined J-R curve.

2.1 Influence of Temperature on the J-R Curve

In Figure 1, two sets of data, presented as Figures B-3 and B-5, have been superimposed. The two data sets are for SA 106 Grade B steel. Both data sets are coded as ZP-14; set one (Figure B-3) for C-L orientation and the second set (Figure B-5) for a L-C orientation. Both data sets for the temperatures shown were determined using specimens of 17.8 mm thickness which were side grooved to a thickness of 14.24 mm.

The J-R curves for both sets show a steep curvature for the 25°C tests, which flattens for the 149°C and thereafter increases with a further increase in temperature. This same trend is evident in Figure B-4, again for a ZP-14 specimen set. The only other data set which shows this trend is given in Figure B-14. It should be noted that Reference 3 states "It is known that ductility of SA 106B steel, as measured by the lateral contraction during a tensile test, shows a minimum in the neighborhood of 250°C and 300°C to confirm that the toughness of the material, when characterized by J_{IC} and R curve, also goes through a minimum near 250°C.

2.2 Influence of Orientation of Specimen on the J-R Curve

A significant difference in the J-R curves for the C-L and L-C orientation are evident from the comparative plots in Figure 1. The L-C data for all temperatures shows a higher J-resistance for the equivalent crack length. Similar trends for J-R curves have been shown from the results in Appendix C (Figures C-1 to C-6) and the Ontario Hydro results in Appendix D (Figures D-1 to D-6). Figure 2 which is a composite of Figures D-3 and D-4 also illustrates this trend for the Ontario Hydro data. This is a particularly consistent result confirmed by all data sets.

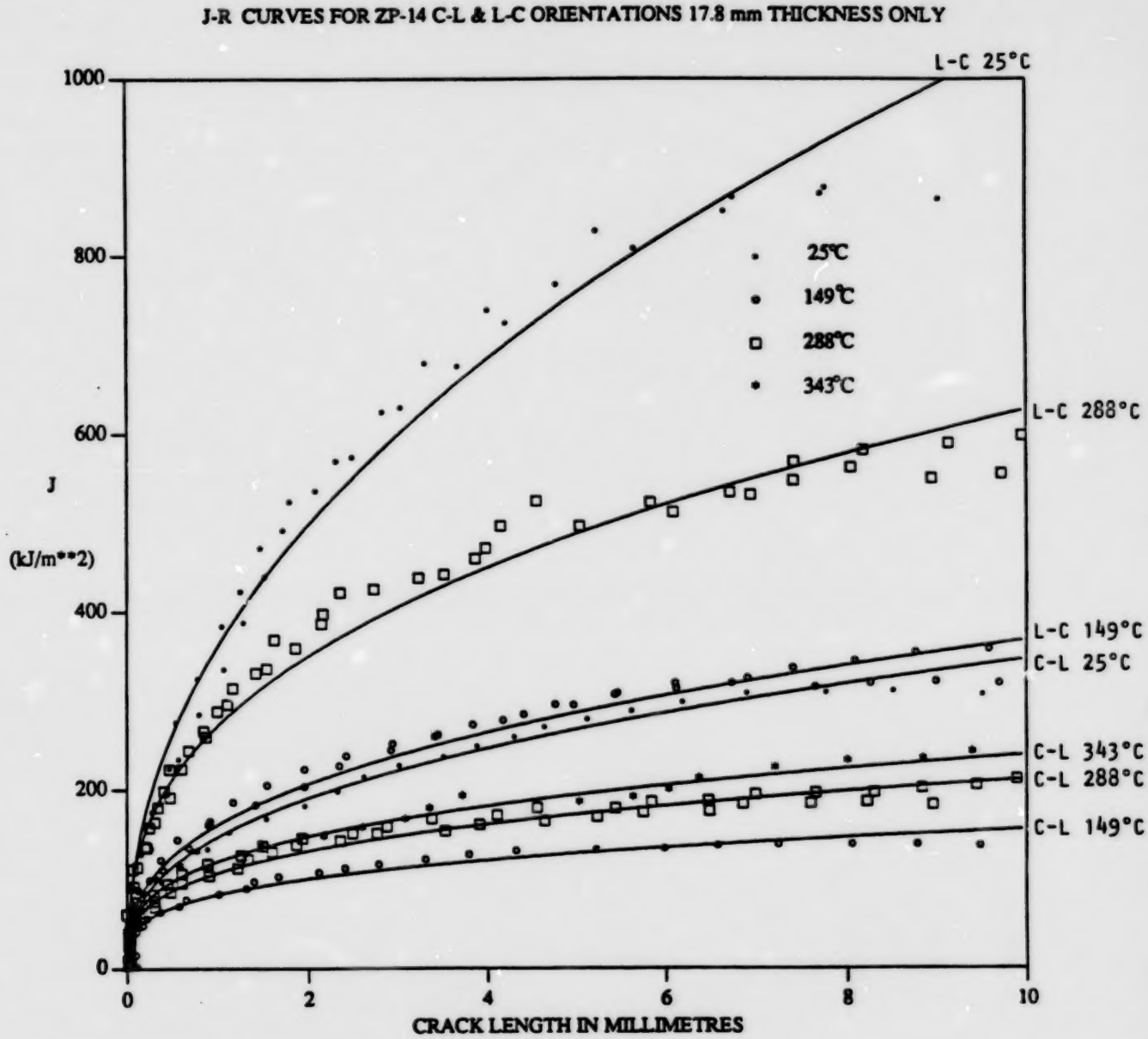

Figure 1: Variation in J-R Curves with Temperature.

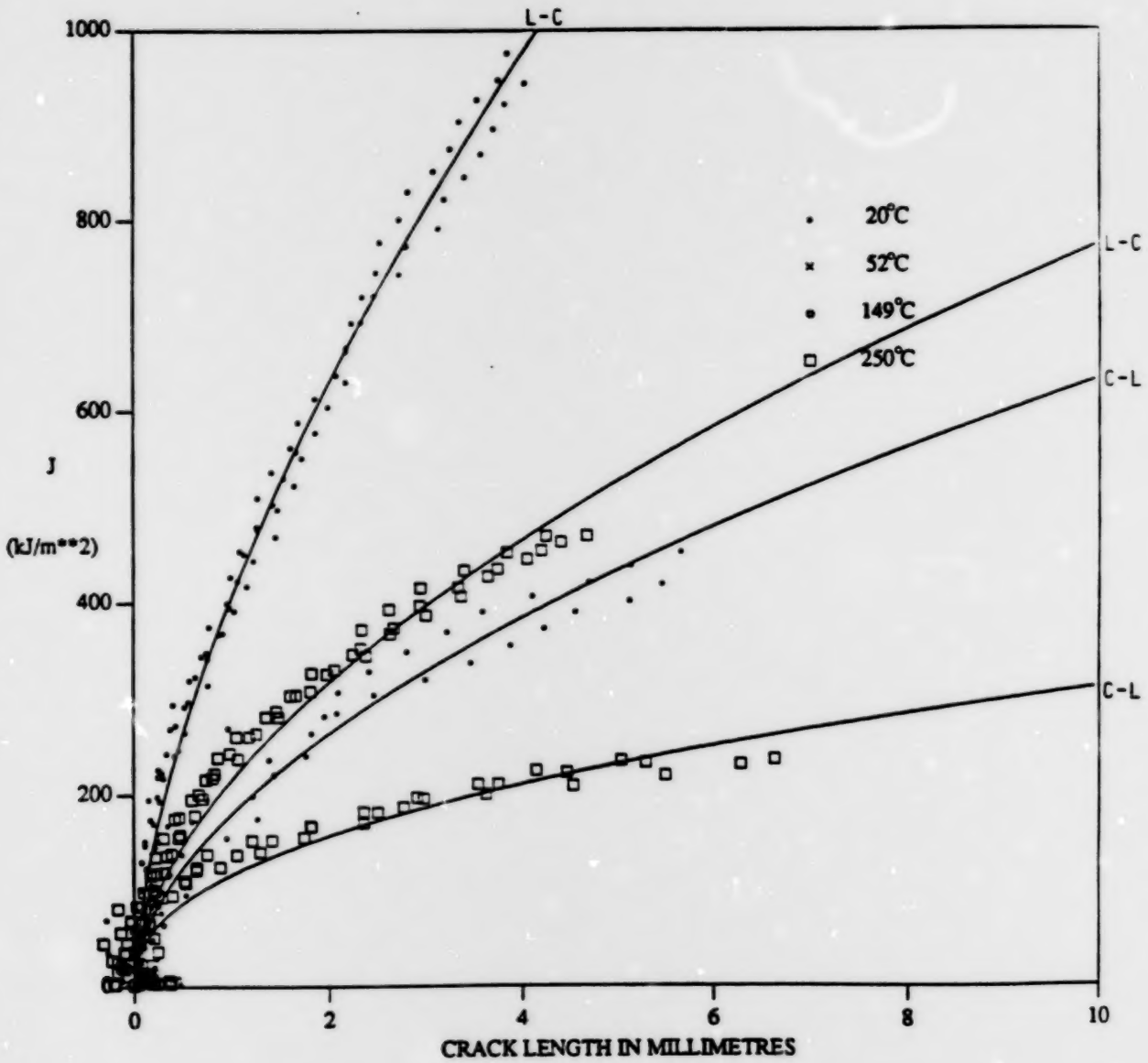

Figure 2: Variation in J-R Curves with Orientation.

2.3 Influence of Specimen Thickness on the J-R Curve

Figures B-4 and B-5 provide an illustration of the effect of side grooving a specimen. The J-resistance curves at 149°C for each of these test series are superimposed and presented as Figure 3. The 15.2 mm specimen appears to have a considerably higher J-resistance for the equivalent crack length as compared with the 17.8 mm thick specimen side grooved to 14.24 mm. As is evident from Figures B-4 and B-5, the equivalent observation is obtained at temperatures of 25°C and 288°C. See also Figures B-2, B-7, B-15 and B-16 for a comparison of non-grooved and grooved specimen results.

Figures 4 and 5 provide a composite of J-R curve results for side grooved specimens for C-L and L-C specimen orientation respectively. The significance of the orientation has been established and it is therefore of interest to observe the grouping of the grooved specimen results for thicknesses ranging from 7.28 mm to 25.4 mm for both the C-L and L-C orientations at 25°C. It should, however, be noted that each of the curves presented in Figures 4 and 5 does not represent a complete experimental data set over the full crack length shown; the curves are numerical extrapolations and it is therefore necessary to refer to each of the curves identified in the respective appendices.

It can be concluded from an examination of most data (Figures B-2, B-7, B-15, B-16) that a more conservative J-R curve will be obtained when the specimen has been side grooved. This is to be expected as a result of the plane strain constraint. What , as yet unclear is if any minimum plateau can be defined for the J-R curve which is independent of the grooved specimen thickness above a particular value. To illustrate the type of result which is obtained the reader is referred to Figures 6 and 7 which are composites of results presented in Appendix D. In Figure 6, two sets of data for L-C type J-R curves obtained from 12 inch and 22 inch diameter SA 106 Grade B pipe steel are given. The 30.5 mm specimens have a reduced thickness of 24.58 mm, while the 19 mm specimens have a reduced thickness of 15.2 mm. At 250°C, for which this comparison is made, the effect of specimen thickness is not significant even though the pipes are of different diameter. This result contrasts sharply with the result provided in Figure 7 for the C-L of the same two pipes. Here the spread in J-R curve results is significantly different with the thicker specimen, as might be anticipated, yielding the more conservative result.

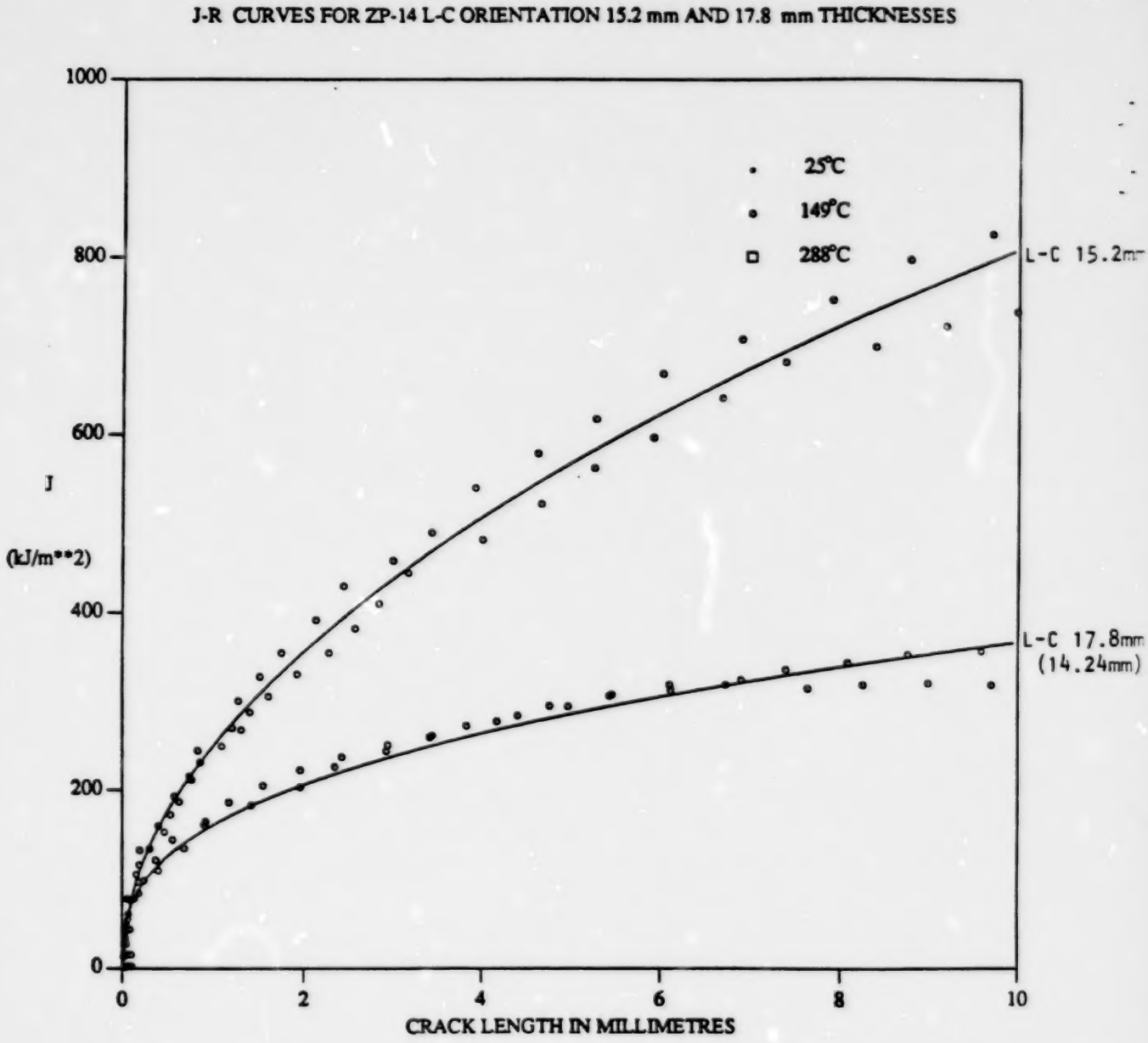

Figure 3: Variation in J-R Curves with Specimen Thickness.

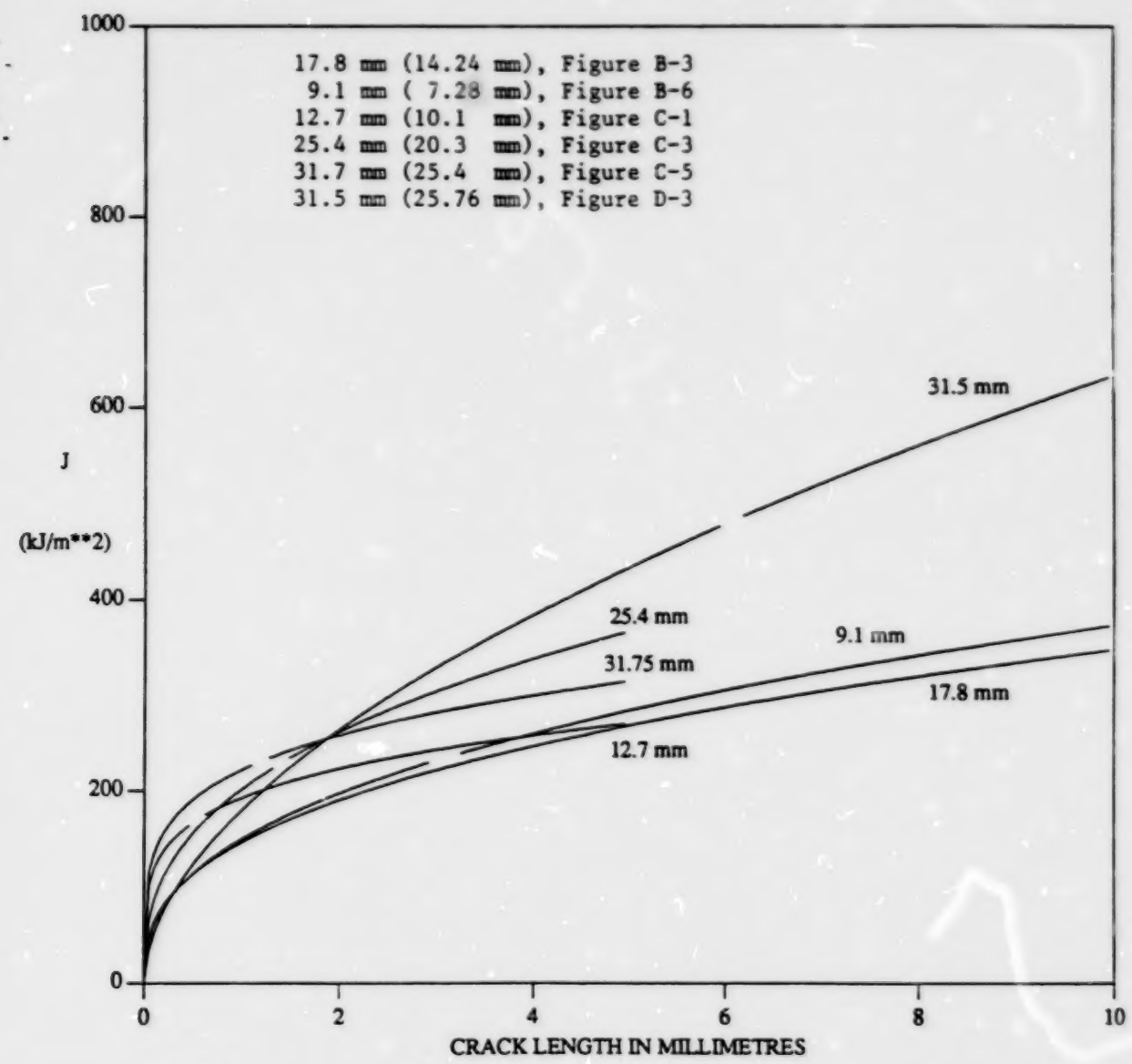

Figure 4: Composite of J-R Curves for C-L Orientation, Side Grooved Specimens at 25°C. (graph beyond the break is an extrapolation based on the fitted experimental data presented in Appendices B, C and D).

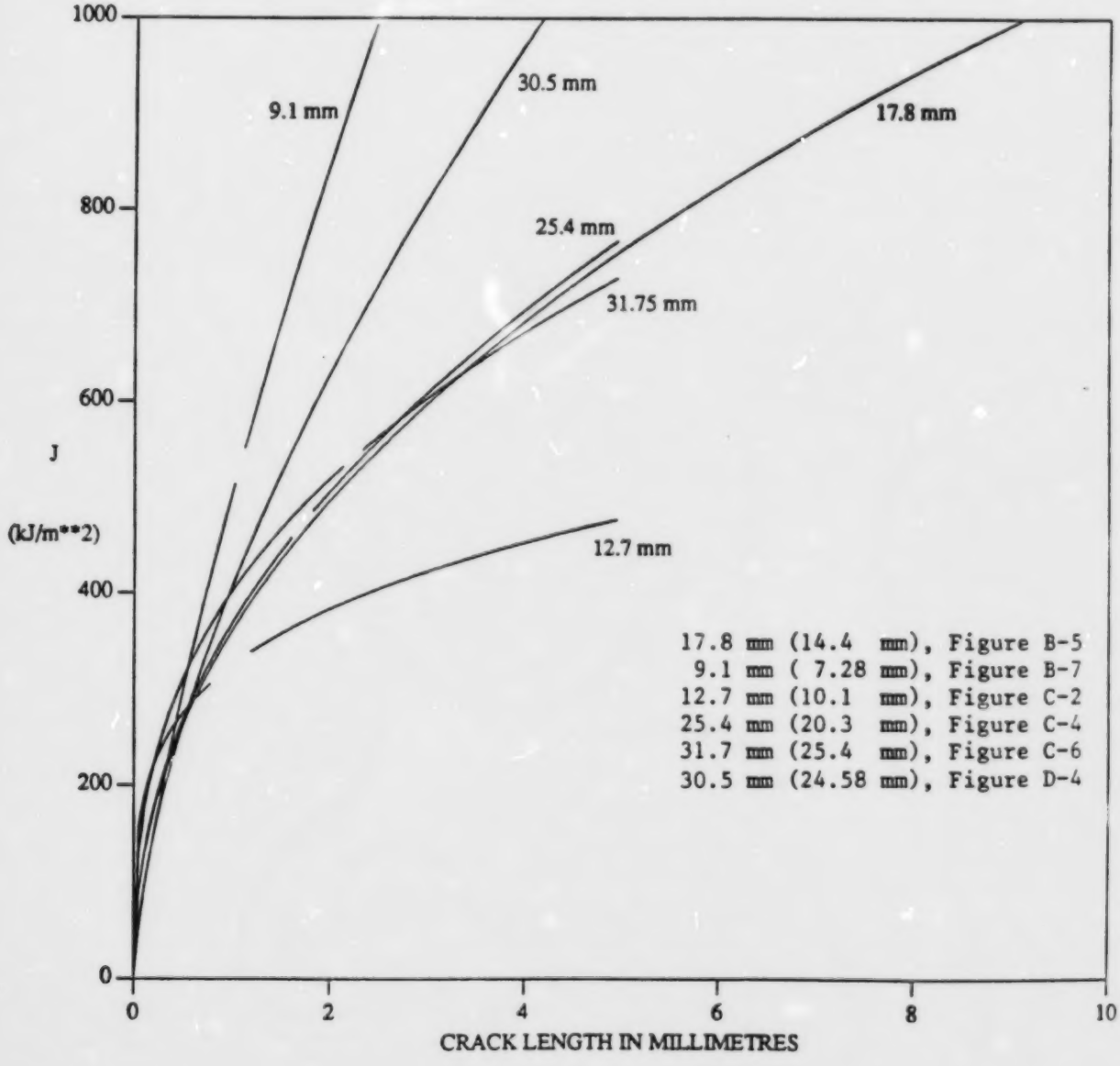

Figure 5: Composite of J-R Curves for L-C Orientation, Side Grooved Specimens at 25°C. (graph beyond the break is an extrapolation based on the fitted experimental data presented in Appendices B, C and D).

L-C TYPE J-R CURVES FOR ONTARIO HYDRO TESTS OF 12 INCH AND 22 INCH DIAMETER NPS SCH 100 PARENT SPECIMEN THICKNESSES 19.0 mm AND 30.5 mm

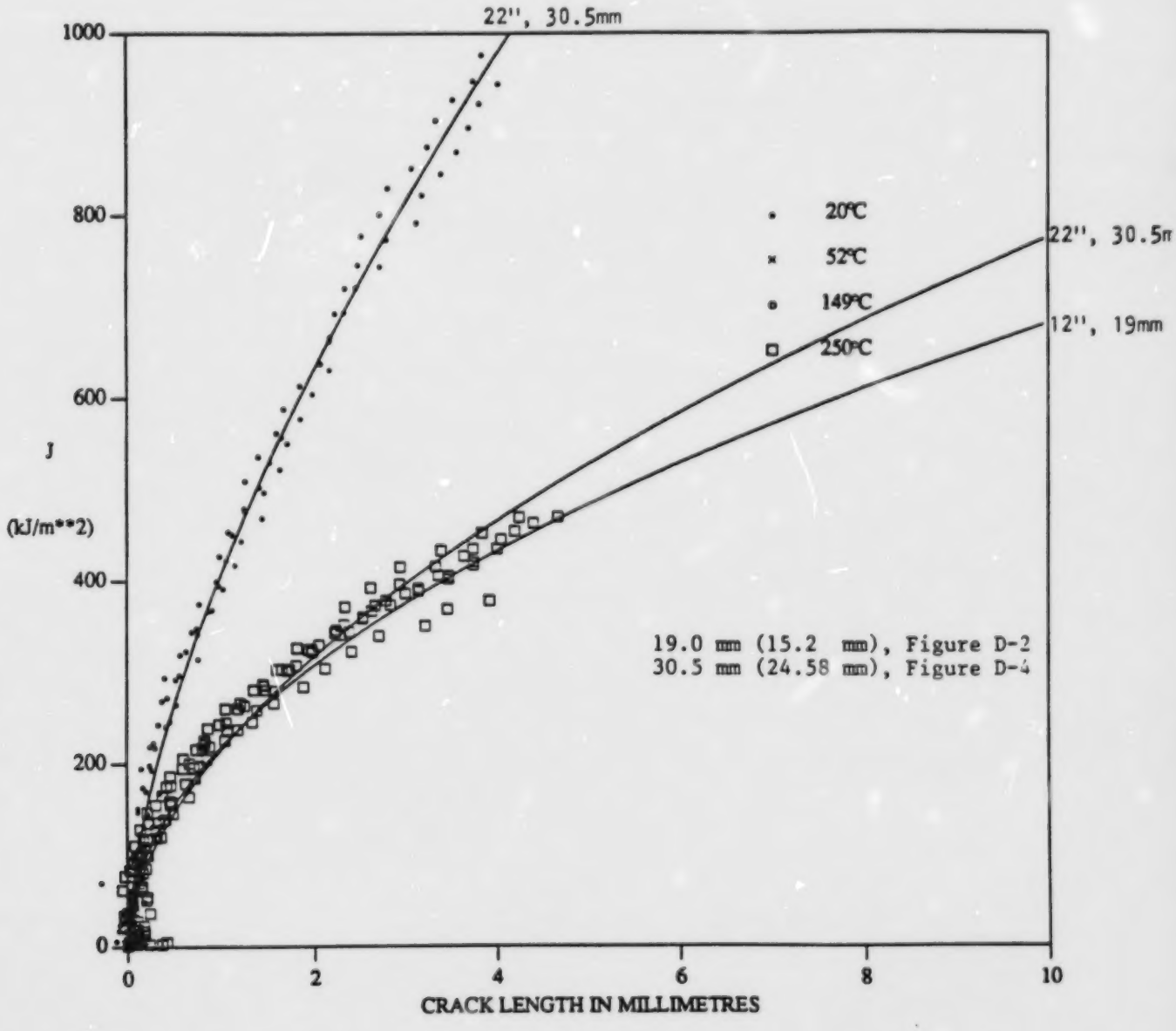

Figure 6: Variation in J-R Curves with Specimen Thickness cut from 12inch and 22inch diameter Pipe in L-C Orientation.

C-L TYPE J-R CURVES FOR ONTARIO HYDRO TESTS OF 12 INCH AND 22 INCH DIAMETER
NPS SCH 100 PARENT SPECIMEN THICKNESSES 19.0 mm AND 30.5 mm

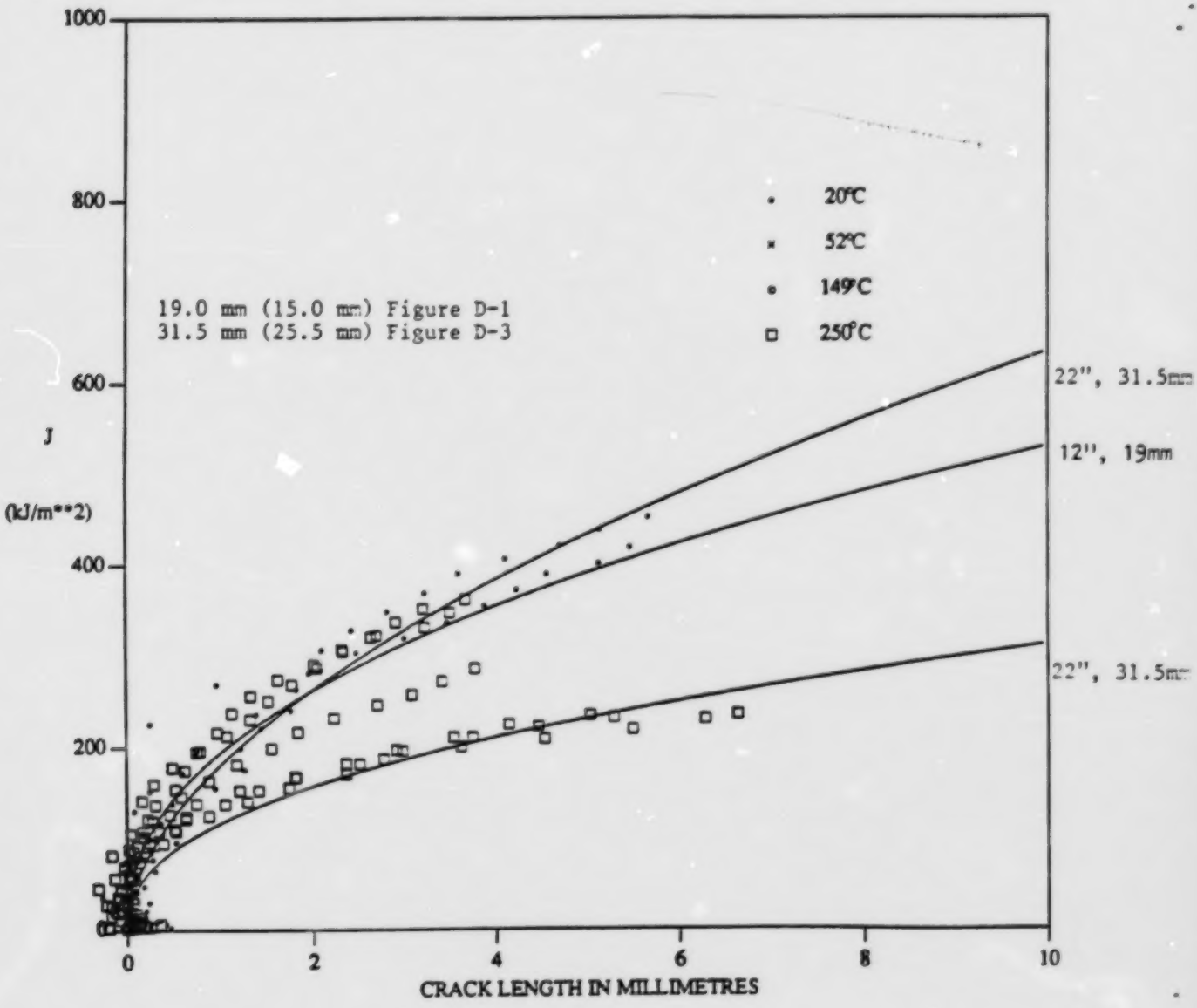

Figure 7: Variation in J-R Curves with Specimen Thickness cut from 12inch and 22inch diameter Pipe in C-L Orientation.

C. STRESS STRAIN DATA

1. General

In addition to the determination of J-R curves which have been presented in Section B, it is appropriate to examine the true stress-true strain data characterized by the Ramburg-Osgood relationship given by the expression:

$$\frac{\epsilon}{\epsilon_o} = \frac{\sigma}{\sigma_o} + \alpha \left[\frac{\sigma}{\sigma_o}\right]^n \qquad 3.1$$

A series of true stress-true strain curves are presented in Appendices B and D for the PIFRAC data (Figures B-8 to B-10) and the Ontario Hydro data (Figures D-7 to D-9) respectively.

A comparison of the true stress-true strain curves as a function of the temperature at which the tests were undertaken is provided in Figure 8 for tests carried out at 25°C, 149°C, 288°C and 343°C respectively. Figure 8 is a composite of the individual results presented in Figures B-9(a)-(d) for specimens cut from the circumferential direction. The results indicate a reasonable scatter within the experimental procedures used; this scatter is less significant at low values of strain, but becomes more pronounced as the level of strain is increased. The empirical relationships, based on the Ramburg-Osgood formulation, were determined using a minimization of the error (least squares) as fitted to the power law. The approach is similar to that adopted for the J-R curves, but in the case of the stress-strain relationship, the yield stress, σ_o, was provided with the data base so that ϵ_o could be directly determined from a knowledge of the Youngs Modulus. Once values for σ_o and ϵ_o are known, the constants α and n were determined. It will be noted that none of the curves correlate well with the small values of strain.

A comparison of Figures B-8(a) and (b) illustrate similar trends to that of Figure 8 for a second test set using longitudinal orientation specimens at 149°C and 288°C, i.e. a similar scatter with the higher stress-strain curve being obtained for the higher temperature. In Figures B-8(c)-(e), which identify the stress-strain curves for the same test set as presented in Figure 8 (with the exception that these tests are for longitudinal orientation specimens) the scatter is again similar, but here the higher stress-strain curve corresponds to the test undertaken at 149°C. From the above, it would appear that the stress-strain results, while different, show no consistent trend and in large measure the scatter must be attributed to experimental error. While interpreting the results in this manner, consideration must be given to the results in Figures B-10(a)-(c) where the difference between the stress-strain curve from tests at 25°C, Figure B-10(a), differs substantially from those tests at 149° and 288°C respectively as shown in Figures B-10(b) and (c).

This lack of any specific trend for stress-strain data at different temperatures and indeed orientations is provided in Figures 9 and 10 for the Ontario Hydro tests. In these figures the stress-strain curves developed by Ontario Hydro are plotted for both the C-L and L-C orientations at 20°C and 250°C. All four curves in both figures practically coincide. This independence of the stress-strain curve, whether obtained from longitudinal or circumferential test specimens, is further confirmed by comparing the test results from PIFRAC for ZP15 (Figures B-10(a) and B-10(d)) and ZP14 (Figures B-8(c) and B-9(a)). Both these sets of data, obtained at 25°C from longitudinal and circumferential test specimens, indicate no dependence of the stress-strain curve on the orientation of the test specimen.

2. Assessment of Curve Fitting.

To assess the range or potential sensitivity of the Ramburg-Osgood formulation in relation to its specific representation of the data points, a detailed investigation of the 'best fit' was undertaken. This is best described with reference to Figures 11(a)-(d). Figure 11(a) represents the 'best fit' through all data points using the Ramburg-Osgood formulation. Figures 11(b) to (d) illustrate the same data points but in each case only data points below the defined levels of strain were incorporated to determine the empirical constants. These constants, together with the imposed strain limit and a small allowable variation in the yield stress, σ_o, are presented in Table 1. All empirical stress-strain curves obtained for each of the

values of σ_o for a particular strain limit are illustrated in each of Figures 11(b), 11(c) and 11(d). In each case the curves coincide exactly.

The purpose of this exercise was simply to ascertain the extent of the variation in the stress-strain curves which result from attempting to force the data to a particular formulation. Clearly, the variation in the stress-strain curves determined using all data points and a limiting strain of 0.05 (Figures 11(a) and 11(b)) would confirm the sizeable scatter which is, therefore, inherent in stress-strain curves.

σ_o (MPa)	Strain Limit	α	n
282.5	0.1	2.01	4.74
282.5	0.075	2.93	4.06
282.5	0.050	3.46	3.69
270	0.1	1.70	4.74
270	0.075	2.56	4.06
270	0.050	3.07	3.69
295	0.1	2.37	4.74
295	0.075	3.35	4.06
295	0.050	3.89	3.69
282.5	all data	1.75	4.967

Table 1: Empirical Constants for Selected Values of σ_o and Strain Limits 0.1, 0.075 and 0.05

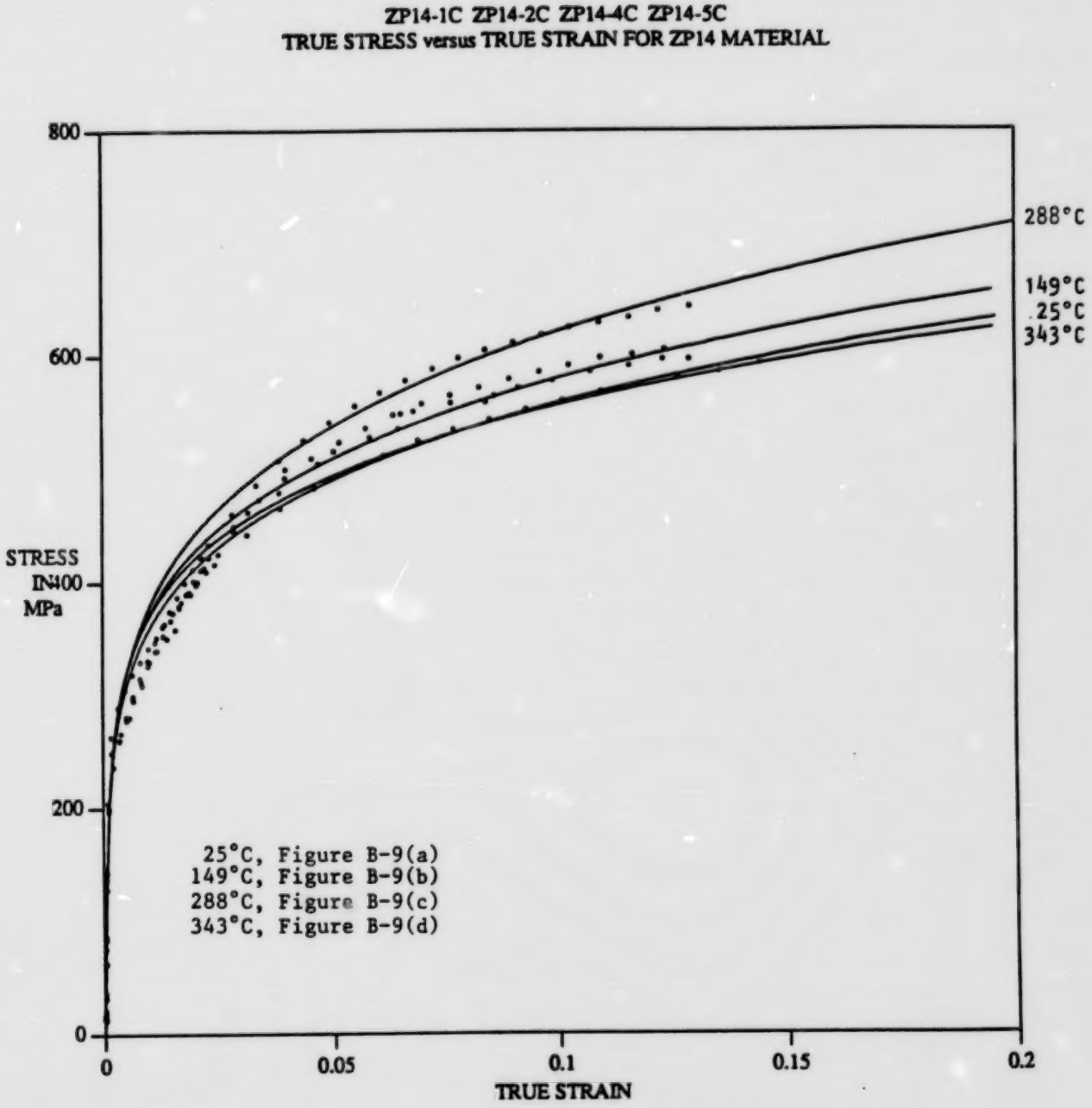

Figure 8: Comparison of True Stress - True Strain Curves, for Circumferential Orientation Specimens, as a Function of Temperature.

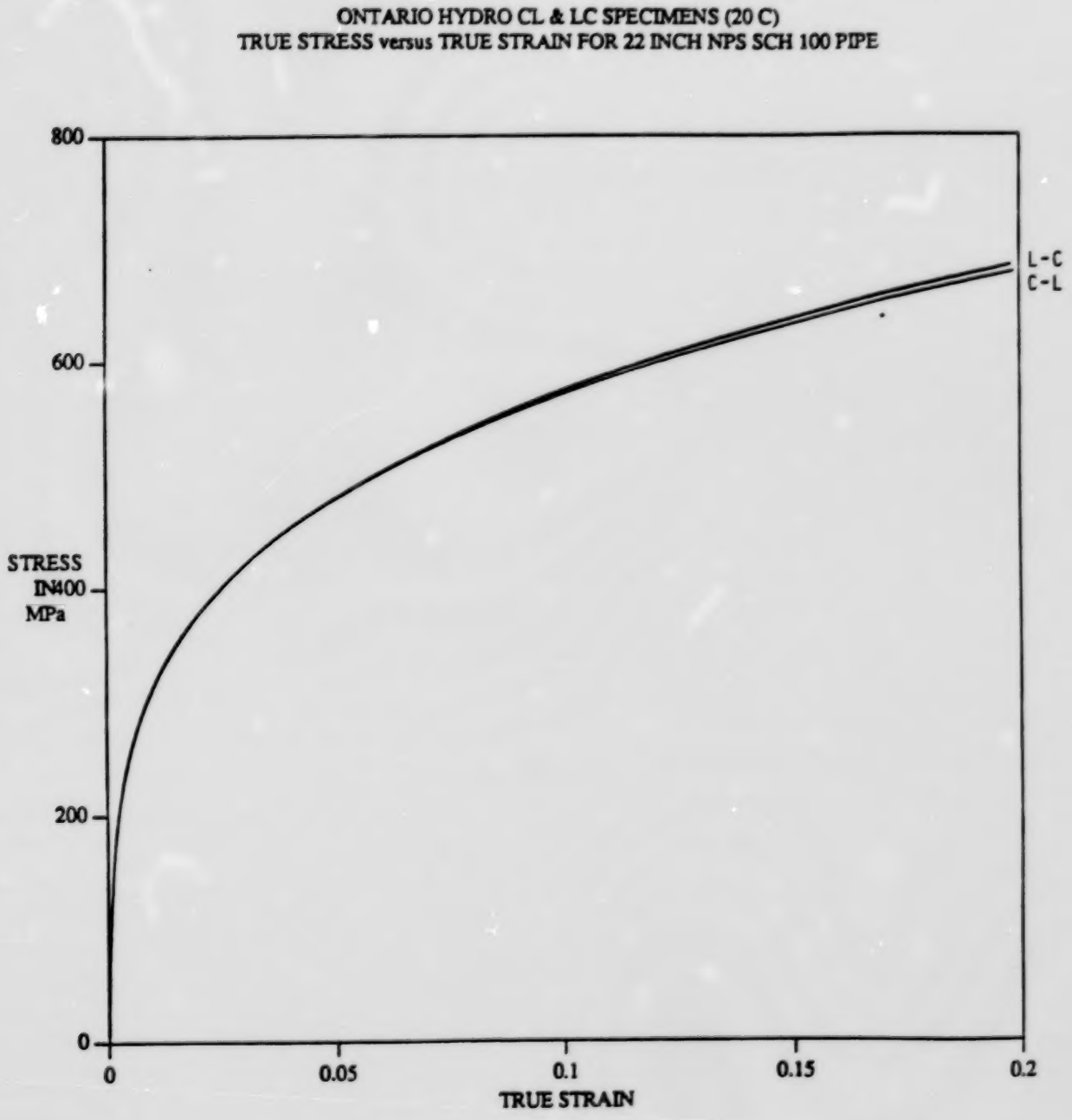

Figure 9: Comparison of True Stress - True Strain Curves for C-L and L-C Orientations at 20°C.

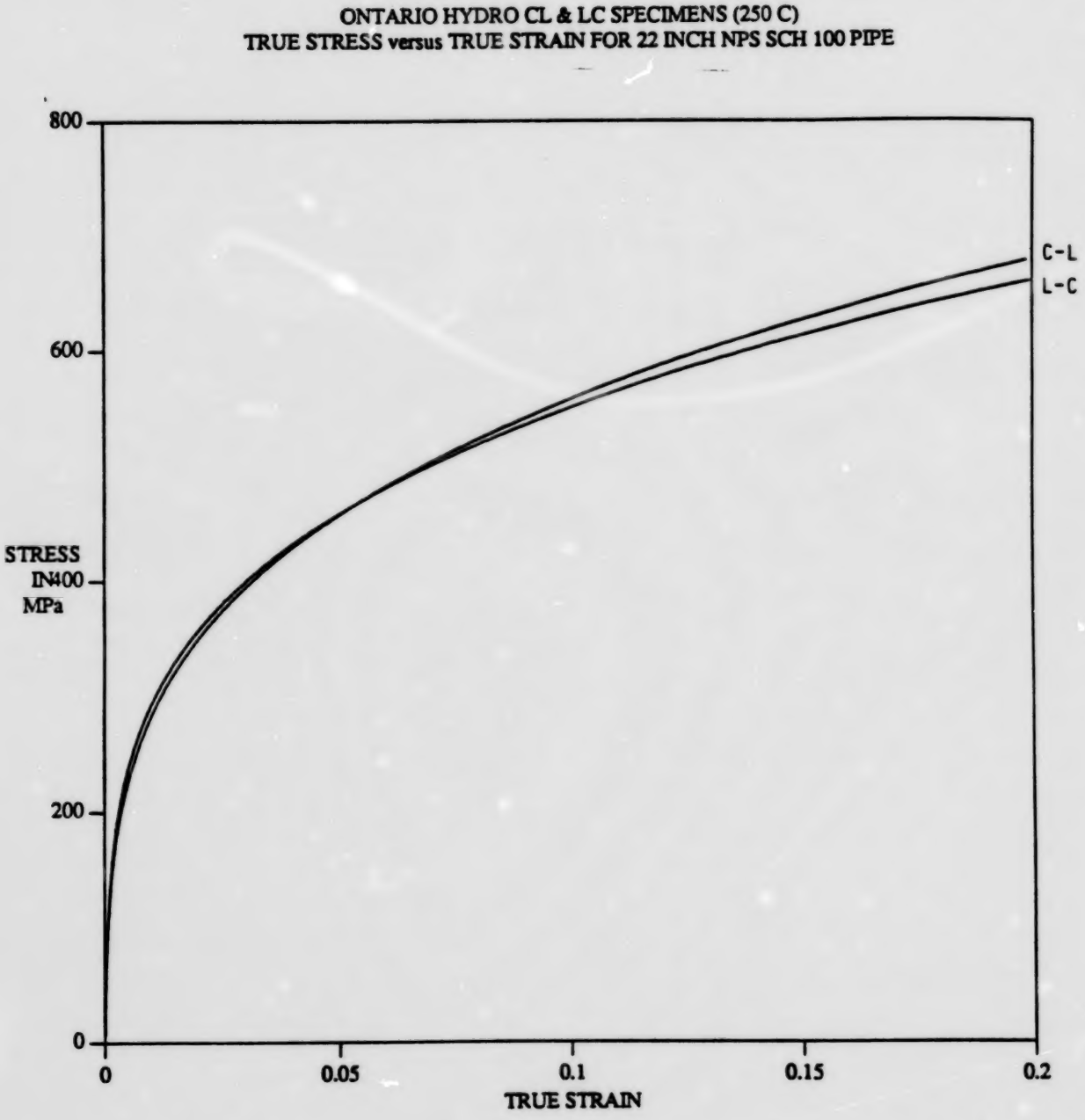

Figure 10: Comparison of True Stress - True Strain Curves for C-L and L-C Orientations at 250°C.

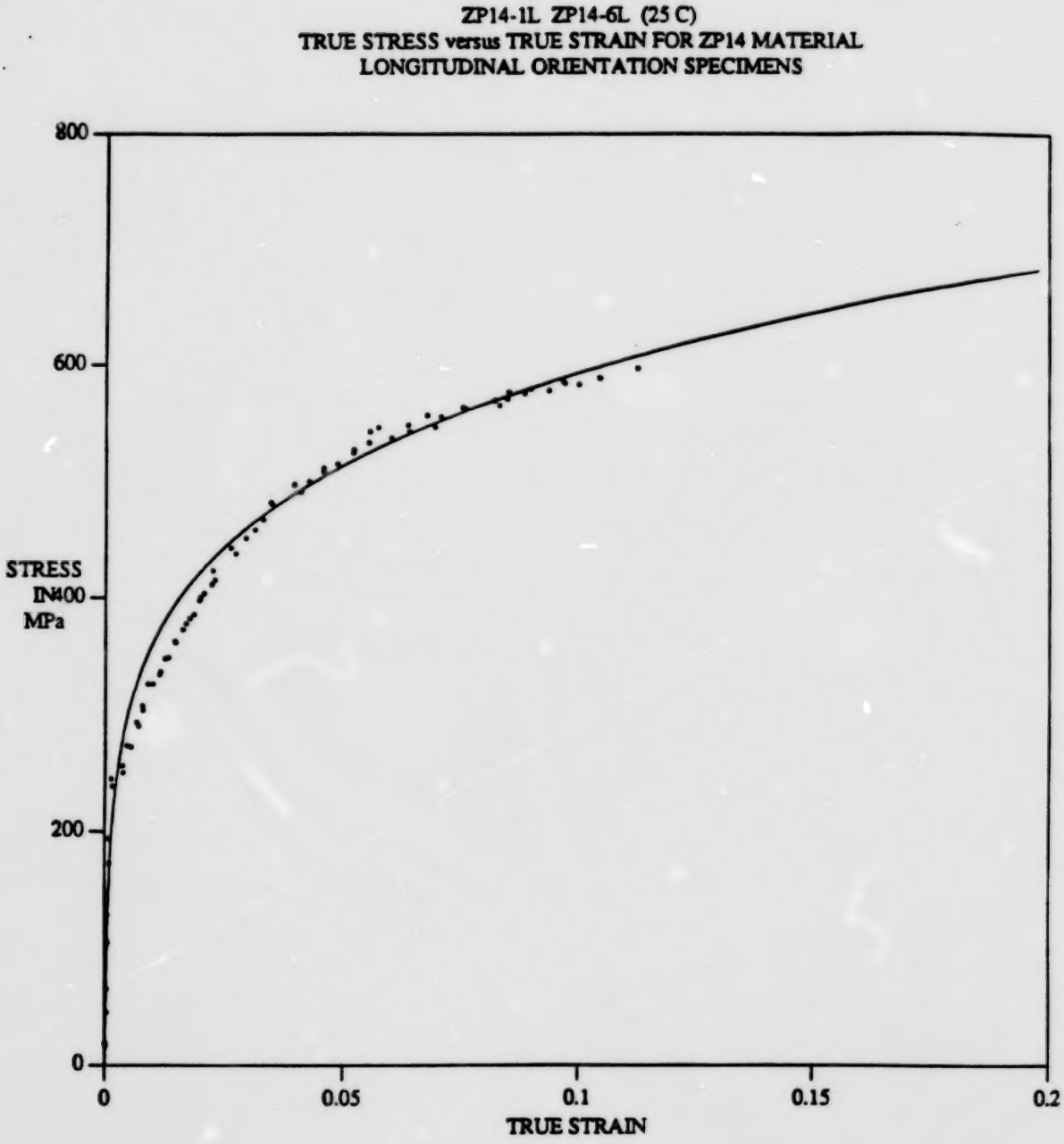

Figure 11(a): True Stress - True Strain Curve using all Data Points.

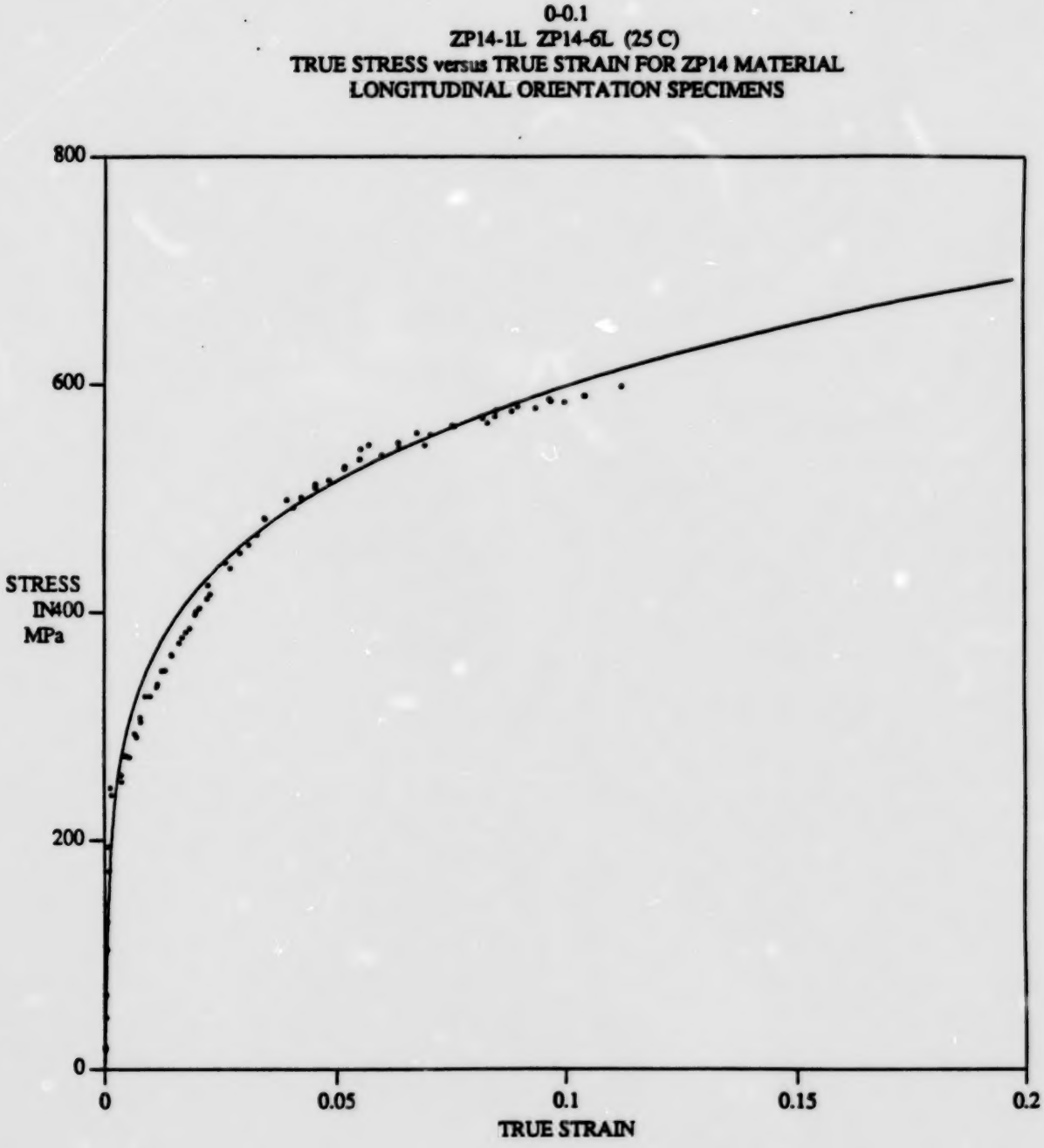

Figure 11(b): True Stress -True Strain Curve using Data Points below True Strain of 0.1.

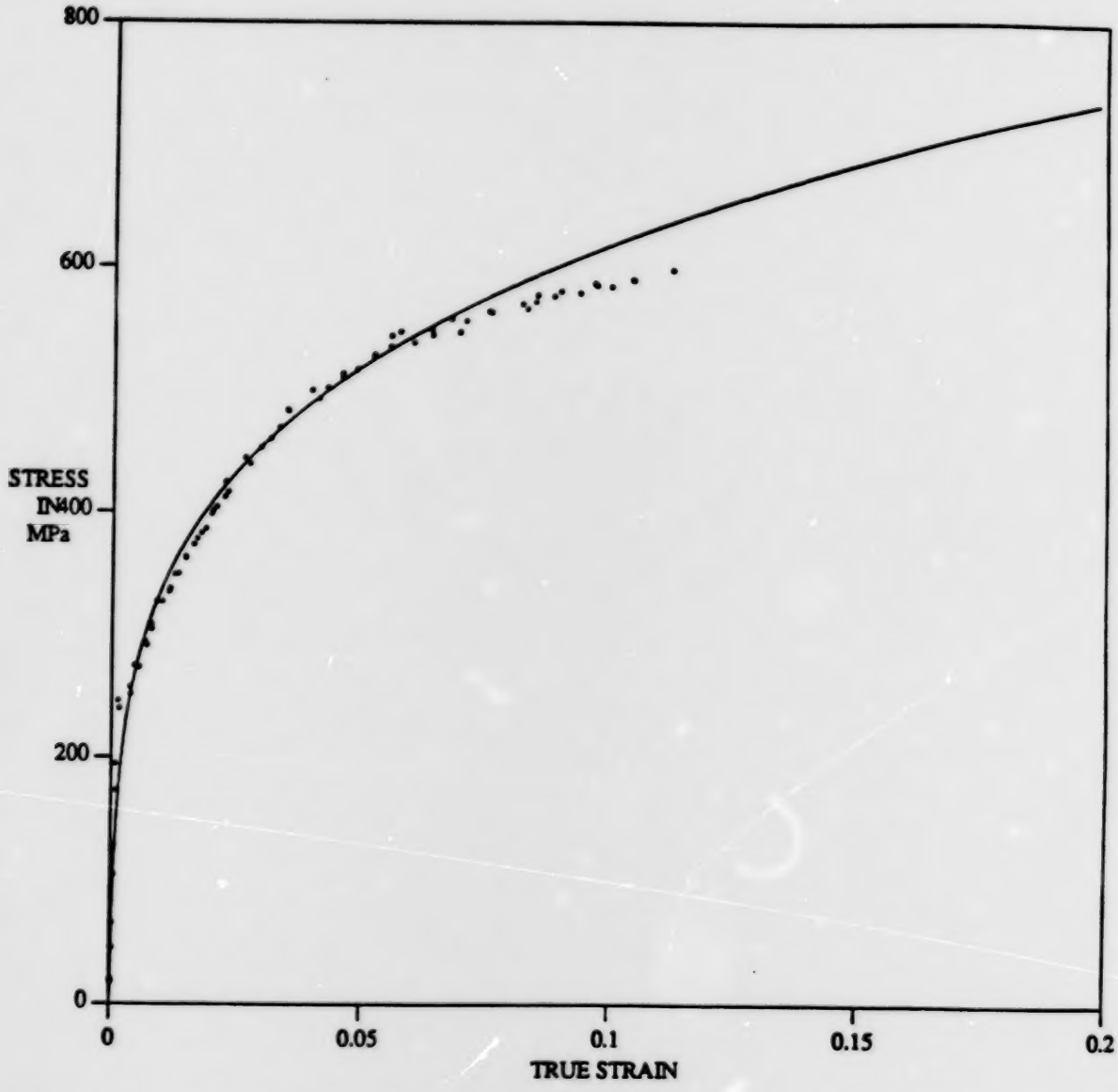

Figure 11(c): True Stress - True Strain Curve using Data Points below True Strain of 0.075.

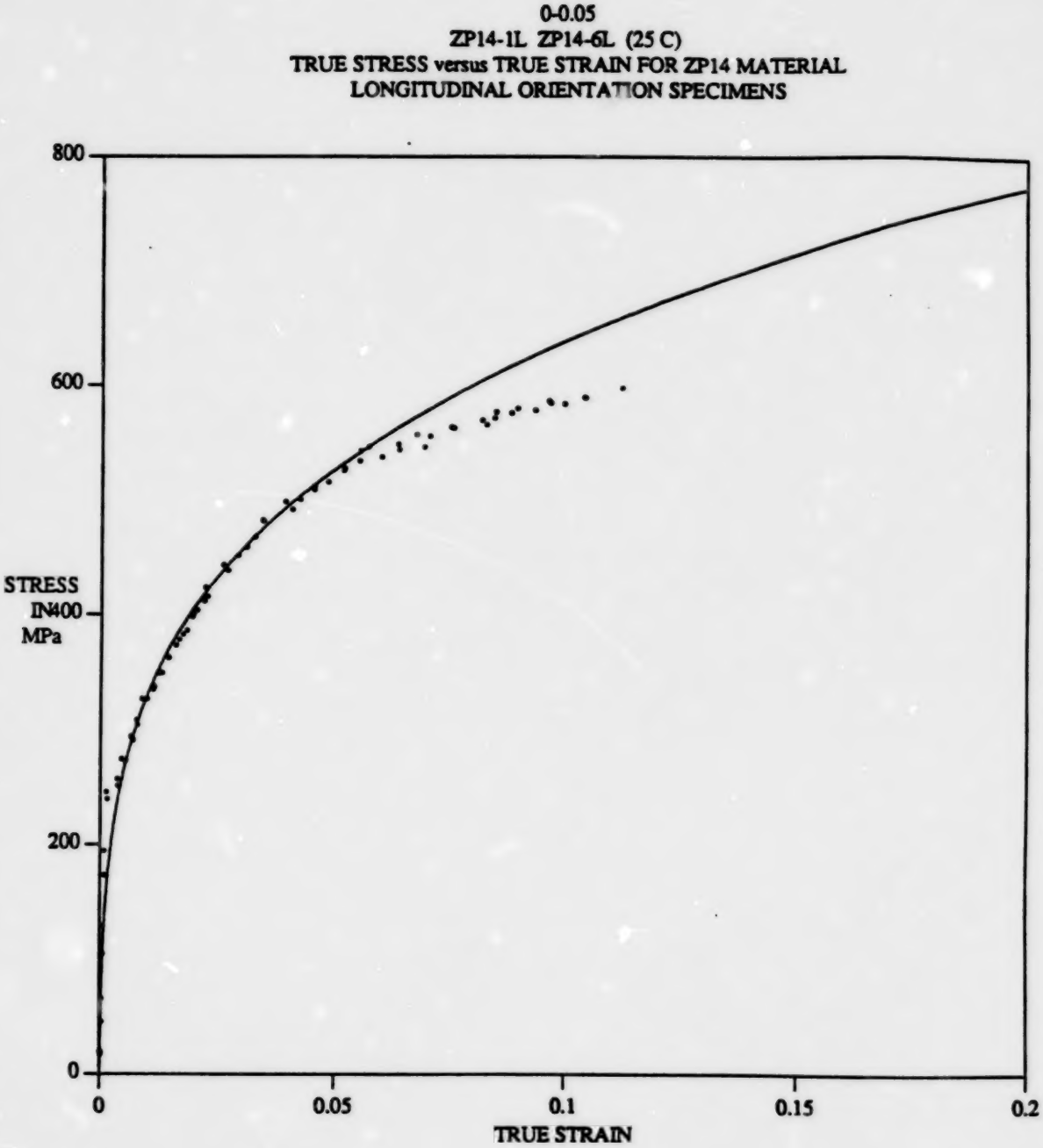

Figure 11(d): True Stress - True Strain Curve using Data Points below True Strain of 0.05.

D. ENGINEERING APPROACH TO ELASTO-PLASTIC ANALYSIS

1. General

The development of the software based on the engineering approach for elastic plastic fracture analysis, outlined in the EPRI documents NP-1931 and NP-3607 [Ref. 4 and 5], is presented in Appendix E. The thrust of this approach is to utilise the results obtained from finite element analyses which have been appropriately tabulated and documented in non-dimensionalised formats to permit the determination of the loading conditions for selected geometries. It will be immediately obvious that such an approach is limited since a comprehensive handbook style catalogue of elastic and fully plastic solutions for evaluating the J driving curves for cracked bodies cannot realistically be compiled to address a useful range of problems. What has been achieved however, albeit limited, is the most basic of problems; these are identified as Conditions A, B and C and are illustrated in Figures E-2(a) through (c).

2. Geometric and Loading Conditions A, B and C

Condition A. This geometry represents an internally pressurized cylinder (pipe) with a part-through-wall axial crack of depth 'a' propagating in the radial direction of the cylinder with wall thickness, b. See Figure E-2(a).

Condition B. This geometry represents a part-through-wall circumferential (radial) crack propagating in the radial direction when the cylinder (pipe) is subjected to a remote tensile loading condition. The depth of the crack is 'a' in the wall of the cylinder of thickness 'b'. See Figure E-2(b).

Condition C. This geometry represents a through-wall circumferential crack propagating in the circumferential direction when the cylinder (pipe) is subjected to a remote tensile loading condition. The length of the crack is 2a, where the full ligament length, 2b, corresponds to the circumference of the pipe. See Figure E-2(c).

Four specific sets of experimental data presented in Appendices C and D have been investigated for each of the Conditions. The particular data sets are:

i) PIFRAC, ZP-14, L-C orientation
ii) PIFRAC, ZP-15, L-C orientation
iii) PIFRAC, ZP-14, C-L orientation
iv) Ontario Hydro, J63-J67, C-L orientation

The results for each of the four data sets for Conditions A, B and C are presented in Figures 12 through to 15. The interpretation of each of these figures is similar, and will be explained with reference to Figure 13(a) for data set ZP-15 with an L-C orientation for Condition A. Figure 13(a) presents a plot of internal pressure/yield strength as a function of the initial crack length/full ligament. While numerous solutions are illustrated, it is suffice to simply describe one such solution: point a_i represents the initial crack length for a test undertaken at 25°C. Using this initial crack length to define the precise geometry as well as the J-R curve from the experimental data set, it is then possible to determine a series of J-driving curves based on an estimated internal pressure loading as indicated in Appendix E for increments in the crack length. This procedure can be repeated automatically using the developed software to finally determine the magnitude of the internal pressure and the final crack length, denoted as, a_f, in Figure 13(a). The equivalent results for tests at both 149°C and 288°C are presented for an increasing initial crack length to full ligament ratio. As is indicated, the coordinate axis records the applied internal pressure divided by the yield strength for an increasing crack length. This normalization allows for an assessment of the complete data set. It is important to emphasize at this time that while an initial crack and final crack length are determined the results must not be interpreted as representing the stable or controlled growth of the crack to the limiting value.

For the results shown in Figures 13(b) and (c) which represent the Conditions B and C respectively, as well as all other experimental sets, the analyses have been undertaken using a 24 inch diameter pipe

with a 2 inch wall thickness, unless otherwise stated. While this is an arbitrary choice of pipe dimensions, it is, nevertheless, representative. For both Conditions B and C the coordinate axis is therefore not dimensionless; it is possible that the pipe geometry could have been incorporated in general terms into this variable plotted on the coordinate axis, but such improvements or generalizations are easily incorporated as required. The intent here was simply to attempt to ascertain how the load and specific geometry conditions will change with an increasing initial crack size, the effect of temperature, and the final crack size which is correlated with the applied loading. Having presented the data in this format is of interest to note the trends that result:

i) while it is evident that the allowable load will be reduced for increased initial crack size, it is of interest to note that the results of a_i increasing to a_f, for each of the individual cases, form a reasonably narrow band.

ii) the results should also be assessed in relation to the C-L and L-C orientations and their relation to the direction of the propagation of the crack. For example in Figures 12(a) and 14(a) the results for the experimental set ZP14 for both the L-C and C-L orientations are presented. The ZP14 C-L results are more representive than the L-C results since the J-R curve for the C-L orientation more closely approximates the material resistance to crack propagation in the radial direction [Ref. 2], see condition A.

iii) following on (ii) above, the results obtained for L-C orientations and the associated J-R curves on which the analysis is dependent, correspond to the direction of crack propagation for condition C.

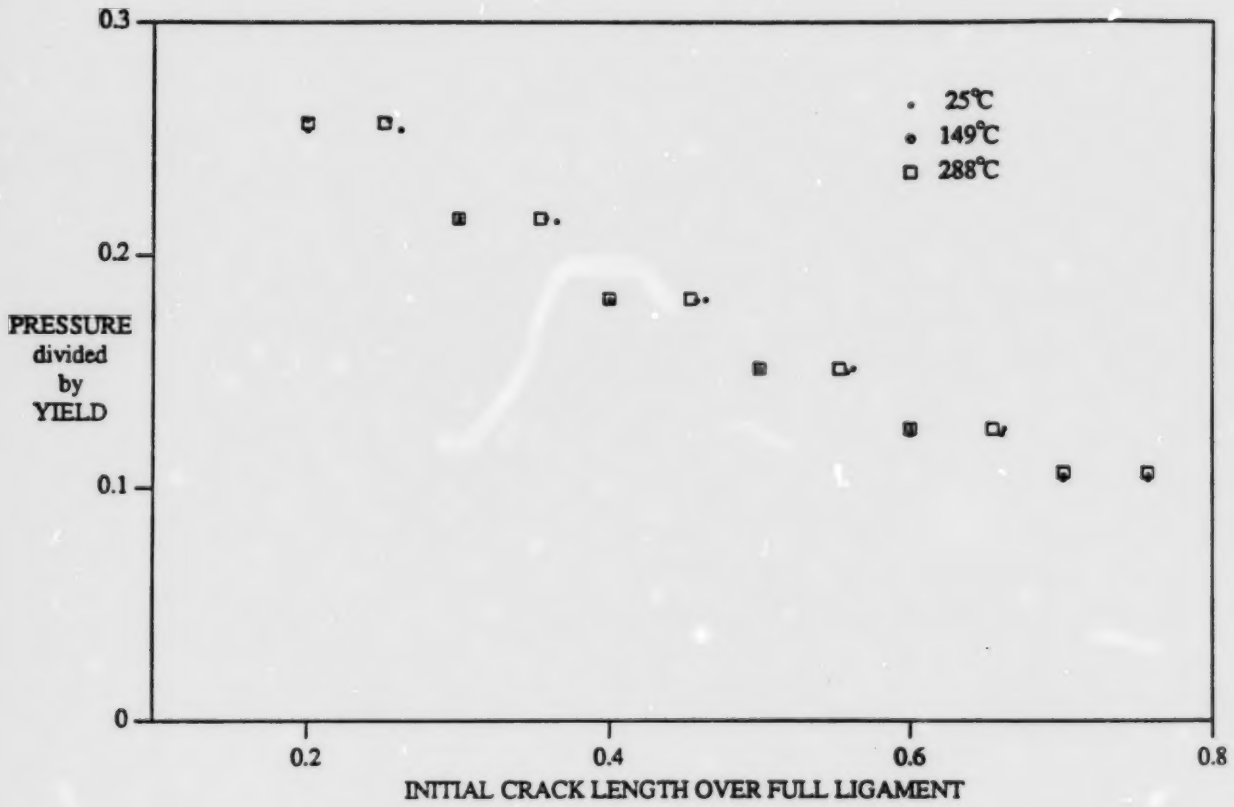

Figure 12(a): Normalised Loading as a Function of Crack Length for Data Set ZP14 (PIFRAC). Condition A.

Developed for a 24 inch diameter pipe of 2 inch wall thickness.

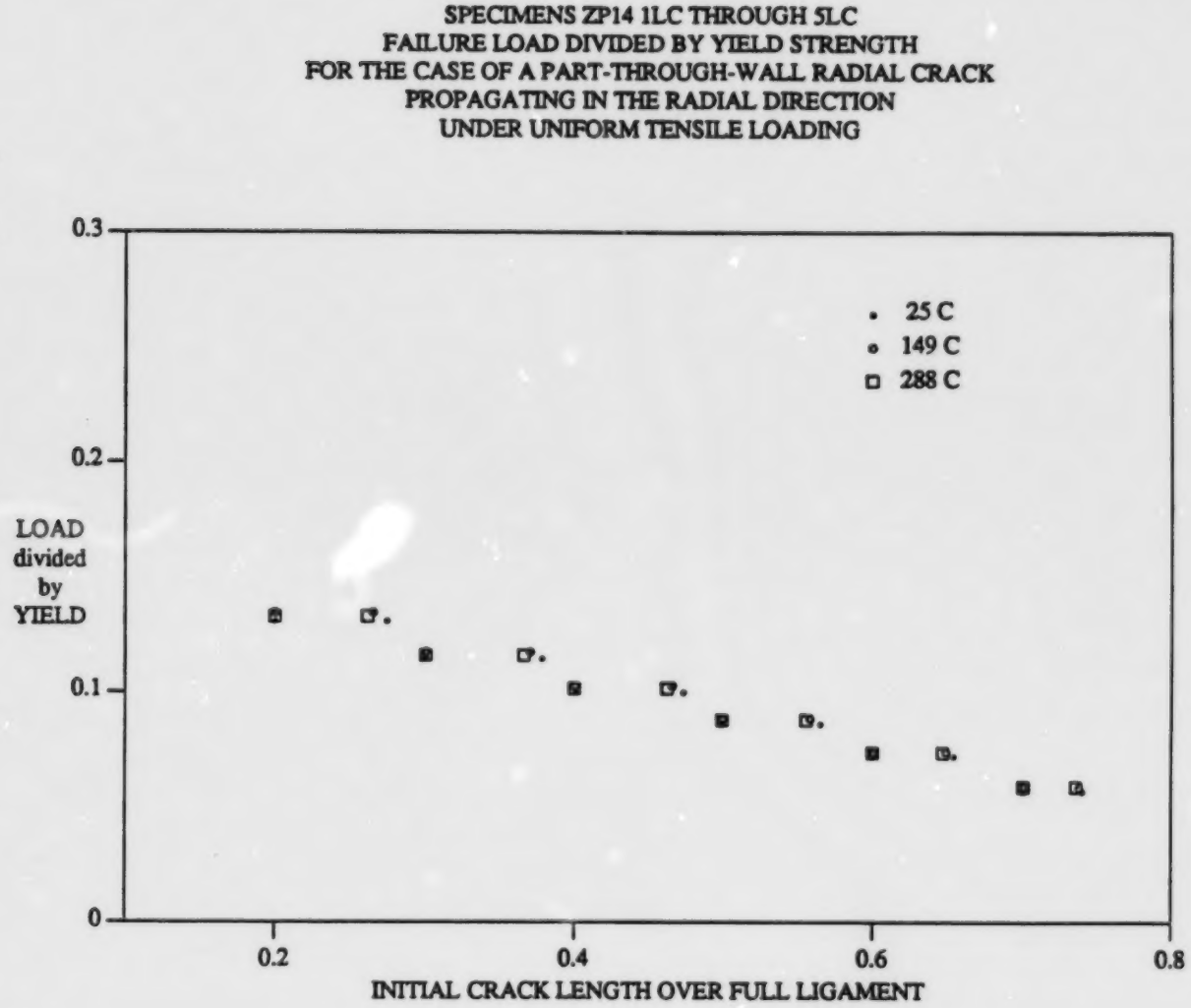

Figure 12(b): Normalised Loading as a Function of Crack Length for Data Set ZP14 (PIFRAC). Condition B.

Developed for a 24 inch diameter pipe of 2 inch wall thickness.

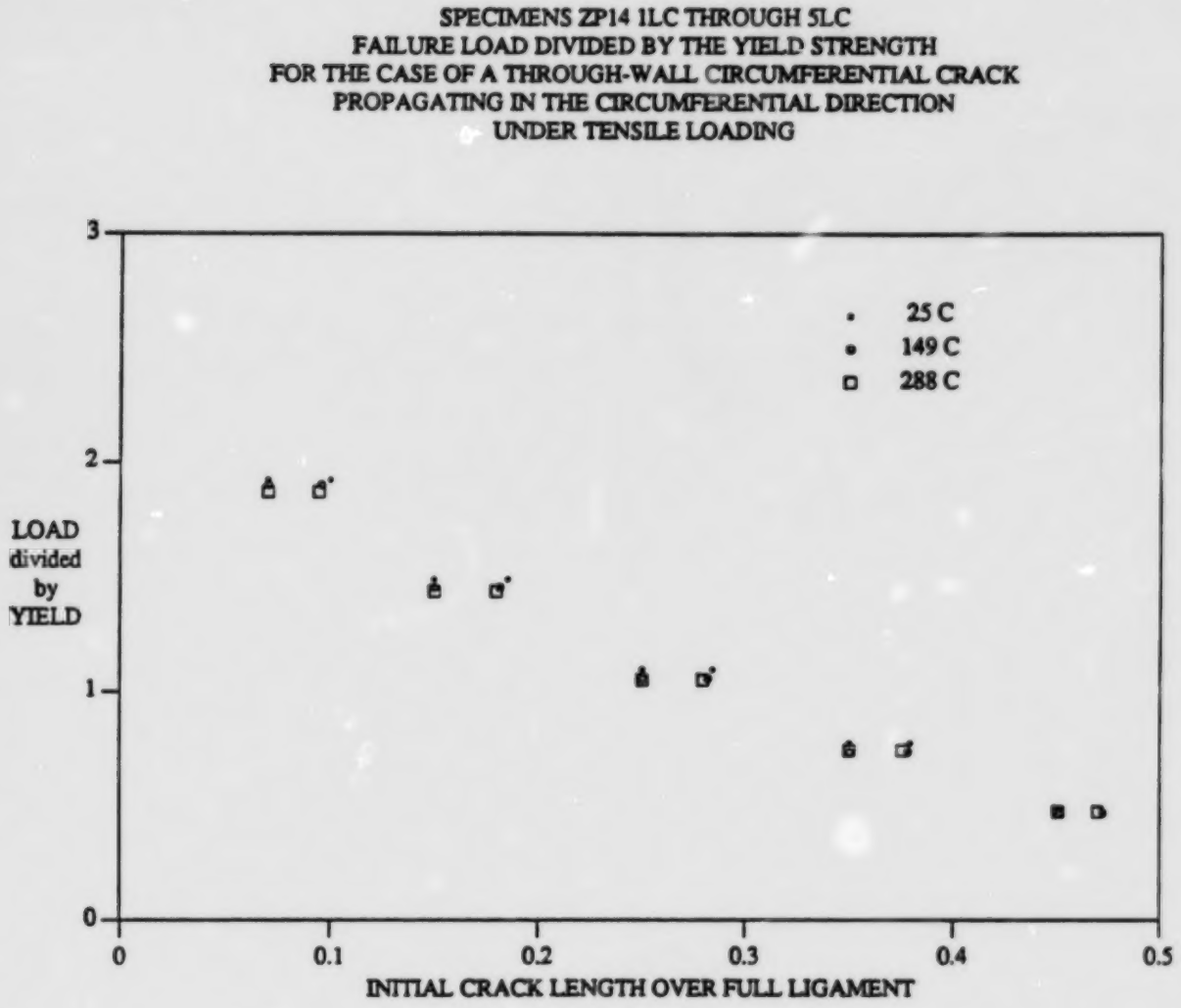

Figure 12(c): Normalised Loading as a Function of Crack Length for Data Set ZP14 (PIFRAC). Condition C.

Developed for a 24 inch diameter pipe of 2 inch wall thickness.

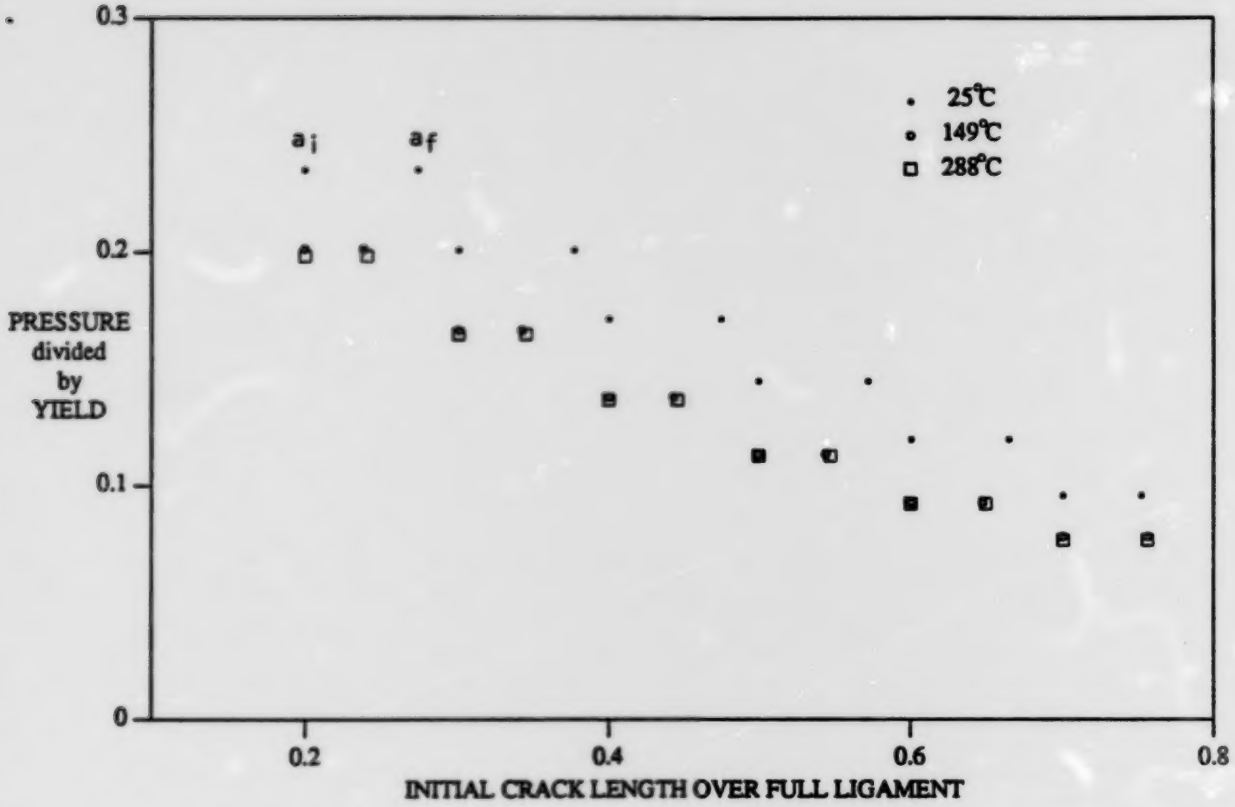

Figure 13(a): Normalised Loading as a Function of Crack Length for Data Set ZP15 (PIFRAC). Condition A.

Developed for a 24 inch diameter pipe of 2 inch wall thickness.

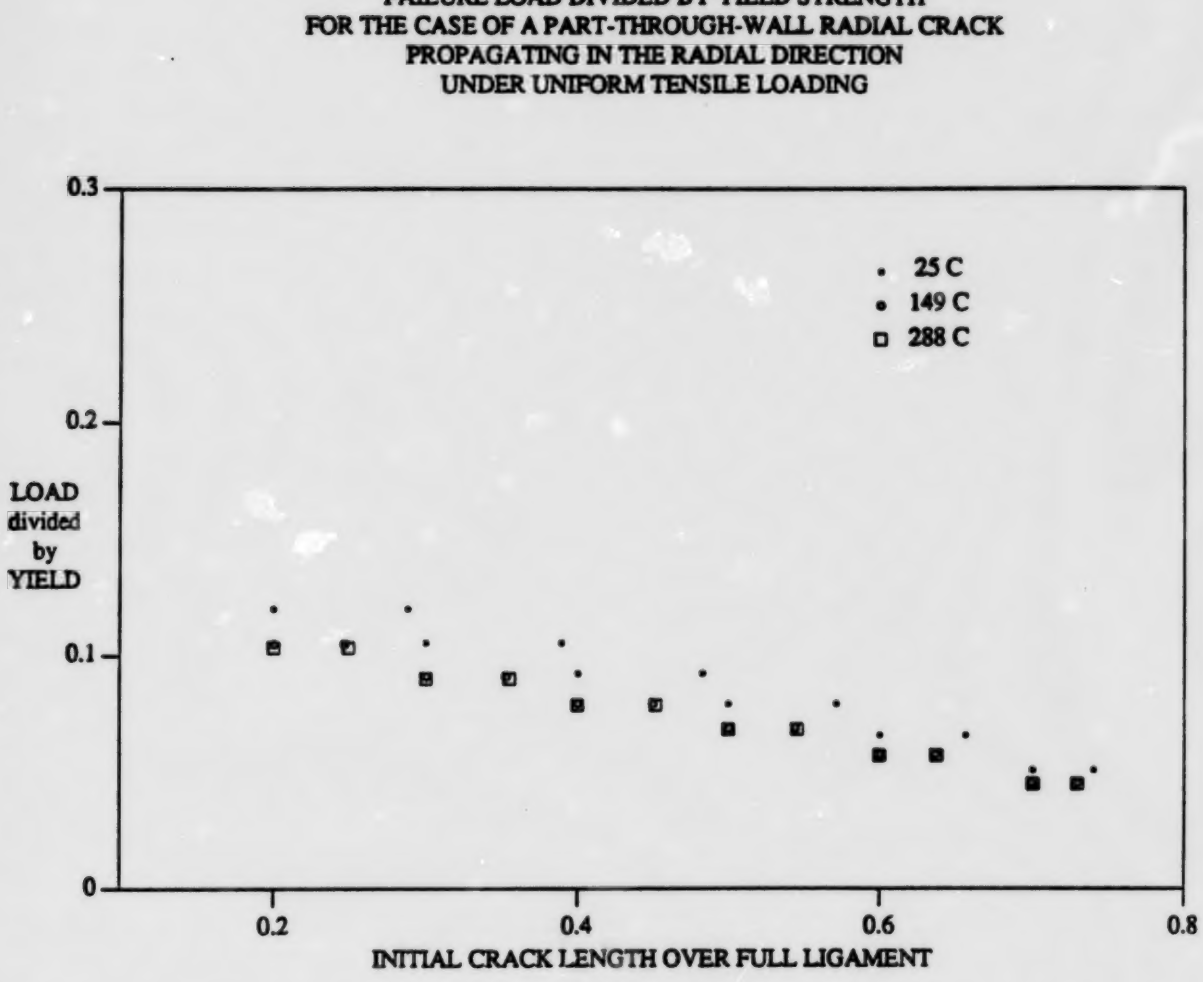

Figure 13(b): Normalised Loading as a Function of Crack Length for Data Set ZP15 (PIFRAC). Condition B.

Developed for a 24 inch diameter pipe of 2 inch wall thickness.

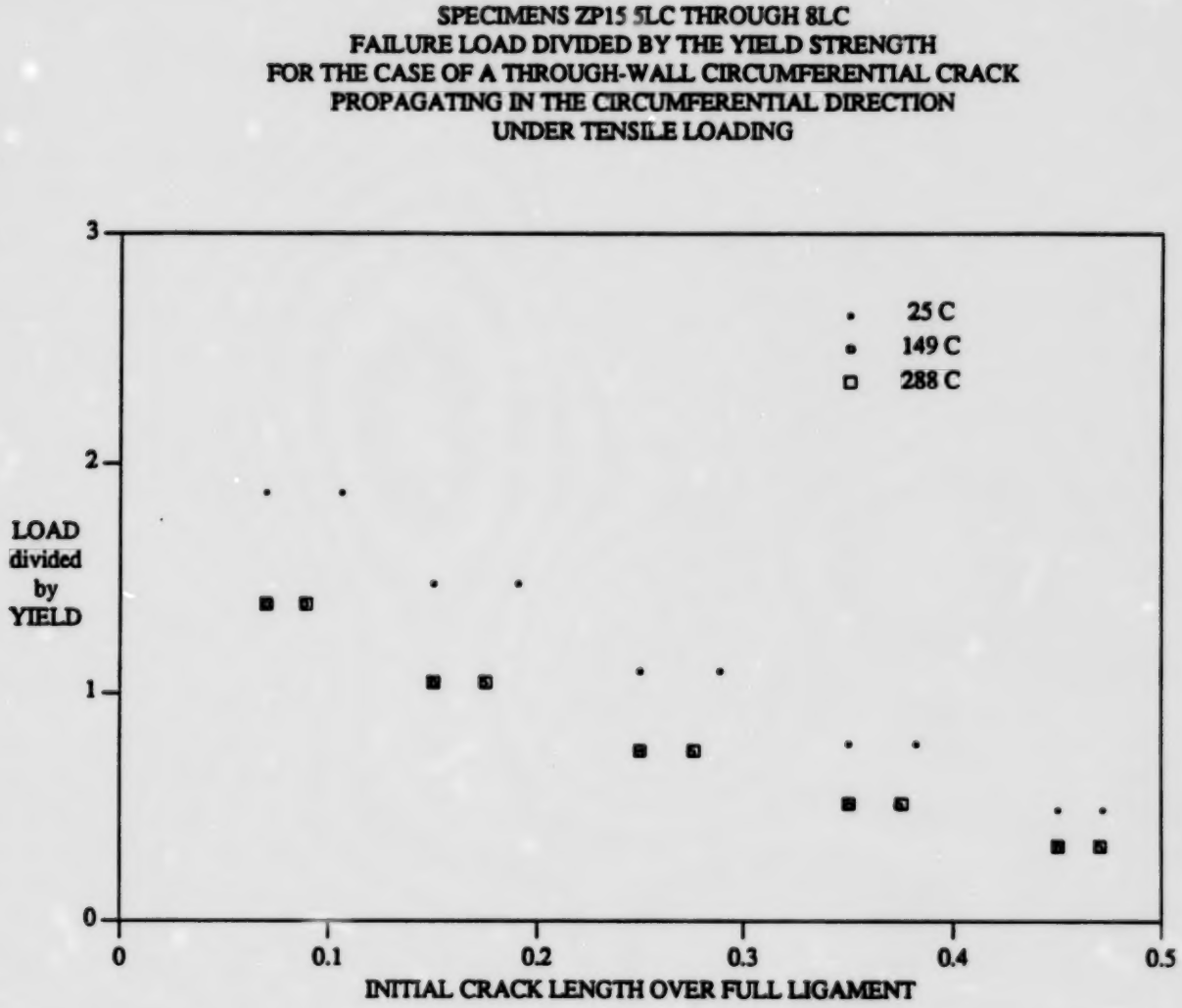

Figure 13(c): Normalised Loading as a Function of Crack Length for Data Set ZP15 (PIFRAC). Condition C.

Developed for a 24 inch diameter pipe of 2 inch wall thickness.

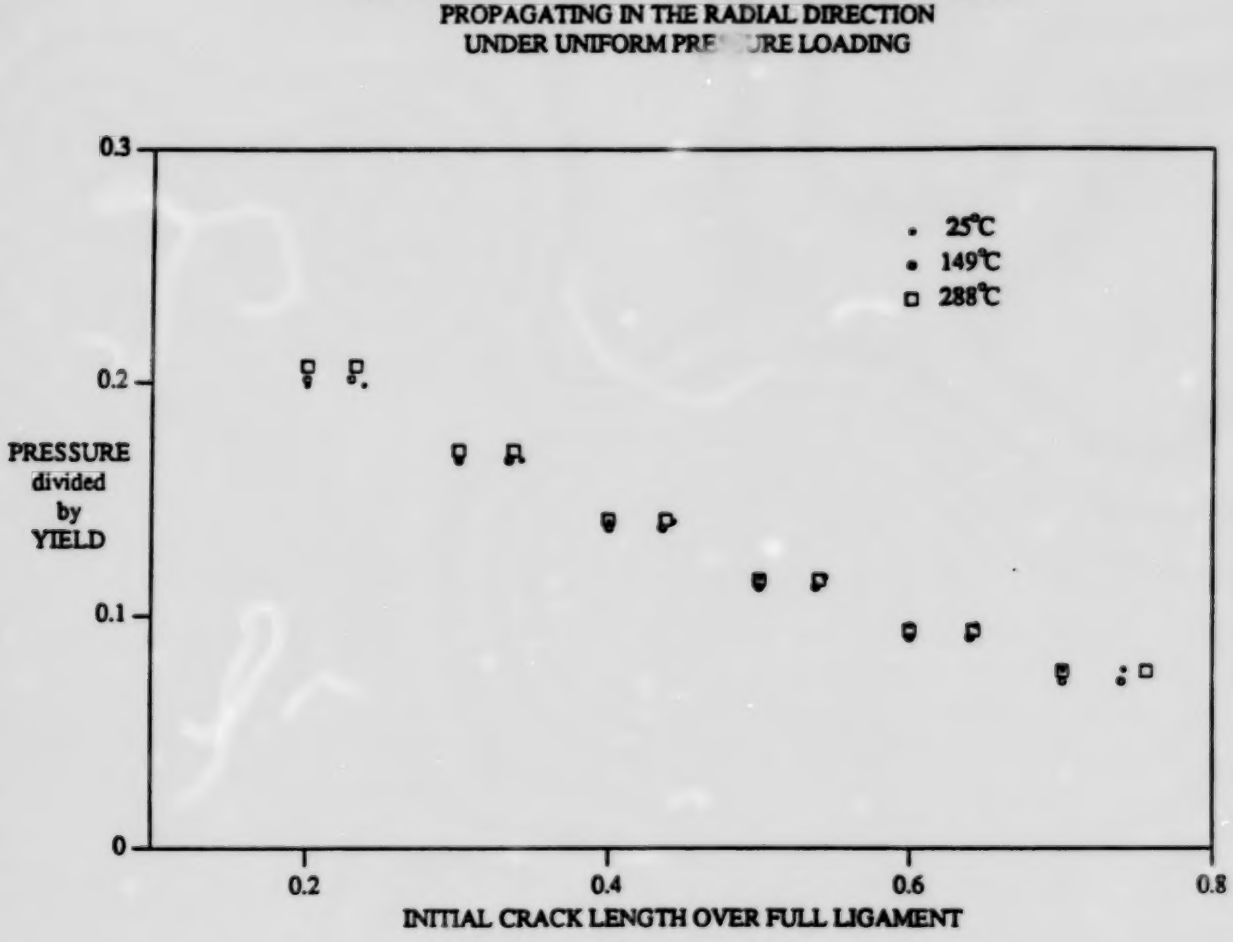

Figure 14(a): Normalised Loading as a Function of Crack Length for Data Set ZP14 C-L (PIFRAC). Condition A.

Developed for a 24 inch diameter pipe of 2 inch wall thickness.

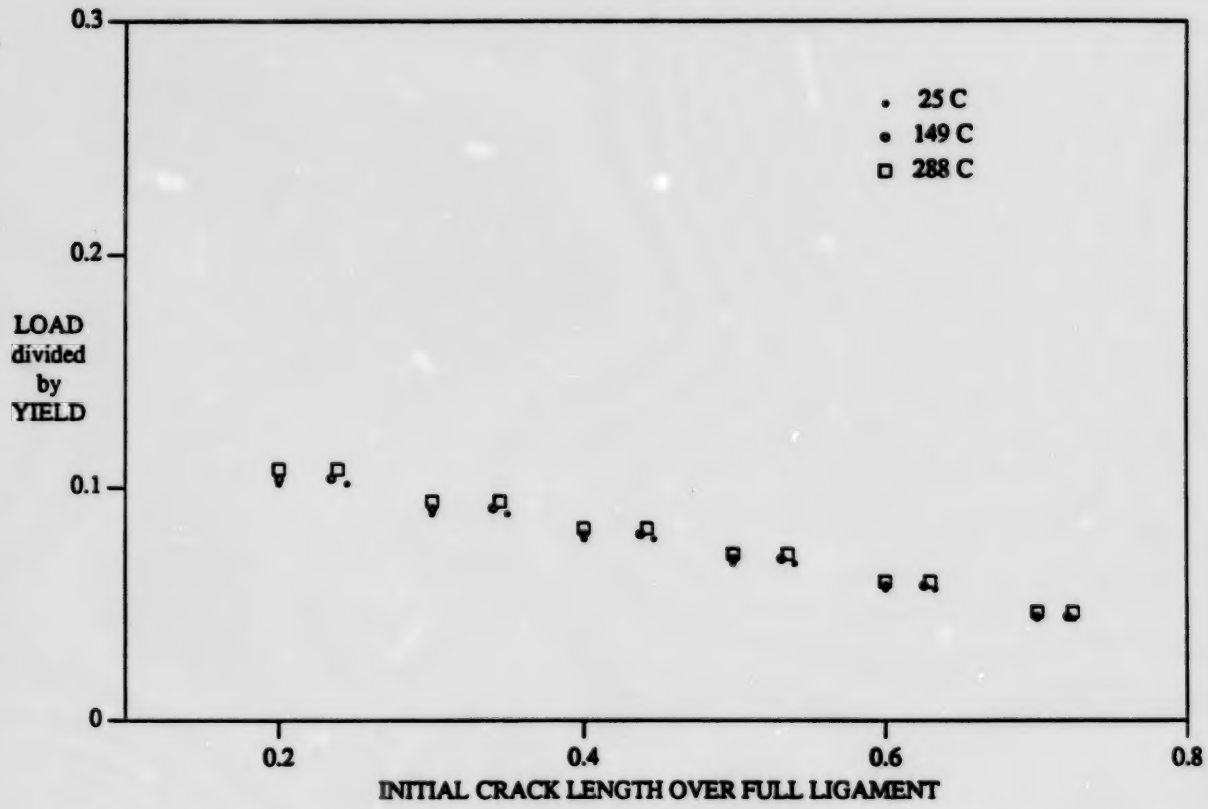

Figure 14(b): Normalised Loading as a Function of Crack Length for Data Set ZP14 C-L (PIFRAC). Condition B.

Developed for a 24 inch diameter pipe of 2 inch wall thickness.

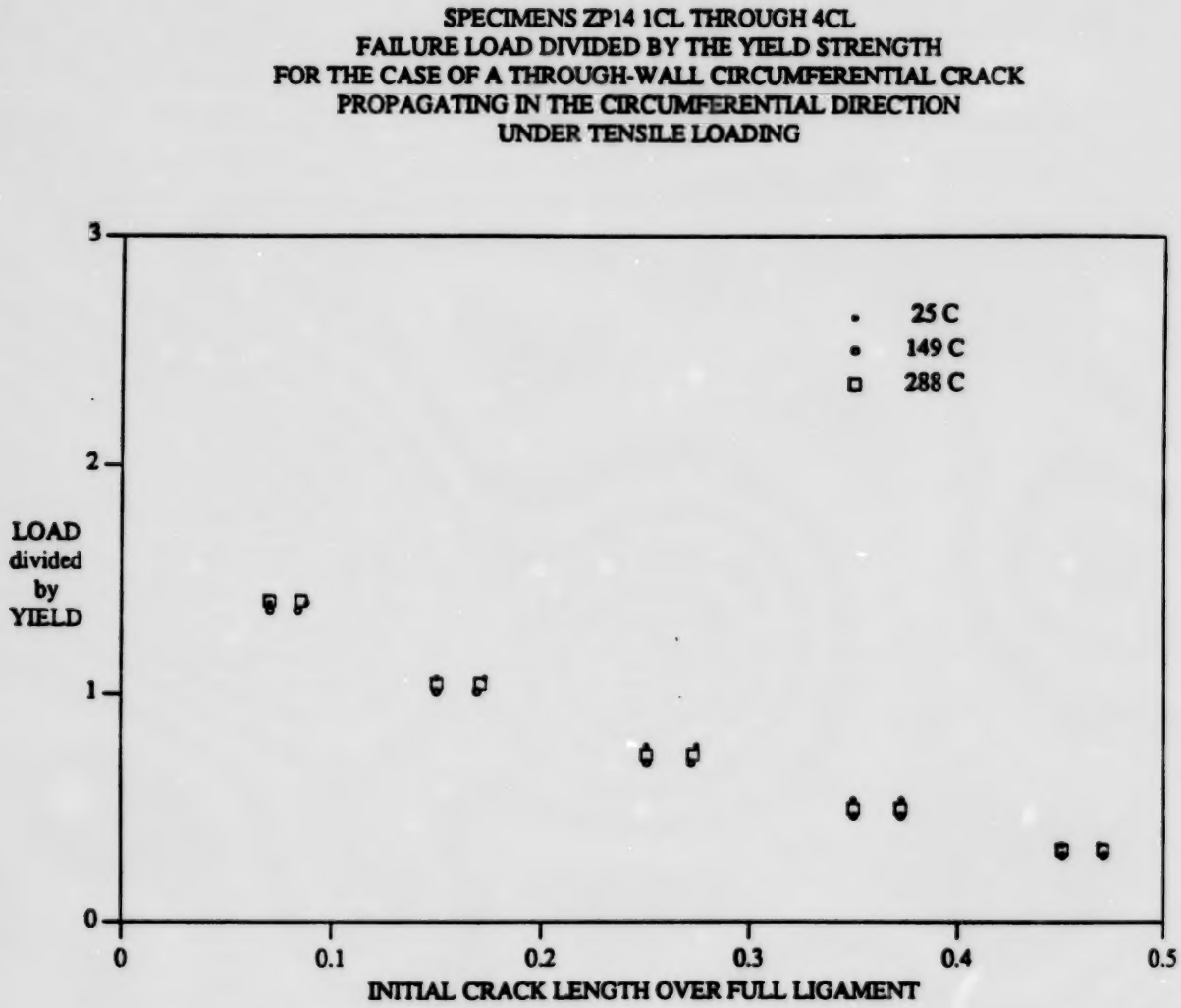

Figure 14(c): Normalised Loading as a Function of Crack Length for Data Set ZP14 C-L (PIFRAC). Condition C.

Developed for a 24 inch diameter pipe of 2 inch wall thickness.

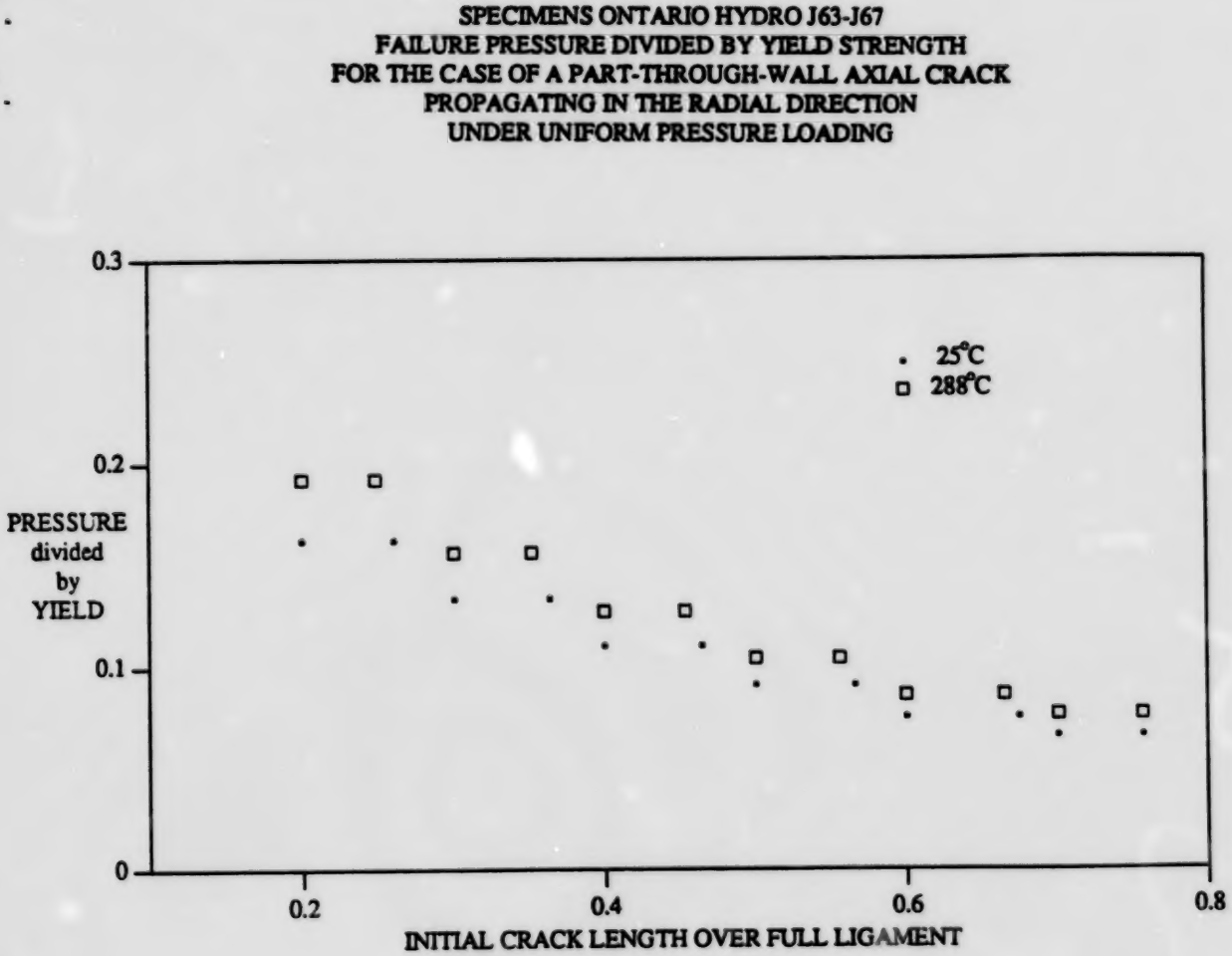

Figure 15(a): Normalised Loading as a Function of Crack Length for Data Set J63-J67 (Ontario Hydro). Condition A.

Developed for a 24 inch diameter pipe of 2 inch wall thickness.

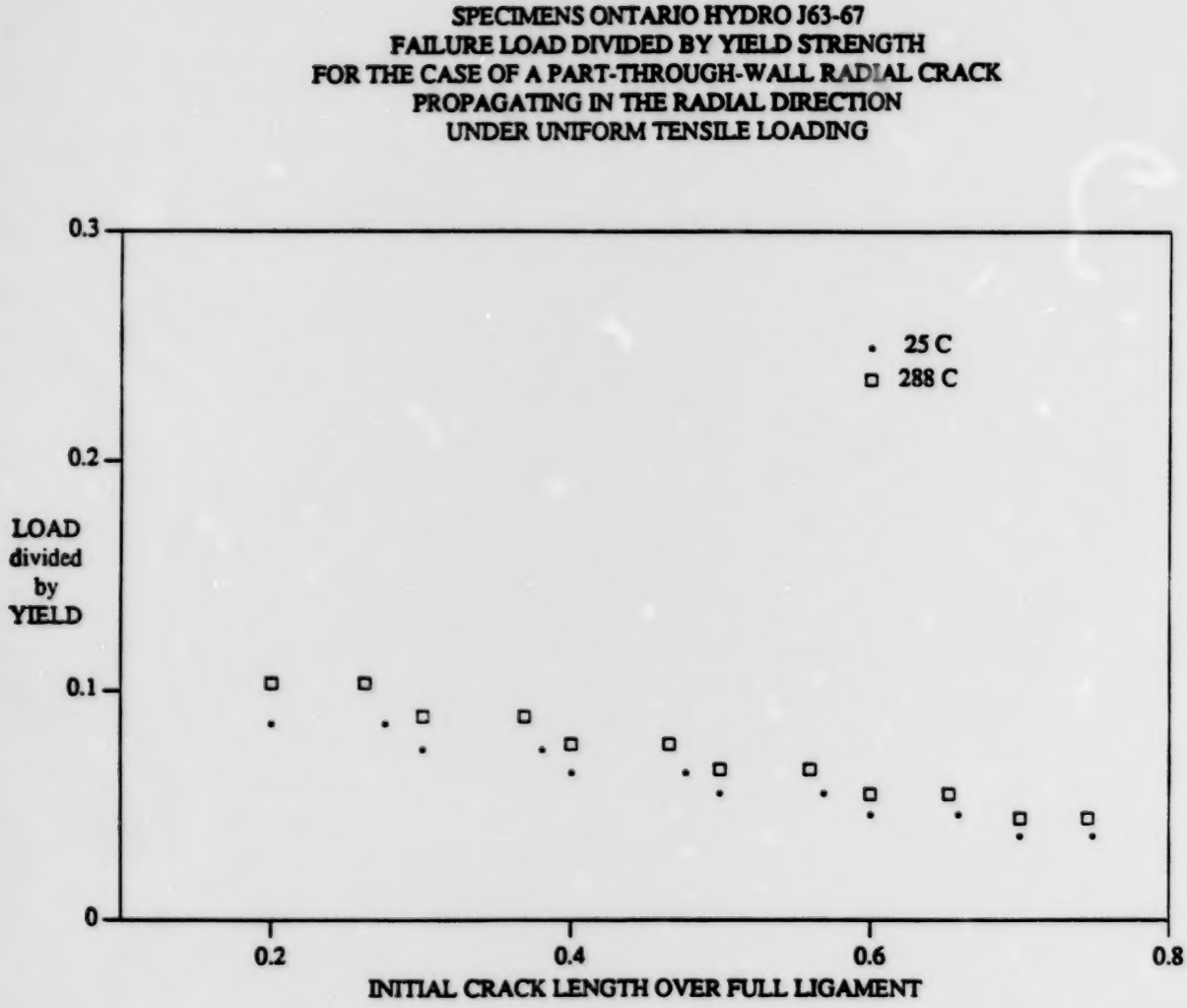

Figure 15(b): Normalised Loading as a Function of Crack Length for Data Set J63-J67 (Ontario Hydro). Condition B.

Developed for a 24 inch diameter pipe of 2 inch wall thickness.

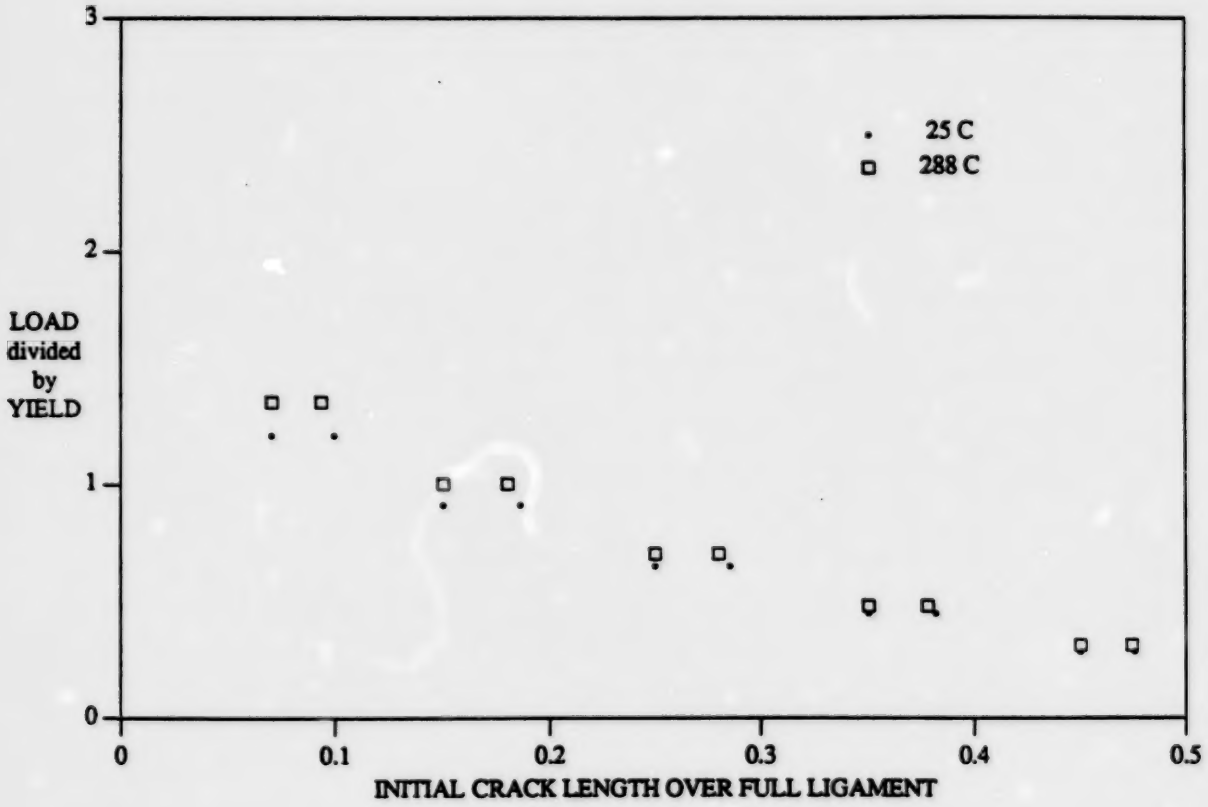

Figure 15(c): Normalised Loading as a Function of Crack Length for Data Set J63-J67 (Ontario Hydro). Condition C.

Developed for a 24 inch diameter pipe of 2 inch wall thickness.

E. ASSESSMENT OF RESULTS AND CONCLUSIONS

A detailed examination of all the results presented, either as individual curves in Appendices B, C and D or as composite curves in the text, will reveal conflicting trends which are extremely difficult to justify and put forward as clear conclusions. The prime reason for this difficulty is that fact that most data is incomplete and lacks key elements of information which if present could strengthen an argument or indeed consolidate a trend.

In spite of these inevitable short-comings, trends do occur, some of which are briefly summarized below:

i) It would appear that the J-R curve if developed for each of a range of temperatures would pass through a minimum value at a temperature value somewhere between 130°C and 250°C.

ii) All results confirm that a significant difference in the J-R curves exist for curves evaluated from test specimens with either L-C or C-L orientations. The J-R curve for the C-L orientation is always substantially lower than the resistance curve for the L-C orientation. The magnitude of this difference (between the L-C and C-L orientations) appears to be at its smallest for the particular temperature when the J-R curve is at its minimum value.

iii) It can be concluded from all data that a more conservative J-R curve will be obtained when the specimen has been side grooved. While this result follows from the increased constraint, it is not evident from the data that a clear minimum thickness specimen, which is side grooved, can be defined which will provide the limiting J-R curve for conservative prediction.

iv) An assessment of the various stress-strain curve results would indicate that while random scatter does exist, there is no consistent evidence to suggest that the stress-strain curves are dependent upon the longitudinal or circumferential orientation of the test specimen.

v) Selected results utilizing the engineering approach to elasto-plastic analyses have been presented. The software developed to investigate each of the three conditions, namely A, B and C is relatively straightforward and has been suitably configured to automatically determine the J driving curve corresponding to maximum crack extension for the particular loading and initial crack geometry. The results presented are useful indicators or estimates of the reduced load carrying capacity given the particular initial geometry and crack length, and as such can be numerically exploited to assess the extent of these changes as well as the 'crack growth' for fictitious J-R curves (for selected orientations) and or stress-strain data.

While it is useful to gain this insight it must be emphasized that this approach cannot easily be extended to a range of geometries and loading conditions, which will require investigation, without an extensive use of finite element programming to develop the catalogued data through tables and graphs to accommodate this engineering approach. For the present the approach has simply been demonstrated and will require further discussion to assess the merits of examining specific application cases to ascertain the type of J-R curve and stress-strain input necessary to generate useful information. The approach, for the three cases developed, is useful but cannot convey useful information on the dynamics of crack propagation.

REFERENCES

1. Venter, R.D., and Hoeppner, D.W. "Crack and Fracture Behaviour in Tough Ductile Materials", Atomic Energy Control Board Report, Ref. AECB INFO-0169, October, 1985.

2. Venter, R.D., Sinclair, A.N., McCammond, D. "Crack Propagation in Tough Ductile Materials (Phase I)", Atomic Energy Control Board Report, Ref. AECB INFO-0254-1, November, 1987.

3. Mukherjee, B. "Darlington Leak Before Break Material Test Program J-Resistance Curves" Ontario Hydro Research.

4. Kumar, V., German, M.D. and Shih, C.F. "An Engineering Approach for Elasto-Plastic Fracture Analysis", NP-1931, Research Project 1237-1, Topical Report, July 1981, prepared by General Electric Company, Corporate Research and Development, Schemectady, New York.

5. Kumar, V., German, M.D., Wilkening, W.W., Andrews, W.R., deLorenzi, H.G. and Mowbary, D.F. "Advances in Elasto-Plastic Fracture Analysis", NP-3607, Research Project 1237-1, Final Report, August 1984, prepared by General Electric Company, Corporate Research and Development, Schenectady, New York.

6. "Standard Test Method for Determining J-R Curves", ASTM, 12th Draft, July 25th, 1985, E24.08 Subcommittee.

APPENDIX A

PIFRAC DATA SHEETS

Tables A-1 and A-2 provide a listing of the data obtained from the PIFRAC data base. Table A-1 is a listing of the specimens identified as the ZP series for SA 106 Grade B 6" diameter pipe; Table A-2 is a miscellaneous set of data for both SA 106 grade B pipe of different diameters, SA 516 grade 70 of different pipe diameters as well 1" thick plate.

In April 1988, the experimental data on J-R curves obtained in the study "Crack Propagation in Tough Ductile Materials (Phase I)" and documented as AECB INFO-0254-1 was compiled and forwarded to Mr. Ken Pereira of AECB for inclusion in the PIFRAC data base. This correspondence is included in Appendix A together with a copy of the standard data format sheets required by the Piping Fracture Mechanics Data Base (PIFRAC).

PIPING FRACTURE MECHANICS DATA BASE (PIFRAC)

Ref.	Specimen ID	Stype	B	Temp °C	JIC	Flow	Ymod	Orient	Comments
1	ZP13-1CL	1	5.8	288	48.6	339.9	190.8	CL	
1	ZP13-1LC	1	5.8	149	402.5	341.3	198.7	LC	
1	ZP13-2CL	1	5.8	288	56.6	339.9	190.8	CL	SA 106 B
1	ZP13-2LC	1	5.8	149	331.4	341.3	198.7	LC	6" pipe
1	ZP13-3LC	1	5.8	288	454.6	339.9	190.8	LC	
1	ZP13-4LC	1	5.8	288	387.7	339.9	190.8	LC	
1	ZP13-7LC	1	5.8	288	274.2	339.9	190.8	LC	
1	ZP13-8LC	1	5.8	288	244.1	339.9	190.8	LC	
2	ZP15-1CL	1	9.1	288	54.2	470.2	190.8	CL	
2	ZP15-1LC	1	9.1	149	122.6	468.0	198.7	LC	
2	ZP15-2CL	1	9.1	288	59.7	470.2	190.8	CL	
2	ZP15-2LC	1	9.1	149	133.8	468.0	198.7	LC	
2	ZP15-3CL	1	9.1	24	96.7	416.4	205.8	CL	SA 106 B
2	ZP15-3LC	1	9.1	288	125.4	470.2	190.8	LC	6" pipe
2	ZP15-4CL	1	9.1	149	60.0	468.0	198.7	CL	
2	ZP15-4LC	1	9.1	288	125.6	470.2	190.8	LC	
2	ZP15-5LC	1	9.1	288	104.2	470.2	190.8	LC	
2	ZP15-6LC	1	9.1	288	110.5	470.2	190.8	LC	
2	ZP15-7LC	1	9.1	24	336.0	416.4	205.8	LC	
2	ZP15-8LC	1	9.1	149	112.4	468.0	198.7	LC	
16	ZP14-1CL	1	17.8	25	81.3	393.6	205.8	CL	
16	ZP14-1LC	1	15.2	25	417.9	398.2	205.8	LC	
16	ZP14-1LC (SG)	1	17.8	25	270.1	398.2	205.8	LC	
16	ZP14-2CL	1	17.8	149	53.1	391.1	198.7	CL	
16	ZP14-2LC	1	15.2	149	161.7	393.1	198.7	LC	
16	ZP14-2LC (SG)	1	17.8	149	108.9	393.1	198.7	LC	
16	ZP14-3CL	1	17.8	288	64.9	411.4	190.8	CL	SA 106 B
16	ZP14-3LC	1	15.2	288	322.1	414.0	190.8	LC	6" pipe
16	ZP14-3LC (SG)	1	17.8	288	183.2	414.0	190.8	LC	
16	ZP14-4CL	1	17.8	288	78.3	411.4	190.8	CL	
16	ZP14-4LC	1	15.2	149	136.2	393.1	198.7	LC	
16	ZP14-4LC (SG)	1	17.8	288	197.4	414.0	190.8	LC	
16	ZP14-5CL	1	17.8	343	92.4	386.7	187.6	CL	
16	ZP14-5LC	1	15.2	288	245.7	414.0	190.8	LC	
16	ZP14-6LC	1	17.8	25	193.4	398.2	205.8	LC	
16	ZP14-7LC	1	17.8	149	89.2	393.1	198.7	LC	

Table A-1: Base Data from PIFRAC for ZP Series

Note: The SG designation refers to the specimen being side grooved when two specimens have the same identification

Ref.	Specimen ID	Stype	B	Temp °C	JIC	Flow	Ymod	Orient	Comments
23	EPCS-1	1	10.0	52	116.1	416.8	204.2		
23	EPCS-2	1	10.0	23	103.3	416.8	205.9		SA 106 B
23	EPCS-3	1	10.0	23	105.0	416.8	205.9		6" pipe
23	EPCS-4	1	10.0	23	92.5	416.8	205.9		
24	106B-F1T1	1	10.0	23	75.5	416.8	205.9		SA 106 B
24	106B-F1T2	1	10.0	23	82.2	416.8	205.9		6" pipe
24	106B-F2T	1	10.0	57	51.3	416.8	204.0		flattened
25	106B-FS1T1	1	10.0	23	76.9	416.8	205.9		SA 106 B
25	106B-FS1T2	1	10.0	23	70.0	416.8	205.8		6" pipe
25	106B-FS2T	1	10.0	57	62.4	416.8	204.0		flattened
51	F13-17	1	9.0	149	91.0	474.7	198.7	LC	SA 106 B
51	F13-18	1	9.0	149	137.0	474.7	198.7	LC	16" pipe
51	F13-19	1	9.0	288	1750.0	436.8	190.8	LC	
51	F13-20	1	9.0	288	138.0	436.8	190.8	LC	
53	F29-17	1	21.0	288	111.0	423.7	190.8	LC	SA 106 B
53	F29-18	1	21.0	288	149.0	423.7	190.8	LC	16" pipe
53	F29-19	1	21.0	149	116.0	427.5	198.7	LC	
53	F29-20	1	21.0	149	52.0	427.5	198.7	LC	
56	F34-17	1	25.0	288	97.0	355.8	190.8	LR	
56	F34-18	1	25.0	288	125.0	355.8	190.8	LR	SA 516 70
56	F34-19	1	25.0	288	179.0	355.8	190.8	LC	37" pipe
56	F34-20	1	25.0	288	190.0	355.8	190.8	LC	
56	F34-21	1	25.0	149	307.0	344.0	198.7	LC	
56	F34-22	1	25.0	149	290.0	344.0	198.7	LC	
57	F40-37	1	25.0	288	287.0	392.0	190.8	LT	
57	F40-38	1	25.0	288	228.0	392.0	190.8	LT	SA 516 70
57	F40-39	1	25.0	288	480.0	392.0	190.8	LT	plate 1"
57	F40-40	1	25.0	288	557.0	392.0	190.8	LT	
57	F40-41	1	25.0	288	789.0	392.0	190.8	LT	
60	F45-18	1	12.0	149	153.0	476.4	198.7	LC	SA 106 B
60	F45-20	1	12.0	149	203.0	476.4	198.7	LC	10" pipe
61	B1	1	66.0	288	190.4	362.2	190.8	LC	SA 516 70
61	B2	1	66.0	288	96.7	362.2	190.8	LC	37" pipe

Table A-2: Base Data from PIFRAC for Various Experimental Sets

University of Toronto -A4-
Department of
Mechanical Engineering

5 King's College Road
Toronto, Ontario, Canada
M5S 1A4

April 25, 1988

Mr. Ken Pereira
Atomic Energy Control Board
270 Albert Street
Ottawa, Ontario
K1P 5S9

Dear Mr. Pereira:

Subject: DSS File No. 38ST.870-55-5-4149

I enclose herewith the PIFRAC data sheets on the SA 106B pipe steel tests. A floppy disk with the experimental data is also enclosed which might be useful in assembling this data. As you will note, there are a sizeable number of questions for which we do not have answers – simply because these tests were not done, i.e. impact, K_{IC} etc.

I have also included Ken Gilbert's name and telephone number should there be any queries on the data compilation.

Yours sincerely,

Professor R.D. Venter
Chairman of Mechanical Engineering

RDV:jf

Enclosure

Re: PIFRAC Data Sheets Enclosed

The following package includes PIFRAC data format sheets. These sheet are presented in two sections, an "Equipment and Procedures" section with the applicable questions answered, and a "Results" section that answers questions 450-475, 480-495, 650, 652, 657 and 658. All results presented are for SA-106 Grade B pipe. In reference to the PIFRAC data sheets the following should be noted:

1 All equations used to calculate J and crack length are as specified in the tentative ASTM standard, "Standard Test Method For Determining J–R Curves", 12th Draft, 25 July 1985, E24.08 Subcommittee Ballot.

2 Questions 80 through 97 are answered based on the average results of four tensile specimens, two from the C-L orientation and two from the L-C orientation. Within experimental variation, there was no detectable difference in the tensile properties for the two orientations tested.

3 No impact tests were conducted, consequently questions 100 through 137 are unanswered.

4 No K_{IC} tests were conducted, consequently questions 140 through 220 are unanswered.

5 All deflections were measured directly, consequently questions 264 through 283 are unanswered.

6 All tests were conducted at room temperature, consequently questions 290 through 296 are unanswered.

7 Questions 330-356, 670-678, and 690-693 are unanswered because the compliance method was used to determine crack length for all tests.

8 Only C(T) tests were undertaken in SA-106 Grade B pipe steel, consequently questions 480-530 and 710-717 are unanswered.

9 Experimental J–R curves were also generated for ASTM 516 Grade 70 plate steel. These results could follow if they are required.

10 A floppy disc containing the data files presented in the results section is supplied. Each file contains five columns of data corresponding to questions 650, 652, 656, 657, and 658 respectively.

Please direct any inquiries about the enclosed directly to:

Mr. Kenneth Gilbert

Dept. of Mechanical Engineering

University of Toronto

5 King's Collage Rd.

Toronto, Ontario

CANADA

Phone 416-978-6853

PIFRAC DATA SHEETS

EQUIPMENT AND PROCEDURES

PIPING FRACTURE MECHANICS DATA BASE (PIFRAC)

DATA FORMAT SHEETS

A. Reference Information

(1) **Title** Crack Propagation in Tough Ductile Materials (Phase I)

(2) **Author(s)** R.D. Venter, A.N. Sinclair and D. McCammond

(3) **Author(s) Affiliation(s)**

Department of Mechanical Engineering, University of Toronto

5 King's College Road, Toronto, Ontario M5S 1A4

(4) **Reference** N/A

(5) **Sponsoring Agency** Atomic Energy Control Board

(6) **Contract Number** DSS File No. 38ST.87055-5-4149

(7) **Date** April 25, 1988

(8) **Remarks**

B. Material Identification

(20) Material Type Carbon steel

(21) Specification ASTM SA 106 Grade B

(22) Product Form 24" OD pipe with a wall thickness of - -

(23) Manufacturer unknown

(24) Heat Number unknown

Composition (Wt. %)

(25) C		(36) Al	
(26) Mn		(37) Co	
(27) P		(38) W	
(28) S		(39) As	
(29) Si		(40) Sn	
(30) Ni		(41) Zr	
(31) Cr		(42) Nb	
(32) Mo		(43) Sb	
(33) Cu		(44) Zn	
(34) V		(45) N	
(35) Ti			

(46) Analysis Code NA

L = Ladle analysis from heat
P = Analysis from product

(47) Thermo-mechanical Processing History unknown

(48) ASTM Grain Size unknown

(49) % Ferrite for Stainless Steel unknown

(50) Location Thru Thickness NA

(51) Hardness/Scale NA

B. Materials Identification (Continued)

Physical Properties

(52) Young's Modulus (GPA)	(53) Poisson's Ratio	(54) Temperature(C)	(55) How was E Determined? See Note Below	(56) How was μ Determined? See Note Below

(55) ASTM E 111 = 1
ASTM E 231 = 2
Other = 3 (Specify)

(56) ASTM E 132 = 1
Other = 2 (Specify)

B.1 Mechanical Properties

Specimen Description

(70) Cross-section shape Circular

(71) Rectangular - (T x W) ____ x ____ (mm)

(72) Circular - (D) 6.35 (mm)

(73) Curved Rectangular (T x W x R curvature) ____ x ____ x ____ (mm)

(74) Specimen Design Code 2

1 = Consistent with ASTM E-8
2 = Other than E-8 designs

(75) If Design Code = 2, Then Describe Design (include drawing)

consistent with E-8 except the length of reduced section "A" was 2" not 1.25".

(76) Additional Thermo-mechanical Processing NA

(77) ASTM Grain Size unknown

(78) Location Thru Thickness ____

(79) Hardness/Scale unknown /

PIFRAC-5

MECHANICAL PROPERTY RESULTS

(80) Specimen Number	(81) Orientation	(82) Specimen Location Thru-Thickness	Strain Rate (min^{-1}) (83) Pre-Yield	(84) Post-Yield	(85) Gage Length (mm)	(86) Irradiation Fluence Level (n/cm^2)> 1MeV	(87) Test Temp (C)	(88) Yield Strength (MPa)	(89) Analysis Code *	(91) UTS (MPa)	(92) Percent Reduction in Area	(93) Percent Elongation	Ramberg-Osgood Coeffs. (95) $\alpha, n, \epsilon_o, \sigma_o$	True σ-ε Values (96) True σ (MPa)	(97) True ε
average of 4	C-L/L-C	center	NA	NA	25.4	N.I	20	288	1	600	NA	24	NA	NA	NA
* see cover page															

* ANALYSIS CODE Describes Method for Determining Yield Strength,
  - = 1 for 0.2% Offset
  - = 2 for 0.5% Total
  - = 3 for Other Criteria

(94) Analysis Method for Determining True σ-True ε data

(94) If Analysis Code = 3, Then Describe Analysis Method

B.2 Impact Test Results NA

(100) Test Type _____ (C_V, DWTT, DT, NDT)

(101) Additional Thermo-mechanical Processing _____

_____

_____

(102) ASTM Grain Size _____

(103) Location Thru Thickness _____

(104) Hardness/Scale _____/_____

Specimen Details

(105) W (mm) _____

(106) B (mm) _____

(107) L (mm) _____

For C_V, DWTT and DT, Complete the Following:

(108) Notch Depth (mm) _____

(109) Notch Angle (Degrees) _____

(110) Notch Root Radius (mm) _____

For NDT Tests, Complete the Following:

(111) Weld Electrode _____

(112) Weld Procedure Description _____

_____

(113) Notch Width (mm) _____

(114) Weld Thickness Above Specimen (mm) _____

(115) Weld Length (mm) _____

(116) Te[illegible] Machine Capacity _____ Joules

PRAC-7

RESULT[illegible] R C_V, DWTT AND DT TESTS

(119) Specimen Type See Note)	(120) Specimen No.	(121) Orientation	(122) Location Thru Thickness	(123) Irradiation Fluence Level (n/cm^2) > 1 MeV	(124) Test Temp (C)	(125) Absorbed Energy (J)	(126) Lateral Expansion (mm)	(127) Percent Shear Area	(128) Hammer Velocity (m/sec)

(119) C_v = 1 DWTT = 2 DT = 3

RESULTS FOR NDT TESTS

PIFRAC-8

(130) Specimen No.	(131) Orientation	(132) Location Thru Thickness	(133) Irradiation Fluence Level (n/cm^2) > 1 MeV	(134) Hammer Velocity at Impact (m/sec)	(135) Hammer Weight (kg)	(136) Test Temperature (C)	(137) Results (B,NB,NT)*

* B = Break, NB = No-Break, NT = No Test

NA

B.3 K_{Ic} Tests

B.3.1 K_{Ic} Test System Description

(140) Test System Description _____

_____

_____

_____

(141) Control Mode _____

Load Measurement

(142) Load Cell Capacity (KN) _____

(143) Sensitivity for Range Used (KN/Volt) _____

Deflection Measurement

(145) Measurement Code _____

1 = Specimen Load Line Only
2 = Specimen Crack Mouth Only
3 = Specimen + Fixture

(146) If Measurement Code = 3, Describe Method Used to Correct For Fixture Deflection

_____

_____

_____

(147) Transducer Type (Clip Gage = CG; LVDT = LV) _____

(148) Deflection Range (mm) _____

(149) Sensitivity (mm/Volt) _____

(150) Linearity (% of Range) _____%

B.3.2 K_{Ic} Test Specimen Description and Test Results

B.3.2.1 Specimen Description

(151) Additional Thermo-Mechanical Processing _____

_____

_____

(152) ASTM Grain Size _____

(153) Location Thru Thickness _____

(154) Hardness/Scale _____ / _____

(155) Specimen Type Code _____

CT = 1
3 pt. Bend = 2
Other = 3

(156) For Specimen Type Code = 3, Describe Specimen and Include Drawing _____

_____

_____

_____

B.3.2.2 Specimen Details For CT Specimens

(157) Specimen Number _____

(158) Specimen Design Code _____

E-399 CT = 1
E-813 CT = 2
Other = 3

(159) For Design Code = 3, Describe Specimen and Include Drawing

_____

_____

Dimensions

(160) B (mm) _____

(161) W (mm) _____

(162) H (mm) _____

(163) Total Side Groove Depth (mm) _____

(164) Describe Clip Gage Attachment (Example: Machined knife edges)

_____

_____

(165) Distance Between Load Line and Clip Gage Attachment (mm) _____

(167) Distance Between Razor Blade Edges (mm) _____

For Other CT Specimen Designs

(168) Describe Deflection Measurement Scheme (Example: Clip gage mounted on razors on load line.)

_____

_____

B.3.2.3 Specimen Details For 3-Pt. Bend Bars

(170) Specimen Number _____

(171) Specimen Design Code _____

E-399 Bend Bar = 1
E-813 Bend Bar = 2
Other = 3

(172) For Design Code = 3, Describe Specimen and Include Drawing

_____

_____

Dimensions

(173) B (mm) _____

(174) W (mm) _____

(175) H (mm) _____

(177) Total Side Groove Depth (mm) _____

(178) Describe Attachment Scheme (Example: Machined knife edges)

_____

_____

_____

(179) Offset Distance Between Attachment Points and Specimen Face (mm) _____

B.3.2.4 Specimen Details For Other Than CT and Bend Bars

(180) Specimen Number _____

(181) Describe Specimen and Include Drawing _____

_____

_____

_____

_____

Dimensions *

	Symbol	Units	Value
(182)	_____	_____	_____
(183)	_____	_____	_____
(184)	_____	_____	_____
(185)	_____	_____	_____
(186)	_____	_____	_____
(187)	_____	_____	_____
(188)	_____	_____	_____
(189)	_____	_____	_____
(190)	_____	_____	_____
(191)	_____	_____	_____
(192)	_____	_____	_____
(193)	_____	_____	_____
(194)	_____	_____	_____
(195)	_____	_____	_____
(196)	_____	_____	_____

* 15 Records Are Provided For Listing Pertinent Dimensions. Relate Symbols To Symbols Used in Analysis Section.

(197) Describe Deflection Measurement Scheme _____

_____

_____

_____

_____

Additional Specimen Data *

(198) _____

(199) _____

(200) _____

(201) _____

(202) _____

(203) _____

(204) _____

(205) _____

(206) _____

* These Records Are Provided For Listing Additional Specimen Data Pertinent To Analysis of the Test Results. Relate Symbols Used Here To Symbols Used in the Analysis Section.

B.3.3 K_{Ic} Test Results Summary

(210) Test Temperature _____ (C)

(211) Irradiation Fluence Level ($n/cm^2 > 1$ MeV) _____

(212) K_{Ic} (MPA$\sqrt{m}$) _____

(213) ASTM E 399 Valid? _____

(214) Load at Failure (kN) _____

(215) Yield Stress at Temperature (MPa) _____

(216) Flow Stress at Temperature (MPa) _____

(217) Young's Modulus at Temperature (GPa) _____

(218) Optically Measured Initial a_o _____ (mm)

(219) Testing Rate _____

(220) Testing Rate Units _____

C. J-R Test System Description

(250) Test System Description 250 kN servohydraulic frame, M.T.S model 312.31 serial 1249

(251) Control Mode load control

Load Measurement

(252) Load Cell Capacity (kN) 250

(253) Sensitivity for Range Used (kN/Volt) (12.52 kN/volt) (4.99 kN/volt) and (2.5 kN/volt)

Deflection Measurement (For Load-Deflection Data)

(255) Measurement Code 1

1 = Specimen Load Line Only
2 = Specimen + Fixture

(256) If Measurement Code = 2, Describe Method Used to Correct For Fixture Deflection

(257) Transducer Type (Clip Gage = CG; LVDT = LV) CG

(258) Deflection Range (mm) 4 mm

(259) Sensitivity (mm/Volt) 0.4 mm/volt

(260) Linearity (% of Range) 0.05 %

(261) Accuracy ± 0.002 (mm)

(262) Precision ± 0.001 (mm)

(263) Calibration Procedure linear regression on 36 points from two passes up and two passes down

LIST ALL OF THE EQUATIONS AND PROCEDURES USED TO CORRECT THE MEASURED DEFLECTIONS TO GIVE THE DESIRED DEFLECTION VALUES USED TO COMPUTE J.

(264) Equation all deflections were measured directly

(265) Discussion of Equation and Purpose

(266) Equation

(267) Discussion of Equation and Purpose

(268) Equation

(269) Discussion of Equation and Purpose

(270) Equation

(271) Discussion of Equation and Purpose

(272) Equation _____

_____

_____

(273) Discussion of Equation and Purpose _____

_____

_____

_____

(274) Equation _____

_____

_____

(275) Discussion of Equation and Purpose _____

_____

_____

_____

(276) Equation _____

_____

_____

(277) Discussion of Equation and Purpose _____

_____

_____

_____

(278) Equation _____

_____

_____

(279) Discussion of Equation and Purpose _____

_____

_____

_____

(281) Discussion of Equation and Purpose _____

(282) Equation _____

(283) Discussion of Equation and Purpose _____

Temperature Control and Measurement

(290) Heating Method Code _____

1 = Oven
2 = Heat Tape
3 = RF Induction
4 = Other

(291) If Method Code = 4, Describe Heating Method _____

(292) Measurement Accuracy ± _____ (C)

(293) Measurement Precision ± _____ (C)

(294) Specimen Temperature Control Accuracy ± _____ (C)

(295) How Determined? _____

(296) Describe Quality Assurance Relating to Temperature Uniformity

C.1 Crack Length Measurement (Single Specimen Tests Only)

(300) Technique Code * 1

1 = Compliance
2 = DC Potential Drop
3 = AC Potential Drop
4 = Other

(301) If Technique Code = 4, Describe Crack Length Measurement Technique _____

(302) Accuracy (after any post-test correction) ± 0.1 (mm)

(303) Precision ± 0.05 (mm)

(304) If Data Were Post-Test Corrected, Describe Correction Procedure

* If more than one technique was used on a test and data from the other technique(s) are being reported, complete additional forms and modify specimen number appropriately.

C.1.1 Details of Compliance Technique

(310) Is Technique Based on Load Line Deflection or Other Deflection? (LL or O) LL

(311) If Other, Describe Attachment Scheme Including Drawings

(312) Transducer Type Code 1

1 = Strain Gaged Clip Gage
2 = LVDT
3 = Capacitance Clip Gage
4 = Other

(313) If Transducer Type = 4, Describe Transducer

(314) Range (mm) 4.0

(315) Sensitivity (mm/Volt) ~ 0.4

(316) Linearity (% of Range) 0.05

(317) Accuracy ± 0.002 (mm)

(318) Precision ± 0.001 (mm)

(319) Deflection to Voltage Calibration Procedure linear regression w. 36 points from two passes up and [illegible]

(320) Calibration Temperature 20 (C)

(321) Is Your Technique Manual or Automated? (M or A) A

(322) Describe Test Procedure Conduct 4 pre-test unloads to check system operation and determine initial crack length. Then unloads at even spacing of ΔP until crack begins to propagate then decrease the size of ΔP.

(323) For Manual Techniques, Describe Method For Determining Un-load Trace Slope From Autographic Record

(324) Equation Relating Measured Parameters to Crack Length

$U = 1/[(B_e E C_i)^{1/2} + 1]$

$a_i/w = 1.00196 - 4.06317 U + 11.242 \cdot U^2 - 106.043 \cdot U^3 + 464.335 \cdot U^4 - 650.677 U^5$

$B_e = B - (B - B_N)^2 / B$

(325) Procedure For Determining Any Calibration Coefficients

(326) Calibration Temperature _____ (C)

(327) Range of Validity _____ $\leq a/w \leq$ _____

(328) Describe Procedure for Including or Excluding Relaxation Phenomenon

NA

C.1.2 Details of AC and DC Potential Drop Techniques

(330) Is Specimen Electrically Isolated From Test Machine? _____

(331) If Yes, Is Specimen Isolated at the Loading Pins or In the Load Train? (P or LT) _____

(332) Describe Current Input Locations (Include Drawing)

_____

_____

_____

(333) Describe Potential Measurement Locations (Include Drawing)

_____

_____

_____

(334) Describe Measurement Procedure _____

_____

_____

(335) Power Supply Stability ± _____ (A)

(336) Voltmeter Sensitivity _____ (Volts)

(337) Equation Relating Measured Parameters To Crack Length

_____

_____

_____

(338) Procedure For Determining Any Calibration Coefficients

_____

_____

_____

_____

(339) Calibration Temperature _____ (C)

(340) Range of Validity _____ $\leq$ a/w $\leq$ _____

C.1.3 Details of Techniques Other Than Compliance or Potential Drop

(350) Equation Relating Measured Parameters To Crack Length

(351) Procedure For Determining Any Calibration Coefficients

(352) Calibration Temperature _____ (C)

(353) Range of Validity _____ $\leq$ a/w $\leq$ _____

C.2 J-R Test Data Analysis Description

(400) Describe Procedure For Computing Area Under Load - Corrected Load Point Deflection Curve

$A_{pl(i)} = A_{pl(i-1)} + [P_i + P_{i-1}][\delta_{pl(i)} - \delta_{pl(i-1)}] / 2$

$\delta_{pl(i)} = \delta_i - (P_i C_i)$

$C_i = (\Delta\delta / \Delta P)_i$

(401) Equation for Computing J $J = J_{el} + J_{pl}$

$J_{el(i)} = (K_{(i)})^2 (1-\nu^2) / E$ $\quad K_{(i)} = [P_i / (B B_N W)^{1/2}] \cdot f(a_i/W)$

$f(a_i/W) = (2+a_i/W)(0.336 + 4.64(a_i/W) - 13.32(a_i/W)^2 + 14.72(a_i/W)^3 - 5.6(a_i/W)^4) / (1-a_i/W)^{3/2}$

$J_{pl(i)} = \{J_{pl(i-1)}[1 - \frac{\gamma_{i-1}}{b_{i-1}}(\frac{a_i - a_{i-1}}{2})] + [\frac{\eta_i P_i}{b_i} + \frac{\eta_{i-1} P_{i-1}}{b_{i-1}}][\frac{\delta_{pl\,i} - \delta_{pl(i-1)}}{2 B_N}]\} \times$

$\{1/[1 + \frac{\gamma_i}{b_i}(a_i - a_{i-1})]\}$ $\quad \eta_i = 2 + 0.522(b_i/W)$ $\quad \gamma_i = 1.76(b_i/W)$

(402) Definition of Parameters *

b_i = incremental $W - a_i$ $\quad$ W specimen width

P = Load $\quad$ B gross specimen thickness

B_N = net specimen thickness

$\delta_{pl(i)}$ is as above in (400)

* For Specimens Other Than CT and Bend Bars, Relate These Parameters to the Parameter List in Records 502 Thru 530.

D. J-R Test Specimen Description and Test Results

D.1 Specimen Description

This sheet duplicated and compleled for each specimen. See results section.

(450) Additional Thermo-Mechanical Processing _____

_____

_____

(451) ASTM Grain Size _____

(452) Location Thru Thickness _____

(453) Hardness/Scale _____ / _____

(454) Test Type Code _____

Multiple Specimen = 1 *
Single Specimen = 2

(455) Specimen Type Code _____

CT = 1
3 pt. Bend = 2
Other = 3

(456) For Specimen Type Code = 3, Describe Specimen and Include Drawing _____

_____

_____

_____

* For Multiple Specimen Tests, Complete the Specimen Detail Sheets For Each Specimen.

D.1.1 Specimen Details For CT Specimens

This sheet duplicated and completed for each specimen.

(460) Specimen Number _____

(461) Specimen Design Code _____

E-399 CT = 1
E-813 CT = 2
Other = 3

(462) For Design Code = 3, Describe Specimen and Include Drawing

_____

_____

Dimensions

(463) B (mm) _____

(464) W (mm) _____

(465) H (mm) _____

(466) Notch Depth (mm) _____

(467) Notch Height, N (mm) _____

(468) Notch Root Angle (Degrees) _____

(469) Notch Root Radius (mm) _____

(470) Total Side Groove Depth (mm) _____

(471) Side Groove Angle (Degrees) _____

(472) Side Groove Root Radius (mm) _____

(473) Describe Clip Gage Attachment _____

_____

_____

(474) Distance Between Load Line and Clip Gage Attachment (mm) _____

(475) Distance Between Attachment Edges (Gage Length) (mm) _____

For Other CT Specimen Designs

(478) Describe Deflection Measurement Scheme _____

_____

_____

(479) Equation Relating Measured Deflection to Load Line Deflections

_____

_____

114

D.1.2 Specimen Details For 3-Pt. Bend Bars

(480) Specimen Number _____

(481) Specimen Design Code _____

E-399 Bend Bar = 1
E-813 Bend Bar = 2
Other = 3

(482) For Design Code = 3, Describe Specimen and Include Drawing

_____

_____

Dimensions

(483) B (mm) _____

(484) W (mm) _____

(485) H (mm) _____

(486) Notch Depth (mm) _____

(487) Notch Height, N (mm) _____

(488) Notch Root Angle (Degrees) _____

(489) Notch Root Radius (mm) _____

(490) Total Side Groove Depth (mm) _____

(491) Side Groove Angle (Degrees) _____

(492) Side Groove Root Radius (mm) _____

(493) If a Clip Gage Was Attached Across the Crack Mouth, Describe Attachment Scheme _____

_____

(494) Offset Distance Between Attachment Points and Specimen Face (mm) _____

(495) Distance Between Attachment Edges (Gage Length) (mm) _____

D.1.3 Specimen Details For Other Than CT and Bend Bars N/A

(500) Specimen Number _____

(501) Describe Specimen and Include Drawing _____

_____

_____

_____

_____

Dimensions *

	Symbol	Units	Value
(502)			
(503)			
(504)			
(505)			
(506)			
(507)			
(508)			
(509)			
(510)			
(511)			
(512)			
(513)			
(514)			
(515)			
(516)			

* 15 Records Are Provided For Listing Pertinent Dimensions. Relate Symbols To Symbols Used in Analysis Section.

(520) Describe Deflection Measurement Scheme _____

(521) Equation Relating Measured Deflection To Deflection Used In Calculating J _____

Additional Specimen Data *

(522) _____

(523) _____

(524) _____

(525) _____

(526) _____

(527) _____

(528) _____

(529) _____

(530) _____

* These Records Are Provided For Listing Additional Specimen Data Pertinent To Analysis of the Test Results. Relate Symbols Used Here To Symbols Used in the Analysis Section.

D.4 RAW DATA FROM POTENTIAL DROP TESTS

(670) Load (kN)	(671) Un-corrected Deflection (mm)	(672) Corrected Deflection (mm)	(673) Total Area (J)	(674) Measured Potential (V)	(675) Computed "a" (mm)	(676) Post-Test Corrected "a" (mm)	(677) J (kJ/m^2)	(678) Corrected Δa (mm)

(690) Load (kN)	(691) Un-corrected Deflection (mm)	(692) Corrected Deflection (mm)	(693) Total Area (J)

D.6 RAW DATA FROM SPECIMENS OTHER THAN CT AND BEND BARS

(710) Load Used In Computing J (kN)	(711) Deflection Used In Computing J (mm)	(712) Total Area (J)	(713) Parameter Used In Computing "a"	(714) Computed "a" (mm)	(715) Post-Test Corrected "a" (mm)	(716) J (kJ/m^2)	(717) Corrected Δa (mm)

Drawing 1

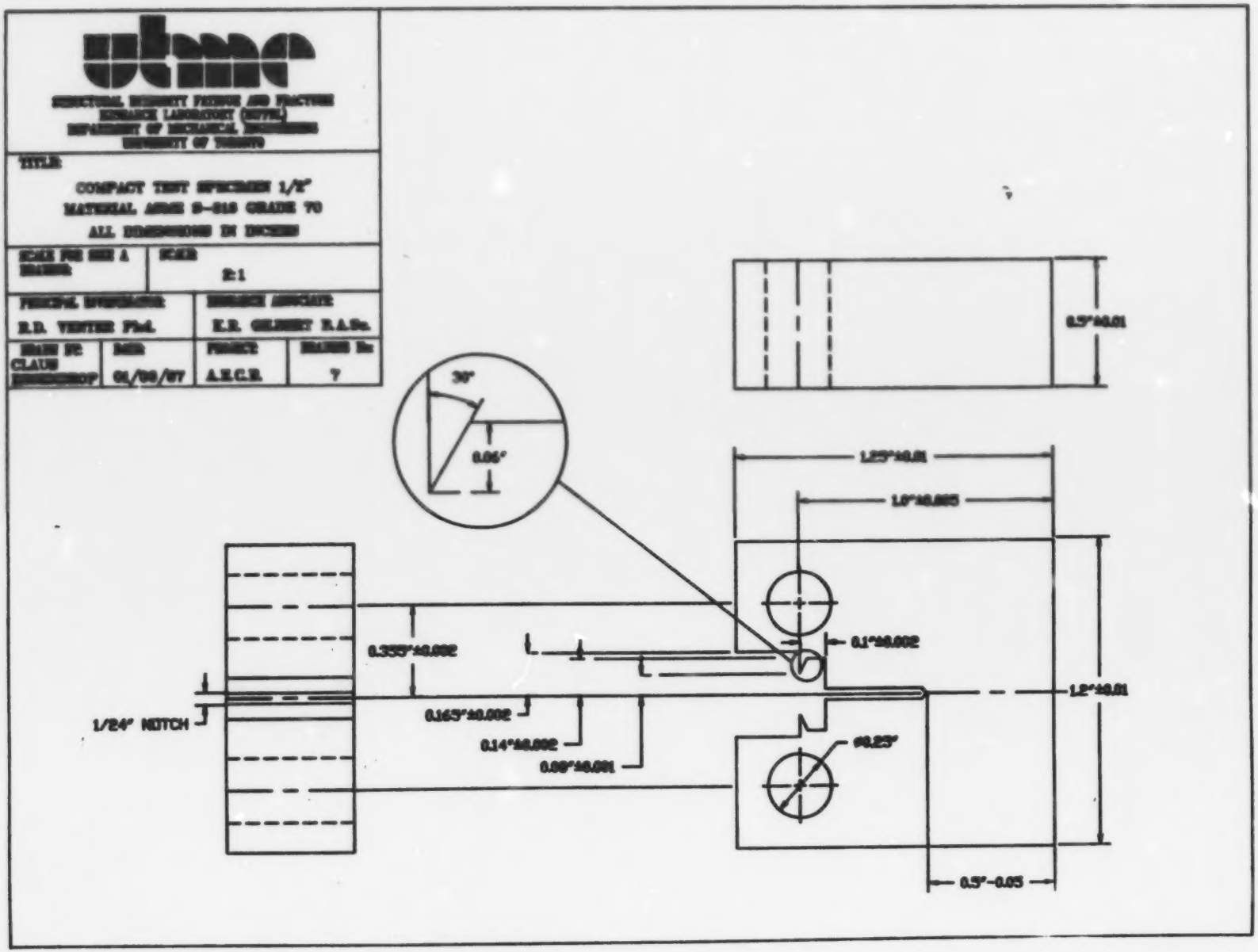
utme
COMPACT TEST SPECIMEN 1/2"
ALL DIMENSIONS IN INCHES
SCALE
2:1
DRAWN BY
CLAUS
DATE
01/20/97
PROJECT
A.E.C.B.
DRAWING No.
7
30°
0.06"
0.5"±0.01
1.225"±0.01
1.0"±0.005
0.355"±0.002
0.1"±0.002
1.2"±0.01
1/24" NOTCH
0.165"±0.002
0.14"±0.002
0.09"±0.001
Ø0.25"
0.5"-0.05

Drawing 2

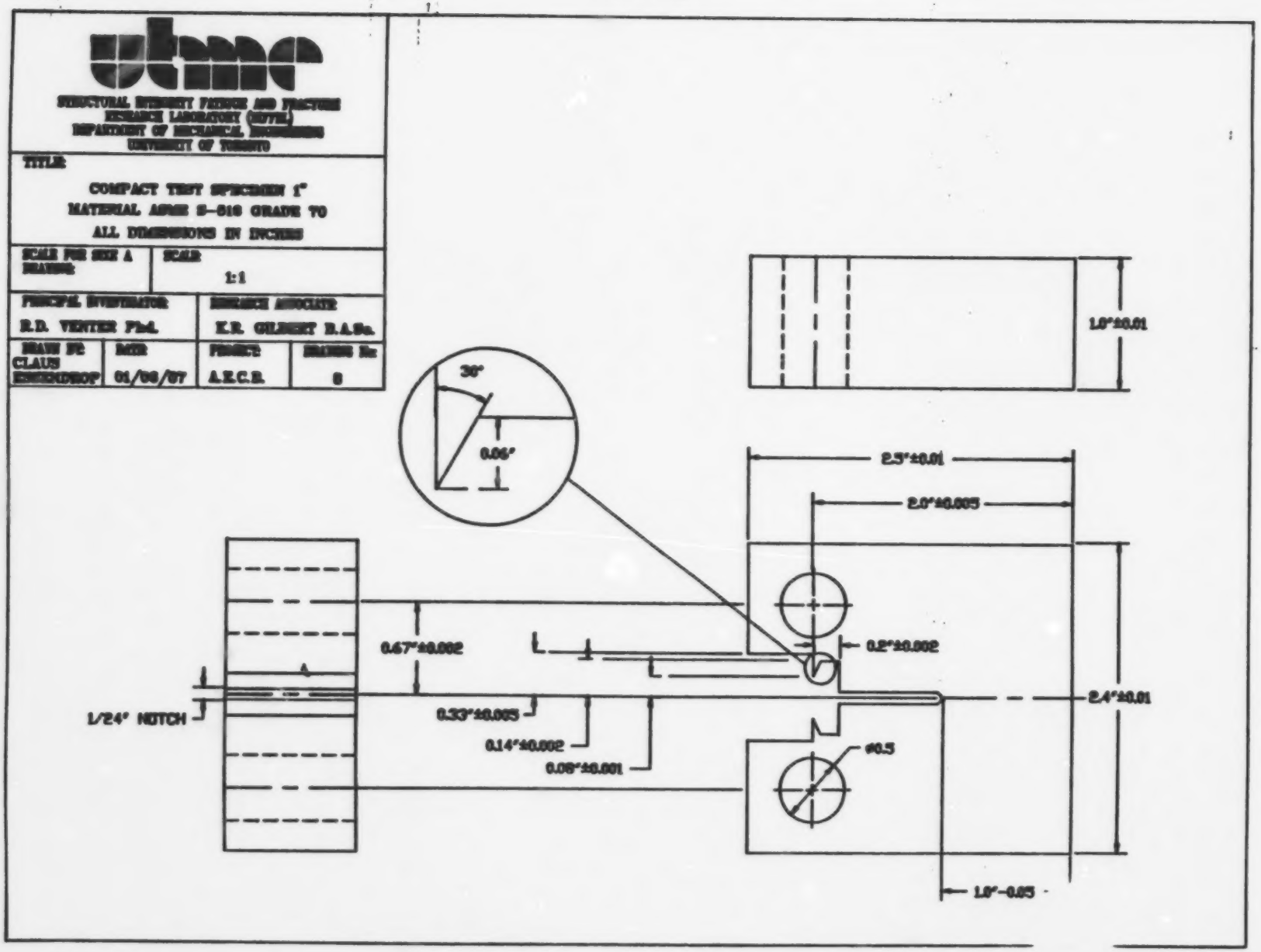
STRUCTURAL INTEGRITY FATIGUE AND FRACTURE RESEARCH LABORATORY (SIFFRL)
DEPARTMENT OF MECHANICAL ENGINEERING
UNIVERSITY OF TORONTO
TITLE:
COMPACT TEST SPECIMEN 1"
MATERIAL ASME S-510 GRADE 70
ALL DIMENSIONS IN INCHES
SCALE FOR SIZE A DRAWING:
SCALE
1:1
PRINCIPAL INVESTIGATOR:
R.D. VENTER P.Eng.
RESEARCH ASSOCIATE:
K.R. GILBERT B.A.Sc.
DRAWN BY:
CLAUS EISENHOFER
DATE:
01/08/07
PROJECT:
A.E.C.B.
DRAWING No:
8
30°
0.05"
1.0"±0.01
2.5"±0.01
2.0"±0.005
0.67"±0.002
0.2"±0.002
2.4"±0.01
1/24" NOTCH
0.33"±0.005
0.14"±0.002
0.08"±0.001
#0.5
1.0"-0.05

Drawing 3

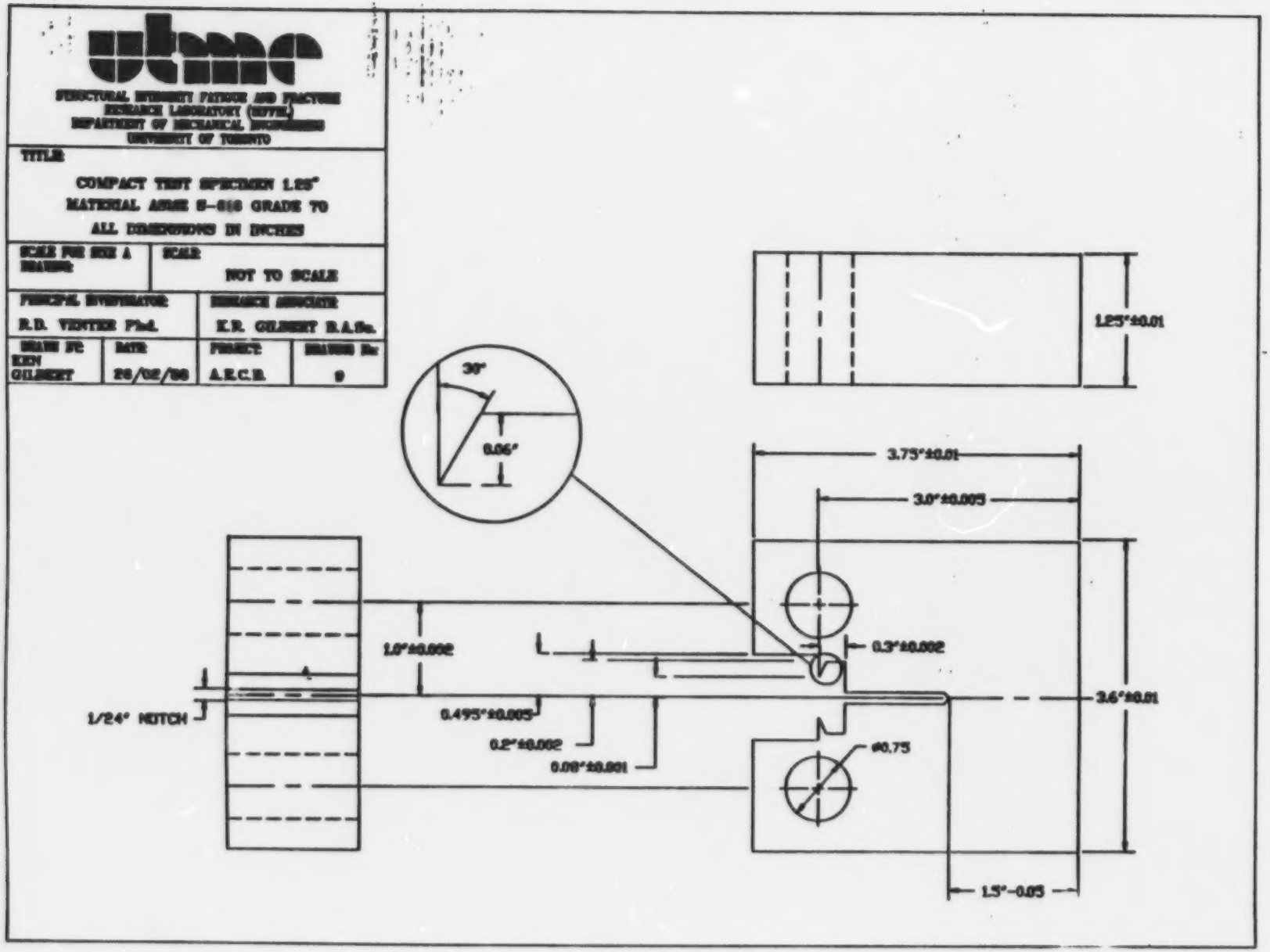
STRUCTURAL INTEGRITY FATIGUE AND FRACTURE RESEARCH LABORATORY (SIFFRL)
DEPARTMENT OF MECHANICAL ENGINEERING
UNIVERSITY OF TORONTO
TITLE:
COMPACT TEST SPECIMEN 1.25"
MATERIAL ASME S-616 GRADE 70
ALL DIMENSIONS IN INCHES
SCALE FOR SIZE A DRAWING
SCALE
NOT TO SCALE
PRINCIPAL INVESTIGATOR:
R.D. VENTER P.Eng.
RESEARCH ASSOCIATE:
K.R. GILBERT B.A.Sc.
DRAWN BY:
KEN GILBERT
DATE:
26/02/98
PROJECT:
A.R.C.B.
DRAWING No:
9
30°
0.06"
1.25"±0.01
3.75"±0.01
3.0"±0.005
1.0"±0.002
0.3"±0.002
3.6"±0.01
1/24" NOTCH
0.495"±0.005
0.2"±0.002
0.08"±0.001
ø0.75
1.5"-0.05

APPENDIX B

TABULATION OF DATA AND GRAPHICAL RESULTS

A considerable amount of data, both tabular and graphical, has been developed from the PIFRAC data which requires inclusion in this report. This data is presented in this Appendix and is referred to in the text.

SPECIMEN DATA FROM PIFRAC FOR SA-106 GRADE B TESTS

Tables B-1 and B-2 provide a listing of the ZP series of test results available from PIFRAC. The J–R exponent and constant when fitted to the curve $J=H(\Delta a)^n$ are provided together with the hardening exponent and alpha constant (see equation B-1) for the Ramburg-Osgood characterization of the material.

The specimen identification includes the orientation L–C or C–L respectively and the temperature at which the test was carried out.

A. The J–R curves for a series of results for each of a like series of tests (thickness, orientation) are presented. These results have been developed for some of the data sets presented in Tables B-1 and B-2. Each curve or set of curves, where the tests were undertaken at different temperatures, is accompanied by tabulated data which correlates with the test data listed in Tables B-1 and B-2. The data points are plotted for each of the test results at the temperatures identified; a 'best fit', J–R curve has been superimposed on these data points and the relevant constants determined. These constants are provided in Tables B-1 and B-2. Furthermore, it should be noted that a standard range for J (0-1000 kJ/m^2) and crack length (0-10 mm) has been used to permit direct comparison of the results.

Summary

Figure B-1	ZP.13	C-L	orientation,	5.8 mm
Figure B-2	ZP.13	L-C	orientation,	5.8 mm
Figure B-3	ZP.14	C-L	orientation,	17.8 mm
Figure B-4	ZP.14	L-C	orientation,	15.2 mm
Figure B-5	ZP.14	L-C	orientation,	17.8 mm
Figure B-6	ZP.15	C-L	orientation,	9.1 mm
Figure B-7	ZP.15	L-C	orientation,	9.1 mm

B. The stress-strain curves for the ZP-13 ZP-14 and ZP-15 data base tests are provided in Figures B-8, B-9 and B-10 respectively for each of the temperatures at which a test was undertaken. The range of both true stress and true strain has also been standardized to permit a direct comparison of these results.

C. Table B-3 provides a listing of all test data other than the ZP series of tests identified in Tables B-1 and B-2. This miscellaneous data base is sketchy at best; stress-strain data is not available for all tests. The J–R data developed for each of these test data sets are provided in Figures B-11 to B-17 together with the limited stress-strain data in Figures B-18 to B-20.

Specimen Data For SA-106 Grade B Tests
J-R and Ramburg-Osgood Constants for ZP Data

Specimen ID	Temp. Deg. C	*J–R* Exponent	*J–R* Constant	Hardening Exponent	Alpha Constant	E GPa
zp13-1cl	288	0.342	88.92	NA	NA	190.8
zp13-2cl	288	"	"	"	"	"
zp13-1lc	149	0.479	377.24	5.262	3.19	198.7
zp13-2lc	"	"	"	"	"	"
zp13-3lc	288	0.559	425.49	4.865	1.38	190.8
zp13-4lc	"	"	"	"	"	"
zp13-7lc	288	0.413	304.05	"	"	190.8
zp13-8lc	"	"	"	"	"	"
zp14-1cl	25	0.373	147.09	5.529	1.44	205.8
zp14-2cl	149	0.275	82.52	5.523	0.71	198.7
zp14-3cl	288	0.298	106.70	4.972	0.86	190.8
zp14-4cl	"	"	"	"	"	"
zp14-5cl	343	0.301	119.74	6.042	0.45	187.6
zp14-1lc	25	0.602	507.87	4.967	1.75	205.8
zp14-2lc	149	0.509	250.66	4.787	0.85	198.7
zp14-4lc	"	"	"	"	"	"
zp14-3lc	288	0.491	409.22	4.798	1.41	190.8
zp14-5lc	"	"	"	"	"	"

Table B-1

Specimen Data For SA-106 Grade B Tests
J-R and Ramburg-Osgood Constants for ZP Data

Specimen ID	Temp. Deg. C	*J–R* Exponent	*J–R* Constant	Hardening Exponent	Alpha Constant	E GPa
zp14-1lc(sg)	25	0.461	361.20	4.967	1.75	205.8
zp14-6lc	"	"	"	"	"	"
zp14-2lc(sg)	149	0.360	160.76	4.787	0.85	198.7
zp14-7lc	"	"	"	"	"	"
zp14-3lc(sg)	288	0.362	272.29	4.798	1.41	190.8
zp14-4lc(sg)	"	"	"	"	"	"
zp15-1cl	288	0.313	377.24	NA	NA	190.8
zp15-2cl	"	"	"	"	"	"
zp15-3cl	25	0.395	150.23	6.186	2.04	205.8
zp15-4cl	149	0.278	87.62	NA	NA	198.7
zp15-1lc	149	0.486	217.48	4.606	1.52	198.7
zp15-2lc	"	"	"	"	"	"
zp15-3lc	288	0.408	214.51	4.830	1.44	190.8
zp15-4lc	"	"	"	"	"	"
zp15-5lc	"	0.379	183.69	"	"	"
zp15-6lc	"	"	"	"	"	"
zp15-7lc	25	0.757	504.37	5.730	2.03	205.8
zp15-8lc	149	0.356	183.57	4.606	1.52	198.7

Table B-2

J-R CURVES FOR ZP-13 C-L ORIENTATION 5.8 mm THICKNESS ONLY

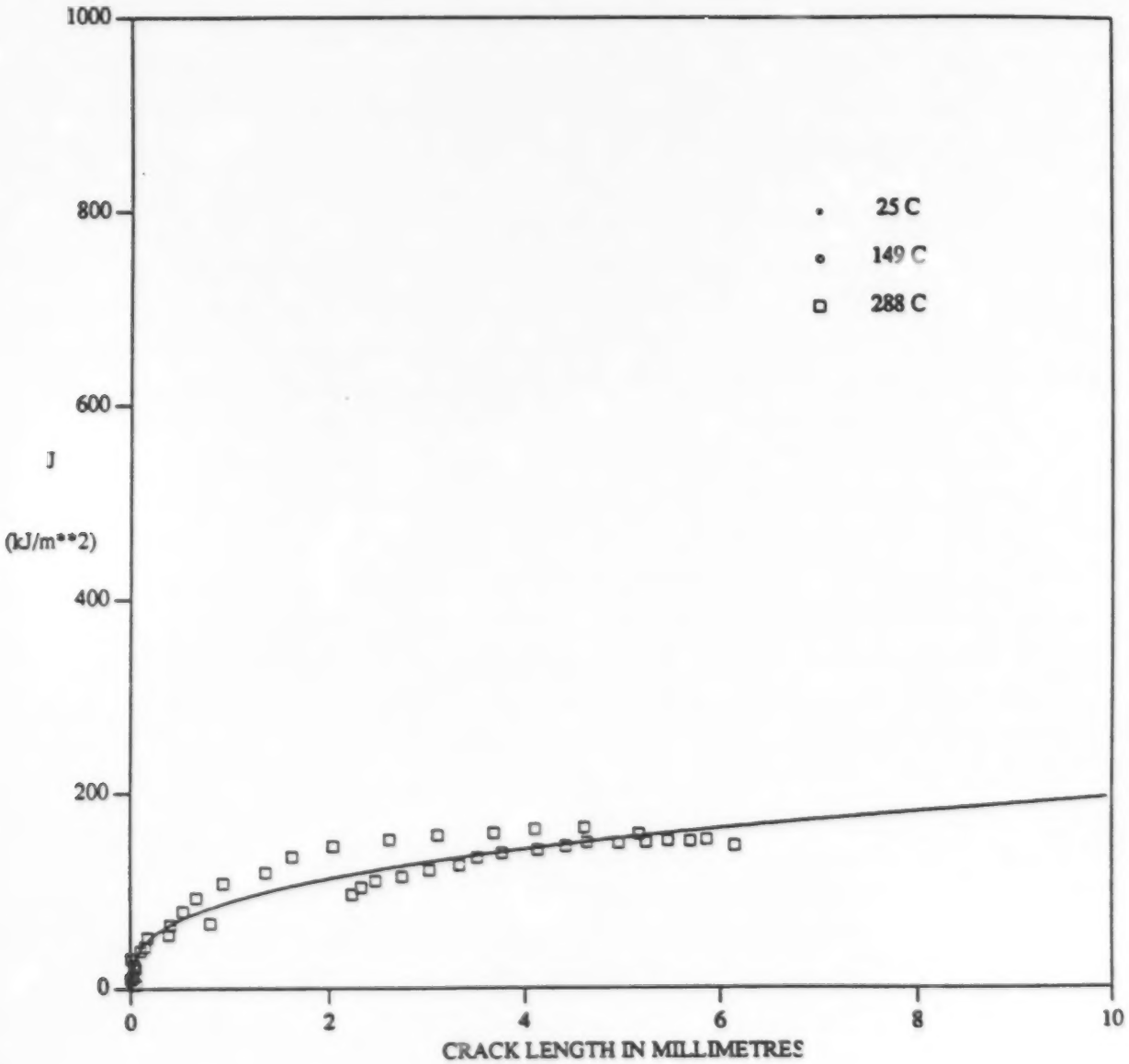

Figure B-1

Specimen Data For SA-106 Grade B Tests C-L Specimens From Lab Group 1							
Specimen ID	Thickness (mm)	Reduced Thickness (mm)	Temperature Degrees C (mm)	J_{IC} kJ/m**2	E GPa	σ_0 MPa	σ_{uts} MPa
zp13-1cl	5.8	4.64	288	48.6	190.8	212	467
zp13-2cl	5.8	4.64	288	56.6	190.8	212	467

Data for Figure B-1

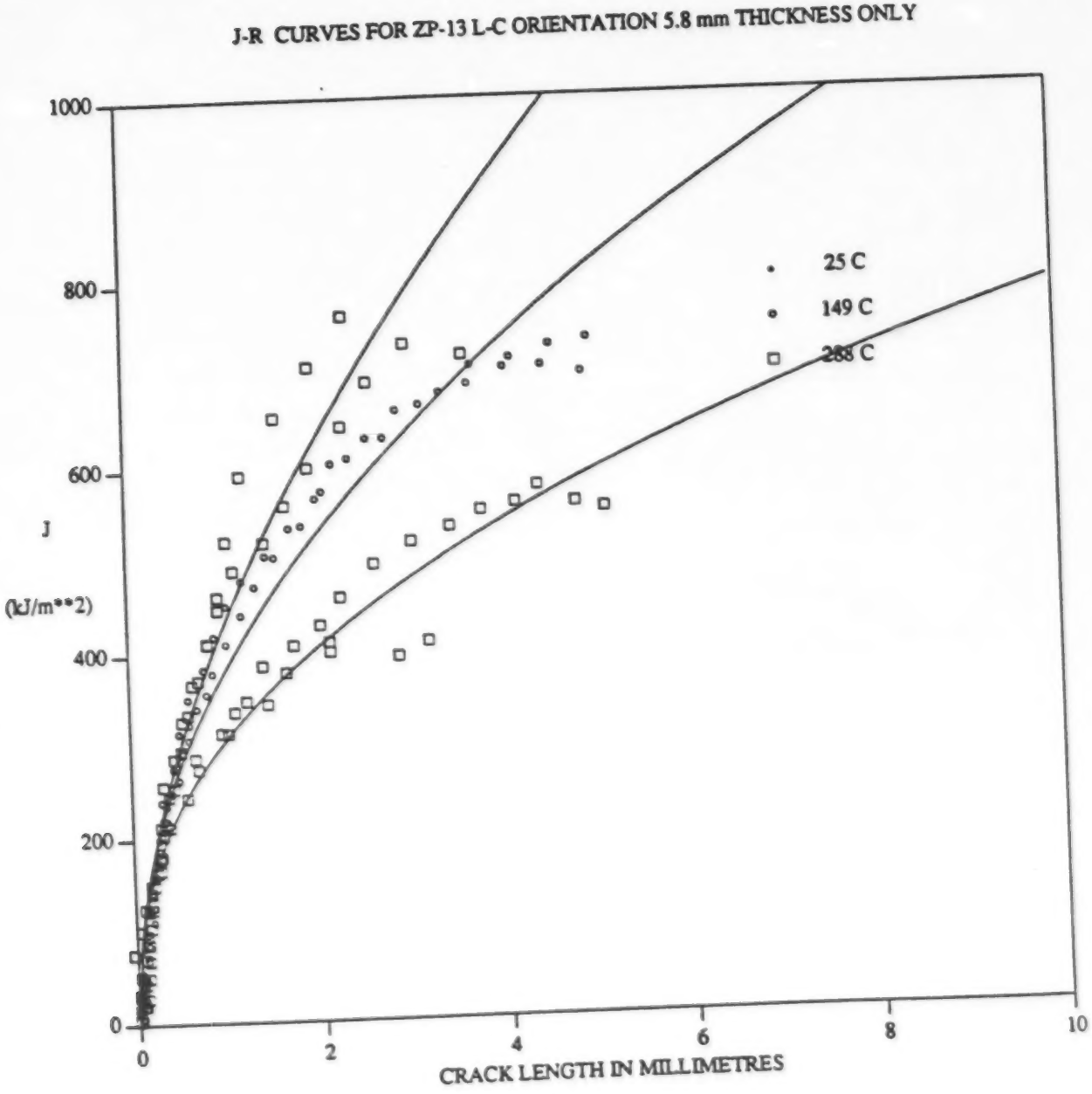
J-R CURVES FOR ZP-13 L-C ORIENTATION 5.8 mm THICKNESS ONLY
1000
800
600
400
200
0
J
(kJ/m**2)
25 C
149 C
288 C
0
2
4
6
8
10
CRACK LENGTH IN MILLIMETRES

Figure B-2

Specimen Data For SA-106 Grade B Tests L-C Specimens From Lab Group 1							
Specimen ID	Thickness (mm)	Reduced Thickness (mm)	Temperature Degrees C	J_{IC} kJ/m**2	E GPa	σ_0 MPa	σ_{uts} MPa
zp13-1lc	5.8	5.8	149	402.5	198.7	253	429
zp13-2lc	5.8	5.8	149	331.4	198.7	253	429
zp13-3lc	5.8	5.8	288	454.6	190.8	212	467
zp13-4lc	5.8	5.8	288	387.7	190.8	212	467
zp13-7lc	5.8	4.64	288	274.2	190.8	212	467
zp13-8lc	5.8	4.64	288	244.1	190.8	212	467

Data for Figure B-2

J-R CURVES FOR ZP-14 C-L ORIENTATION 17.8 mm THICKNESS ONLY

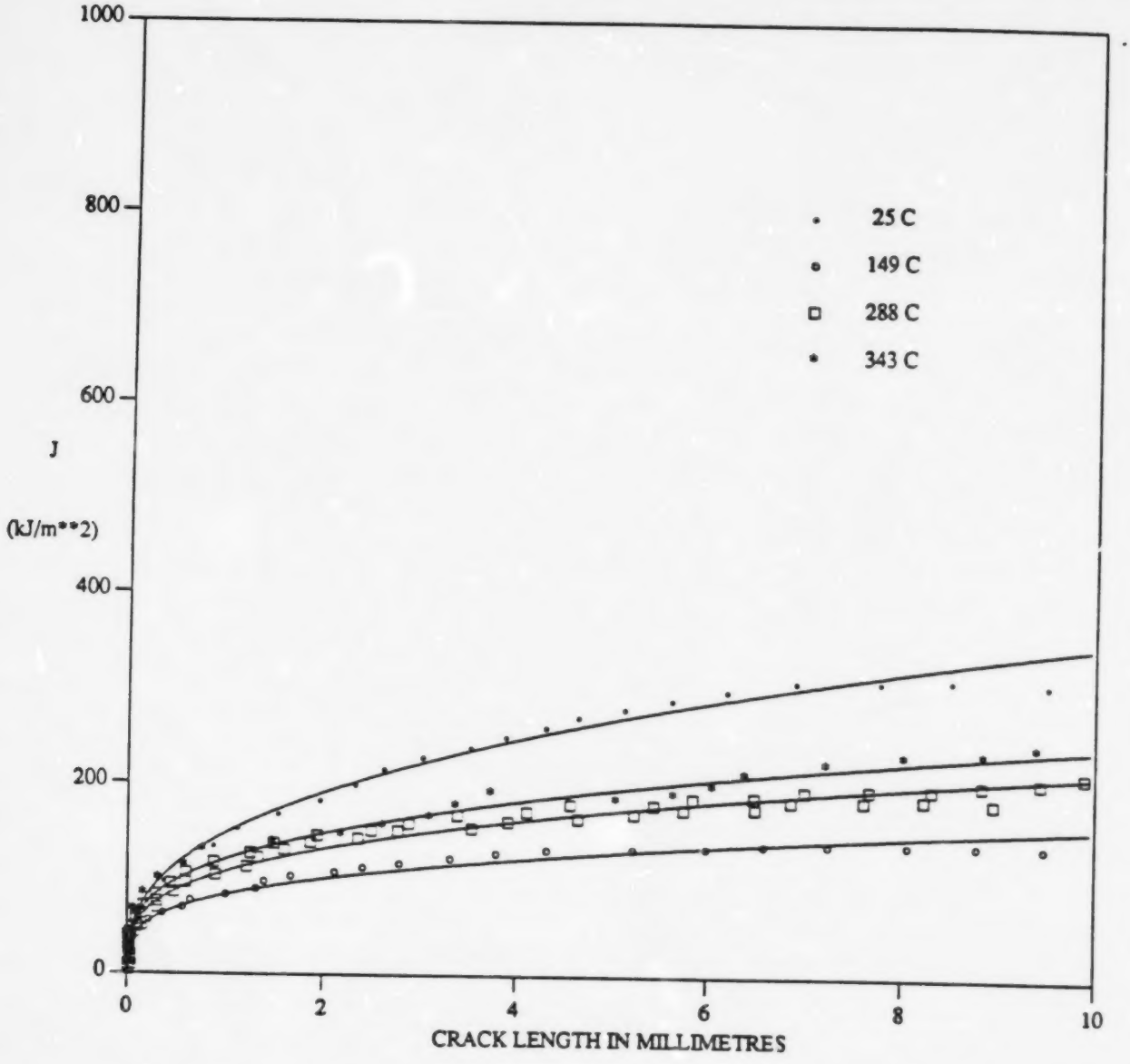

Figure B-3

Specimen Data For SA-106 Grade B Tests 17.8 mm Thickness C-L Specimens From Lab Group 16							
Specimen ID	Thickness (mm)	Reduced Thickness (mm)	Temperature Degrees C	J_{IC} kJ/m**2	E GPa	σ_0 MPa	σ_{uts} MPa
zp14-1cl	17.8	14.24	25	81.3	205.8	275.0	512.0
zp14-2cl	17.8	14.24	149	53.1	198.7	248.0	533.0
zp14-3cl	17.8	14.24	288	64.9	190.8	255.0	567.0
zp14-4cl	17.8	14.24	288	78.3	190.8	255.0	567.0
zp14-5cl	17.8	14.24	343	92.4	187.6	238.0	534.0

Data for Figure B-3

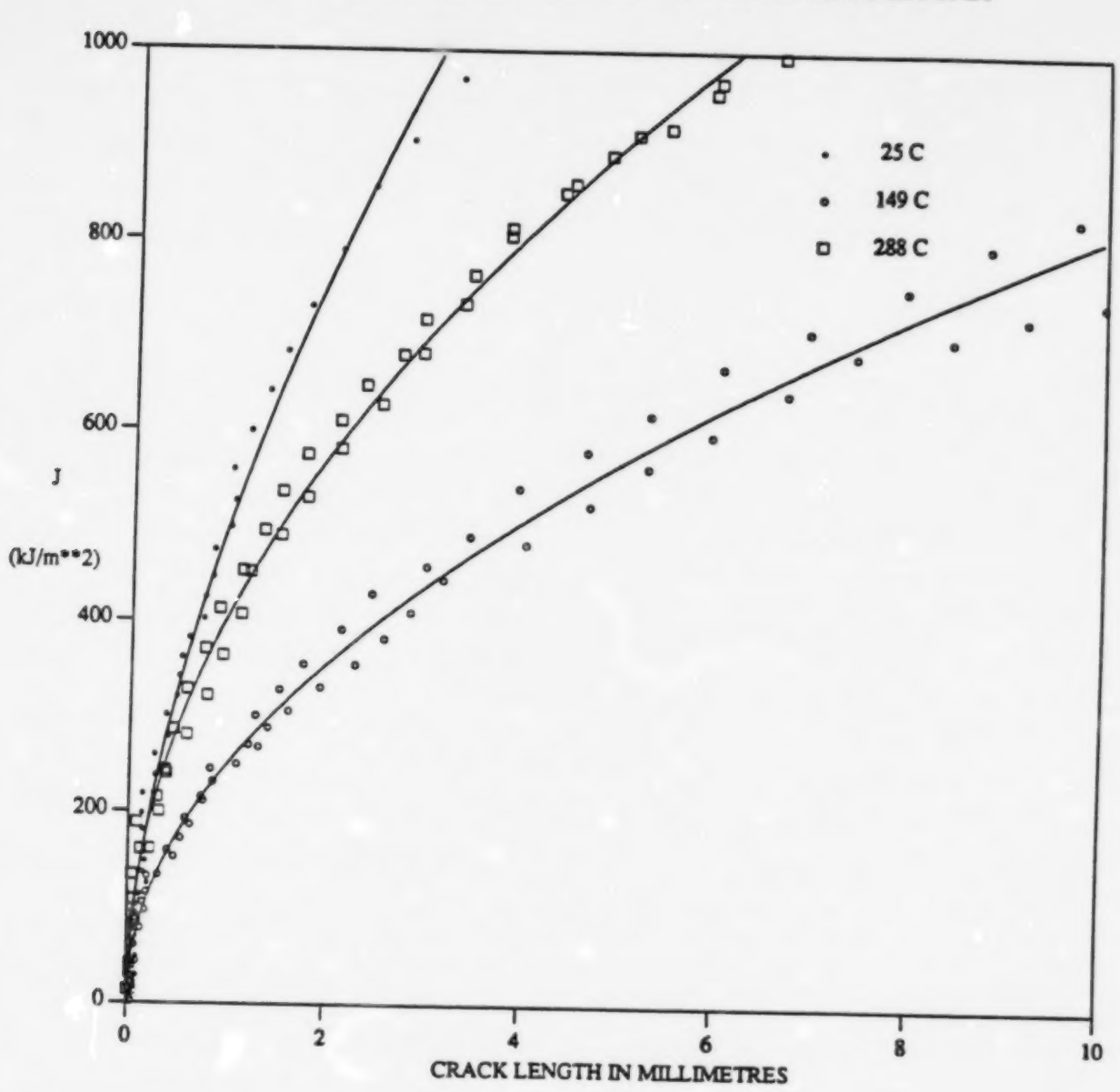
J-R CURVES FOR ZP-14 L-C ORIENTATION 15.2 mm THICKNESS ONLY
1000
800
600
400
200
0
J
(kJ/m**2)
25 C
149 C
288 C
0
2
4
6
8
10
CRACK LENGTH IN MILLIMETRES

Figure B-4

Specimen Data For SA-106 Grade B Tests 15.2 mm Thickness L-C Specimens From Lab Group 16							
Specimen ID	Thickness (mm)	Reduced Thickness (mm)	Temperature Degrees C	J_{IC} kJ/m**2	E GPa	σ_0 MPa	σ_{uts} MPa
zp14-1lc	15.2	15.2	25	417.9	205.8	282.5	513.5
zp14-2lc	15.2	15.2	149	161.7	198.7	253	533
zp14-3lc	15.2	15.2	288	322.1	190.8	258	569.5
zp14-4lc	15.2	15.2	149	136.2	198.7	253	533
zp14-5lc	15.2	15.2	288	322.1	190.8	258	569.5

Data for Figure B-4

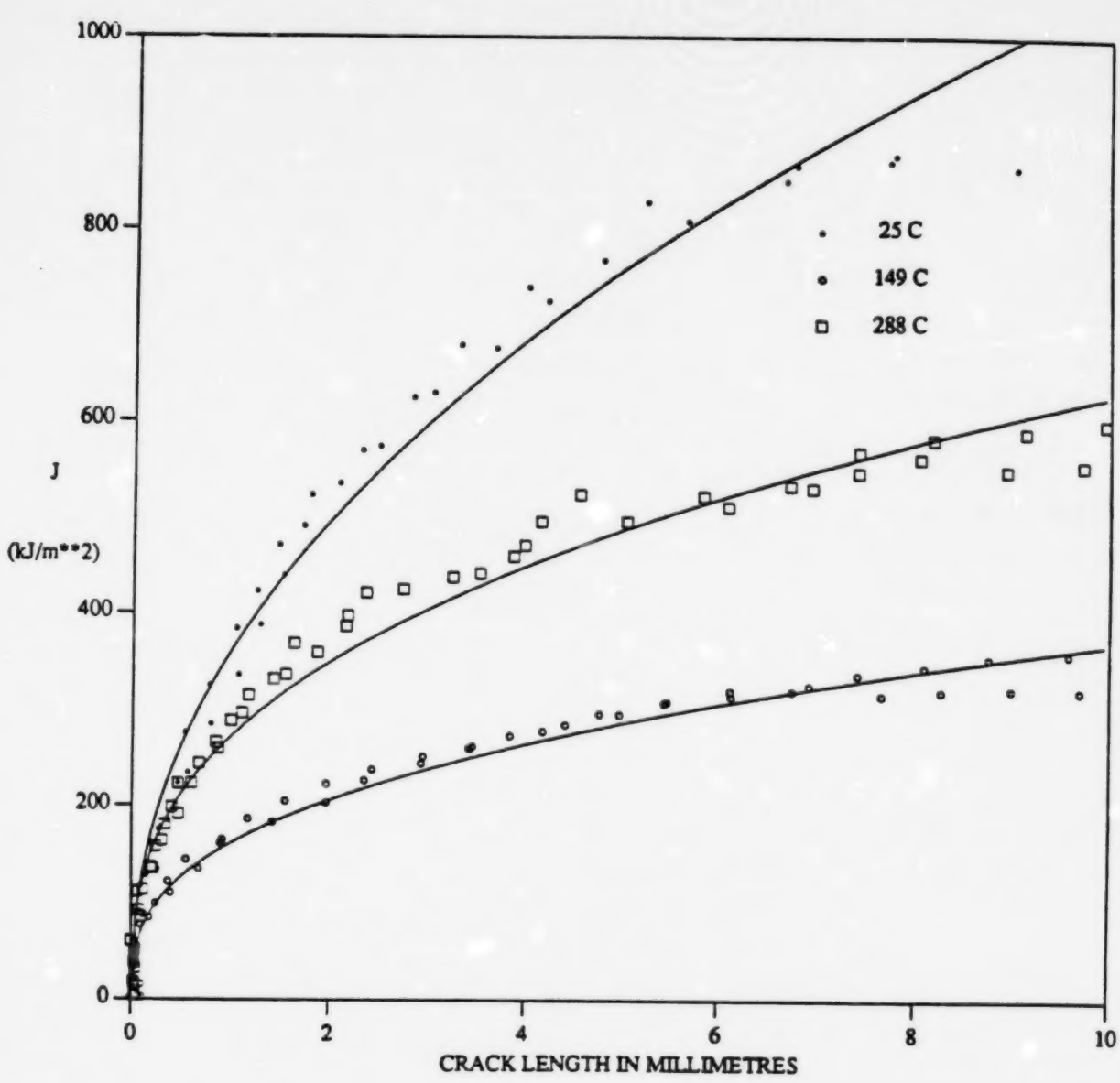
J-R CURVES FOR ZP-14 L-C ORIENTATION 17.8 mm THICKNESS ONLY
1000
800
600
400
200
0
J
(kJ/m**2)
25 C
149 C
288 C
0
2
4
6
8
10
CRACK LENGTH IN MILLIMETRES

Figure B-5

Specimen Data For SA-106 Grade B Tests 17.8 mm Thickness L-C Specimens From Lab Group 16							
Specimen ID	Thickness (mm)	Reduced Thickness (mm)	Temperature Degrees C	J_{IC} kJ/m**2	E GPa	σ_0 MPa	σ_{uts} MPa
zp14-1lc (sg)	17.8	14.24	25	270.1	205.8	282.5	513.5
zp14-2lc (sg)	17.8	14.24	149	108.9	198.7	253.0	533.0
zp14-3lc (sg)	17.8	14.24	288	197.4	190.8	258.0	569.5
zp14-4lc (sg)	17.8	14.24	288	197.4	190.8	258.0	569.5
zp14-6lc	17.8	14.24	25	193.4	205.8	282.5	513.5
zp14-7lc	17.8	14.24	149	89.2	198.7	253.0	533.0

Data for Figure B-5

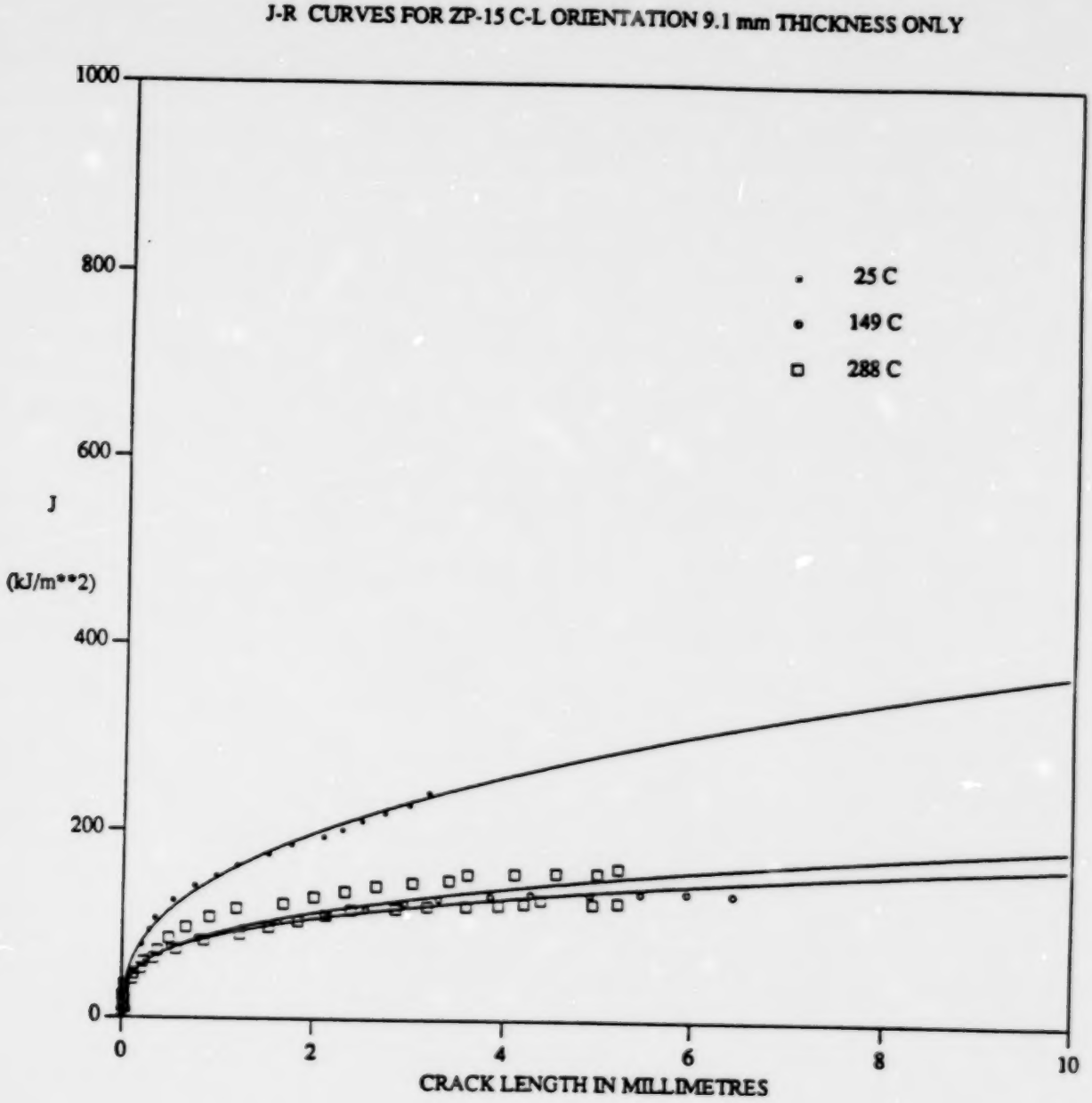
J-R CURVES FOR ZP-15 C-L ORIENTATION 9.1 mm THICKNESS ONLY
1000
800
600
400
200
0
J
(kJ/m**2)
25 C
149 C
288 C
0
2
4
6
8
10
CRACK LENGTH IN MILLIMETRES

Figure B-6

Specimen Data For SA-106 Grade B Tests C-L Specimens From Lab Group 2							
Specimen ID	Thickness (mm)	Reduced Thickness (mm)	Temperature Degrees C	J_{IC} kJ/m**2	E GPa	σ_0 MPa	σ_{uts} MPa
zp15-1cl	9.1	7.28	288	54.2	190.8	319	620
zp15-2cl	9.1	7.28	288	59.7	190.8	319	620
zp15-3cl	9.1	7.28	25	96.7	205.8	320	510
zp15-4cl	9.1	7.28	149	60.0	198.7	308	628

Data for Figure B-6

J-R CURVES FOR ZP-15 L-C ORIENTATION 9.1 mm THICKNESS ONLY

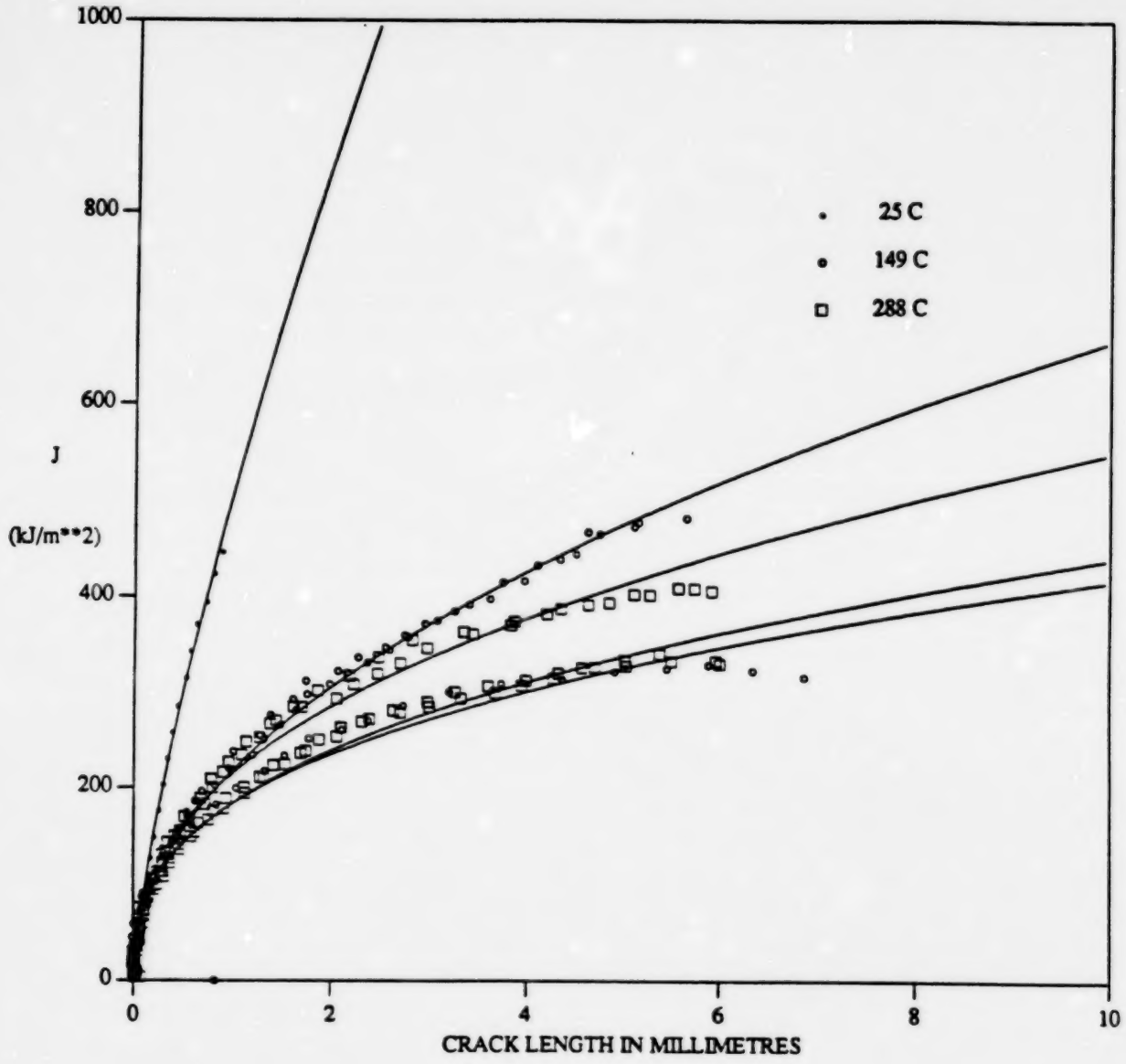

Figure B-7

Specimen Data For SA-106 Grade B Tests L-C Specimens From Lab Group 2							
Specimen ID	Thickness (mm)	Reduced Thickness (mm)	Temperature Degrees C	J_{IC} kJ/m**2	E GPa	σ_0 MPa	σ_{uts} MPa
zp15-1lc	9.1	9.1	149	122.6	198.7	308.0	628.0
zp15-2lc	9.1	9.1	149	133.8	198.7	308.0	628.0
zp15-3lc	9.1	9.1	288	125.4	190.8	319.0	620.0
zp15-4lc	9.1	9.1	288	125.6	190.8	319.0	620.0
zp15-5lc	9.1	7.28	288	104.2	190.8	319.0	620.0
zp15-6lc	9.1	7.28	288	110.5	190.8	319.0	620.0
zp15-7lc	9.1	7.28	25	336.0	205.8	314.0	520.0
zp15-8lc	9.1	7.28	149	112.4	198.7	308.0	628.0

Data for Figure B-7

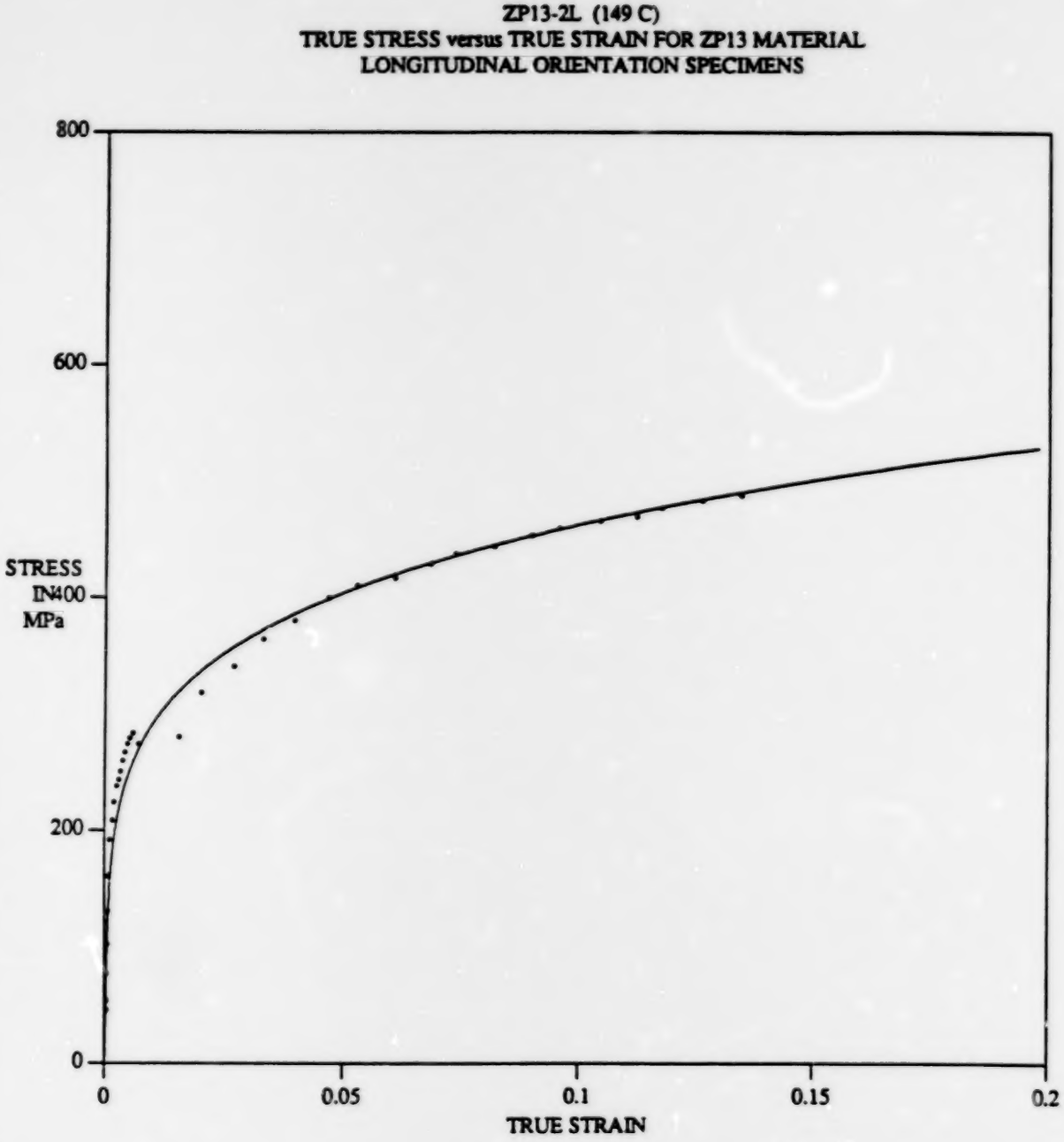
ZP13-2L (149 C)
TRUE STRESS versus TRUE STRAIN FOR ZP13 MATERIAL
LONGITUDINAL ORIENTATION SPECIMENS
800
600
400
200
0
STRESS
IN
MPa
0
0.05
0.1
0.15
0.2
TRUE STRAIN

Figure B-8(a)

ZP13-4L (288 C)
TRUE STRESS versus TRUE STRAIN FOR ZP13 MATERIAL
LONGITUDINAL ORIENTATION SPECIMENS

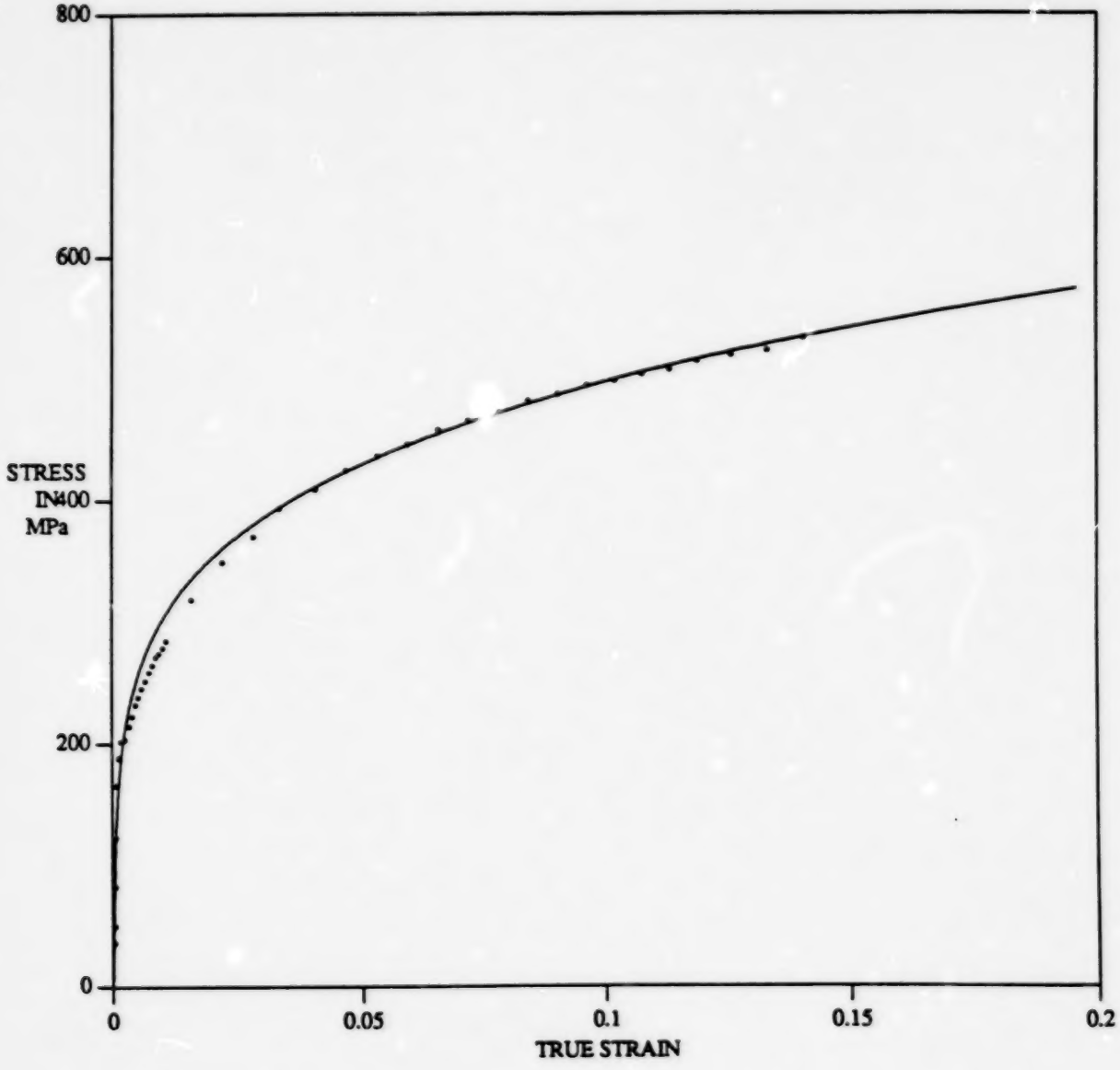

Figure B-8(b)

ZP14-1L ZP14-6L (25 C)
TRUE STRESS versus TRUE STRAIN FOR ZP14 MATERIAL
LONGITUDINAL ORIENTATION SPECIMENS

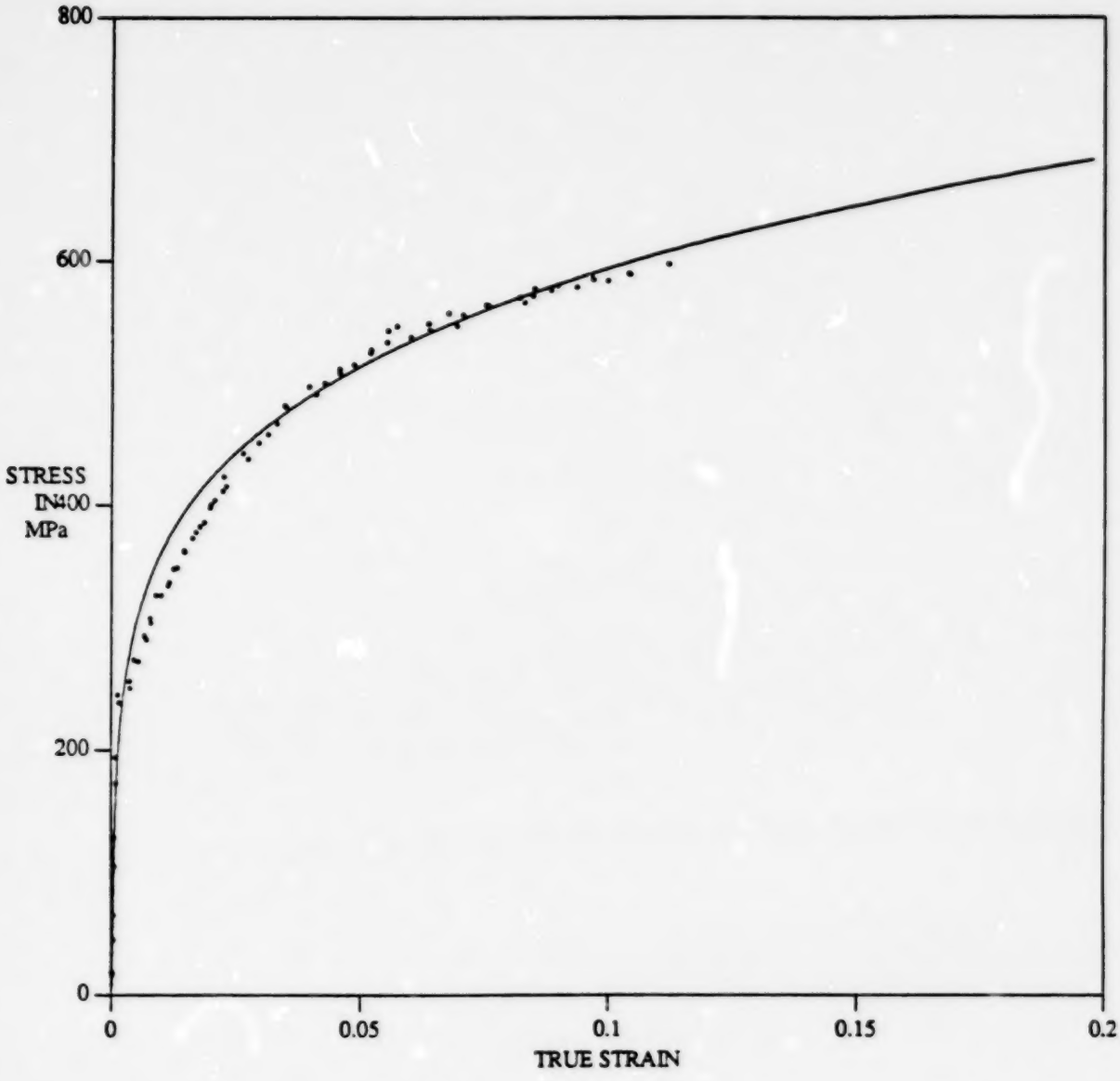

Figure B-8(c)

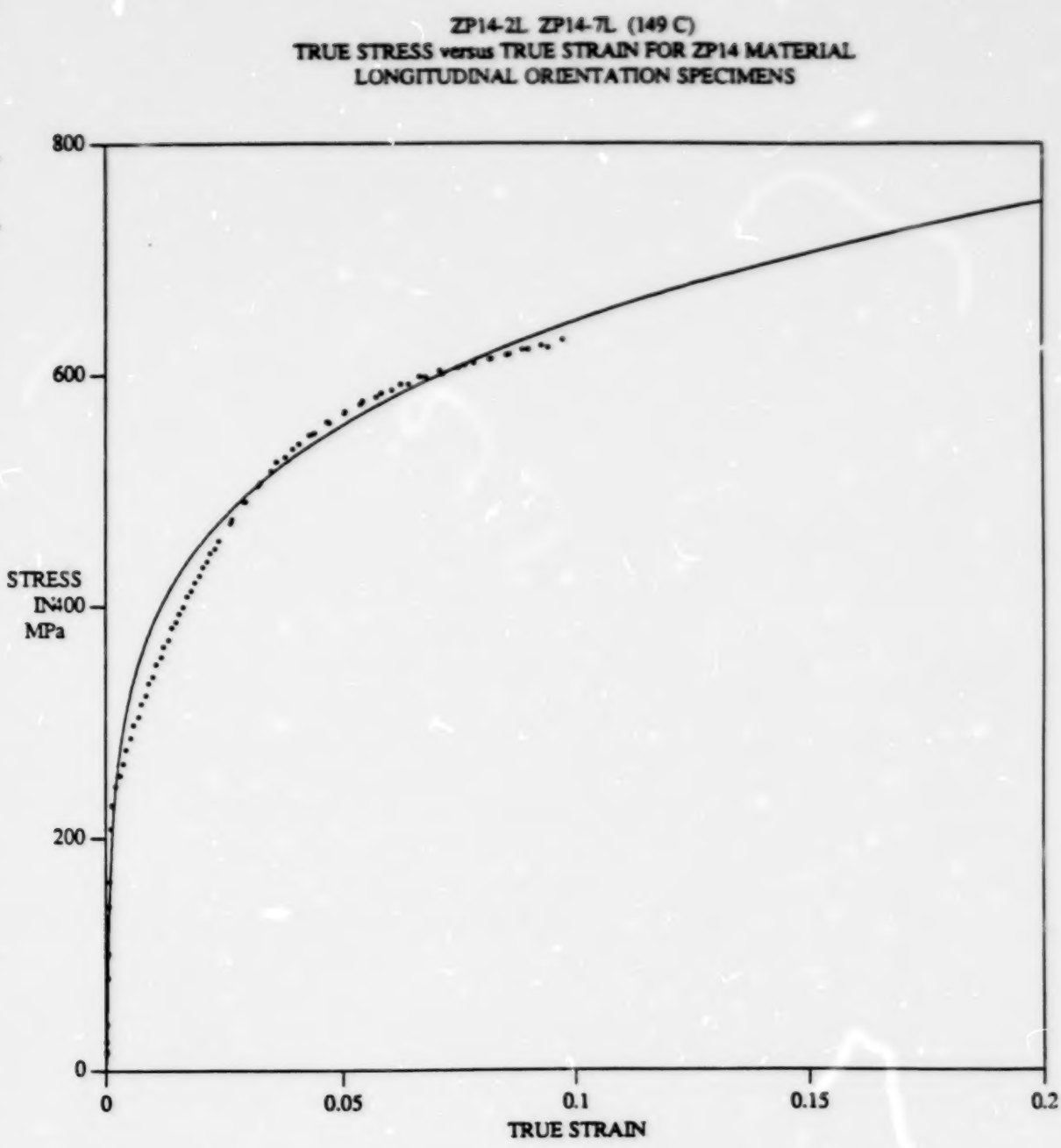
ZP14-2L ZP14-7L (149 C)
TRUE STRESS versus TRUE STRAIN FOR ZP14 MATERIAL
LONGITUDINAL ORIENTATION SPECIMENS
800
600
400
200
0
STRESS
IN
MPa
0
0.05
0.1
0.15
0.2
TRUE STRAIN

Figure B-8(d)

ZP14-4L ZP14-9L (288 C)
TRUE STRESS versus TRUE STRAIN FOR ZP14 MATERIAL
LONGITUDINAL ORIENTATION SPECIMENS

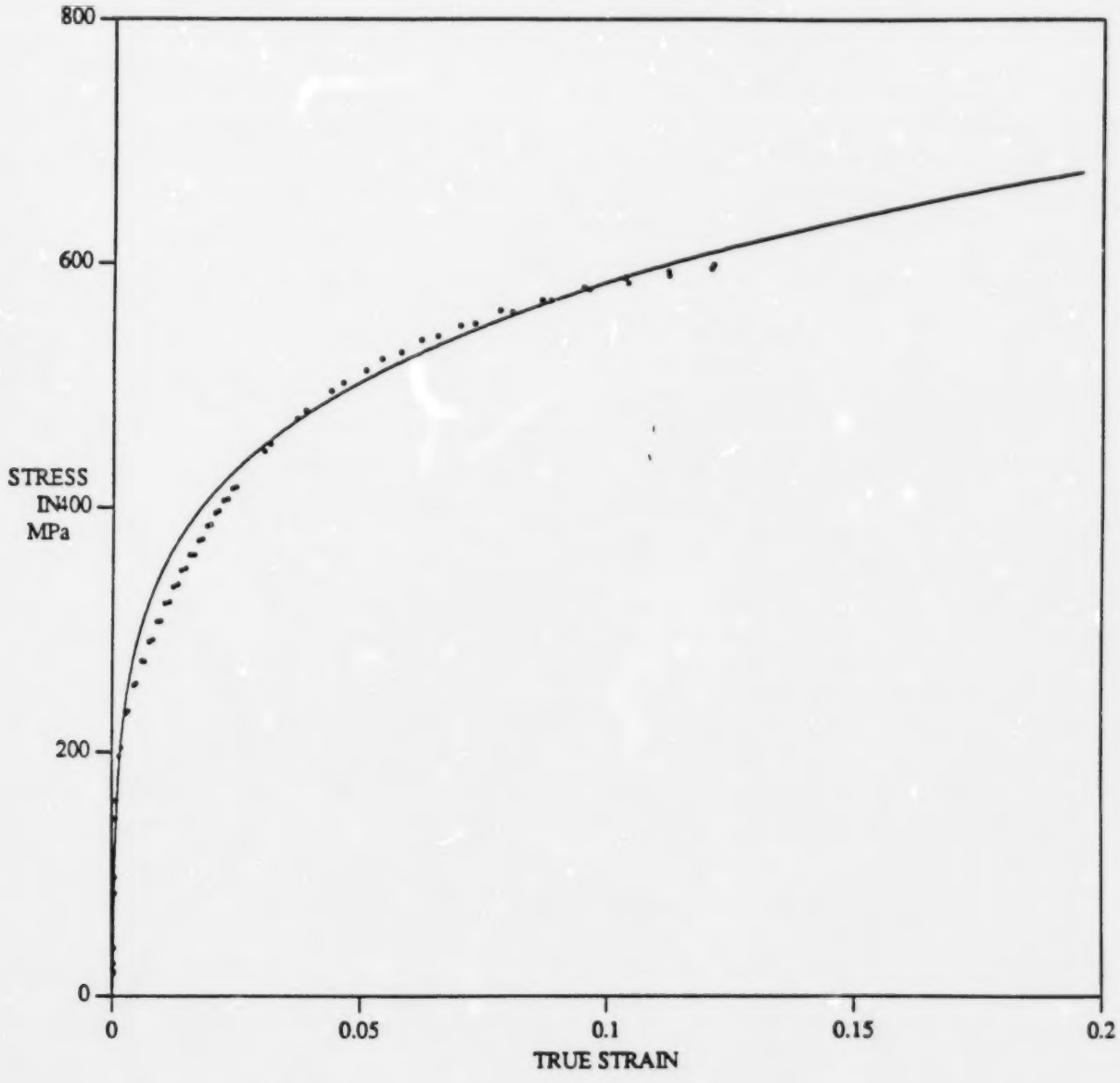

Figure B-8(e)

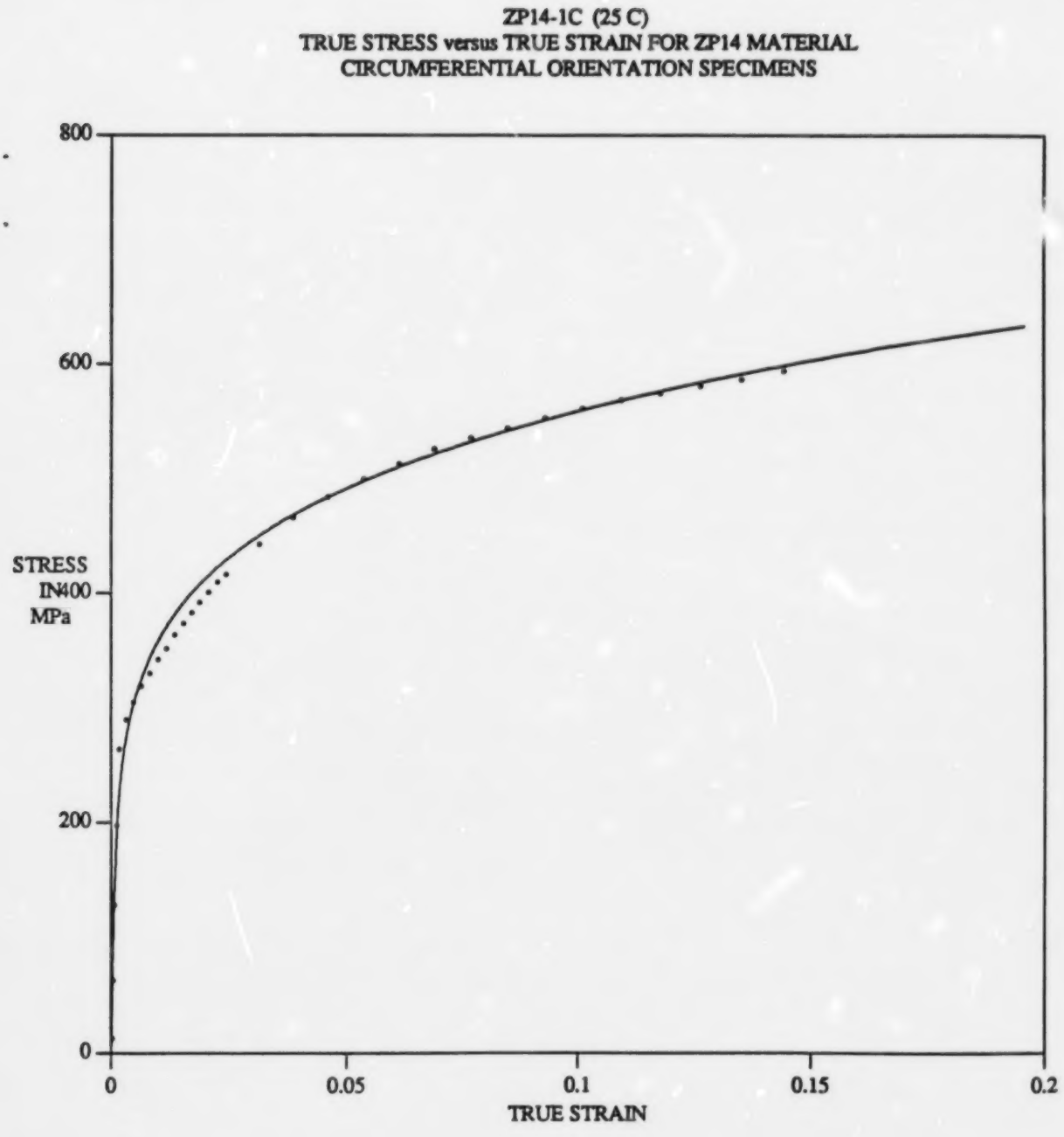
ZP14-1C (25 C)
TRUE STRESS versus TRUE STRAIN FOR ZP14 MATERIAL
CIRCUMFERENTIAL ORIENTATION SPECIMENS
800
600
400
200
0
STRESS
IN
MPa
0
0.05
0.1
0.15
0.2
TRUE STRAIN

Figure B-9(a)

ZP14-2C (149 C)
TRUE STRESS versus TRUE STRAIN FOR ZP14 MATERIAL
CIRCUMFERENTIAL ORIENTATION SPECIMENS

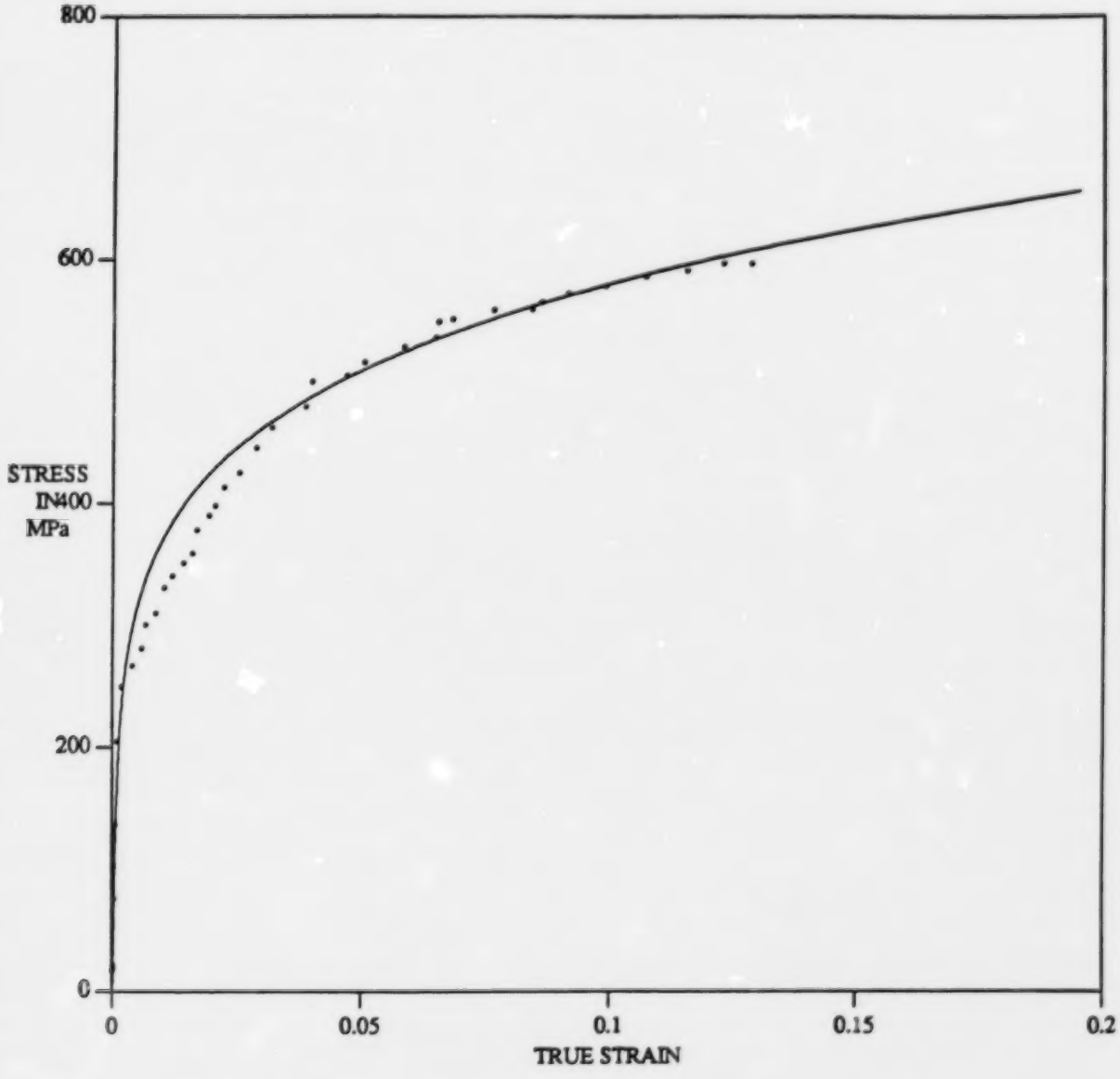

Figure B-9(b)

ZP14-4C (288 C)
TRUE STRESS versus TRUE STRAIN FOR ZP14 MATERIAL
CIRCUMFERENTIAL ORIENTATION SPECIMENS

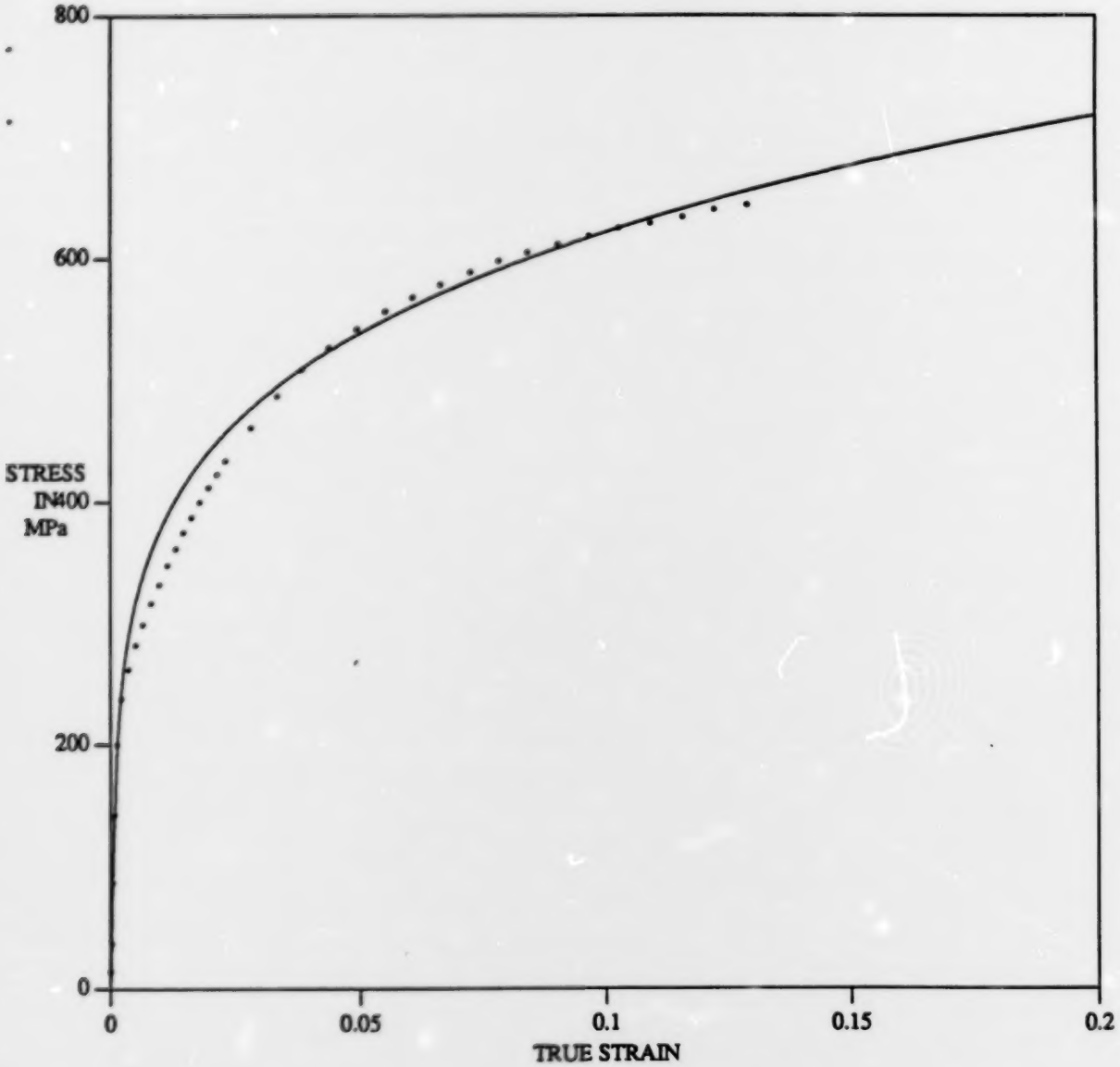

Figure B-9(c)

ZP14-5C (343 C)
TRUE STRESS versus TRUE STRAIN FOR ZP14 MATERIAL
CIRCUMFERENTIAL ORIENTATION SPECIMENS

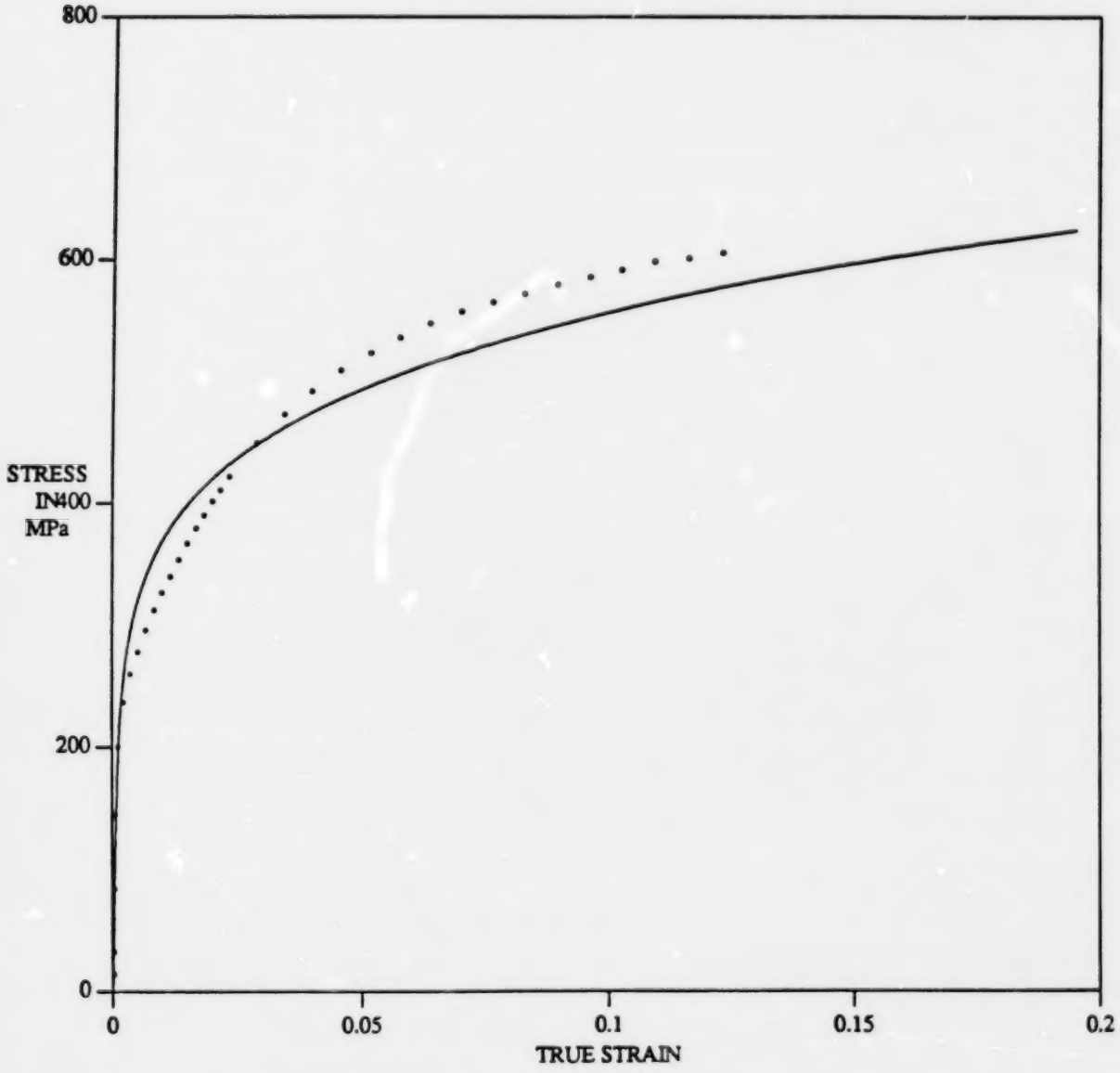

Figure B-9(d)

ZP15-1L (25 C)
TRUE STRESS versus TRUE STRAIN FOR ZP15 MATERIAL
LONGITUDINAL ORIENTATION SPECIMENS

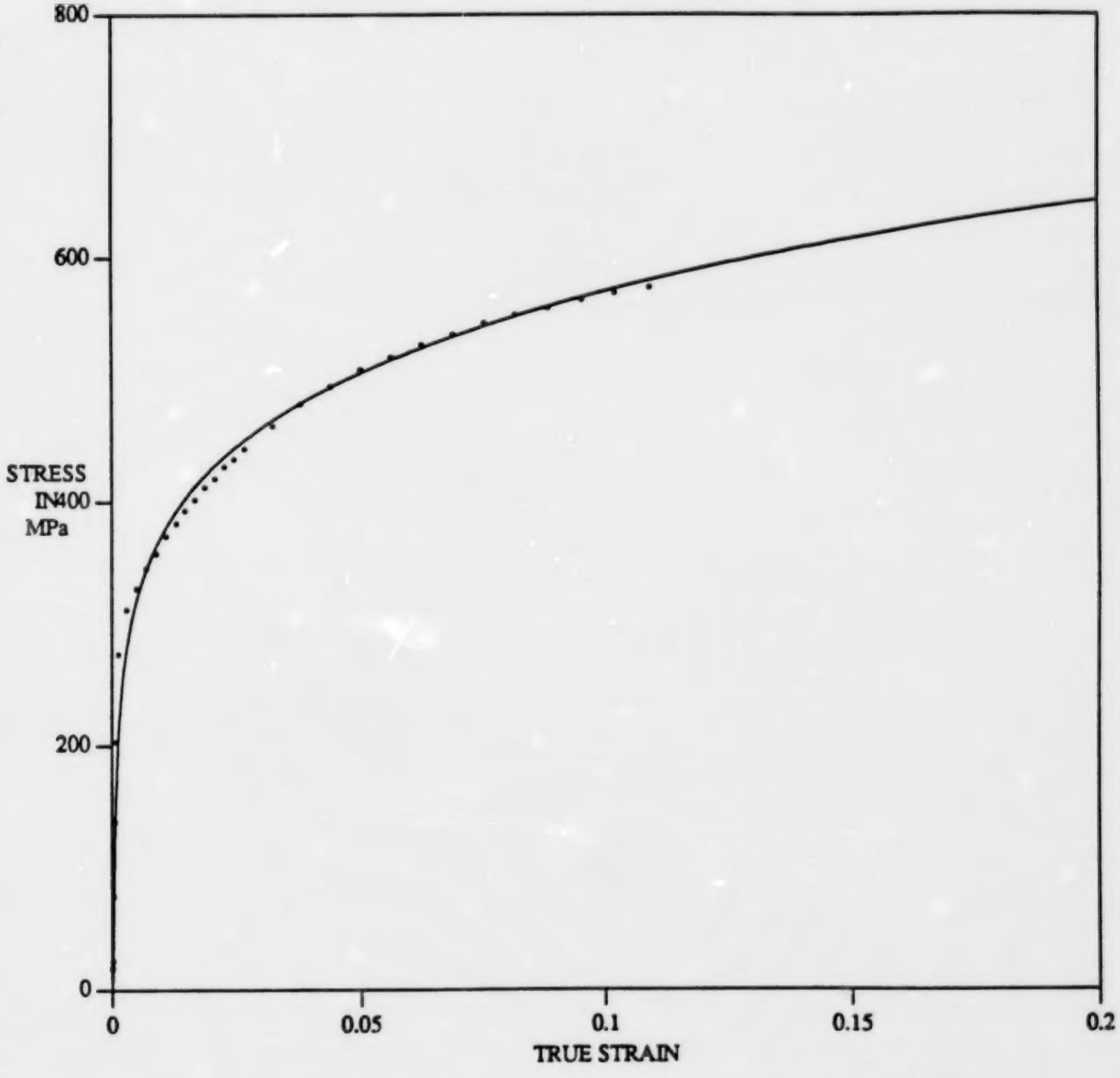

Figure B-10(a)

ZP15-2L (149 C)
TRUE STRESS versus TRUE STRAIN FOR ZP15 MATERIAL
LONGITUDINAL ORIENTATION SPECIMENS

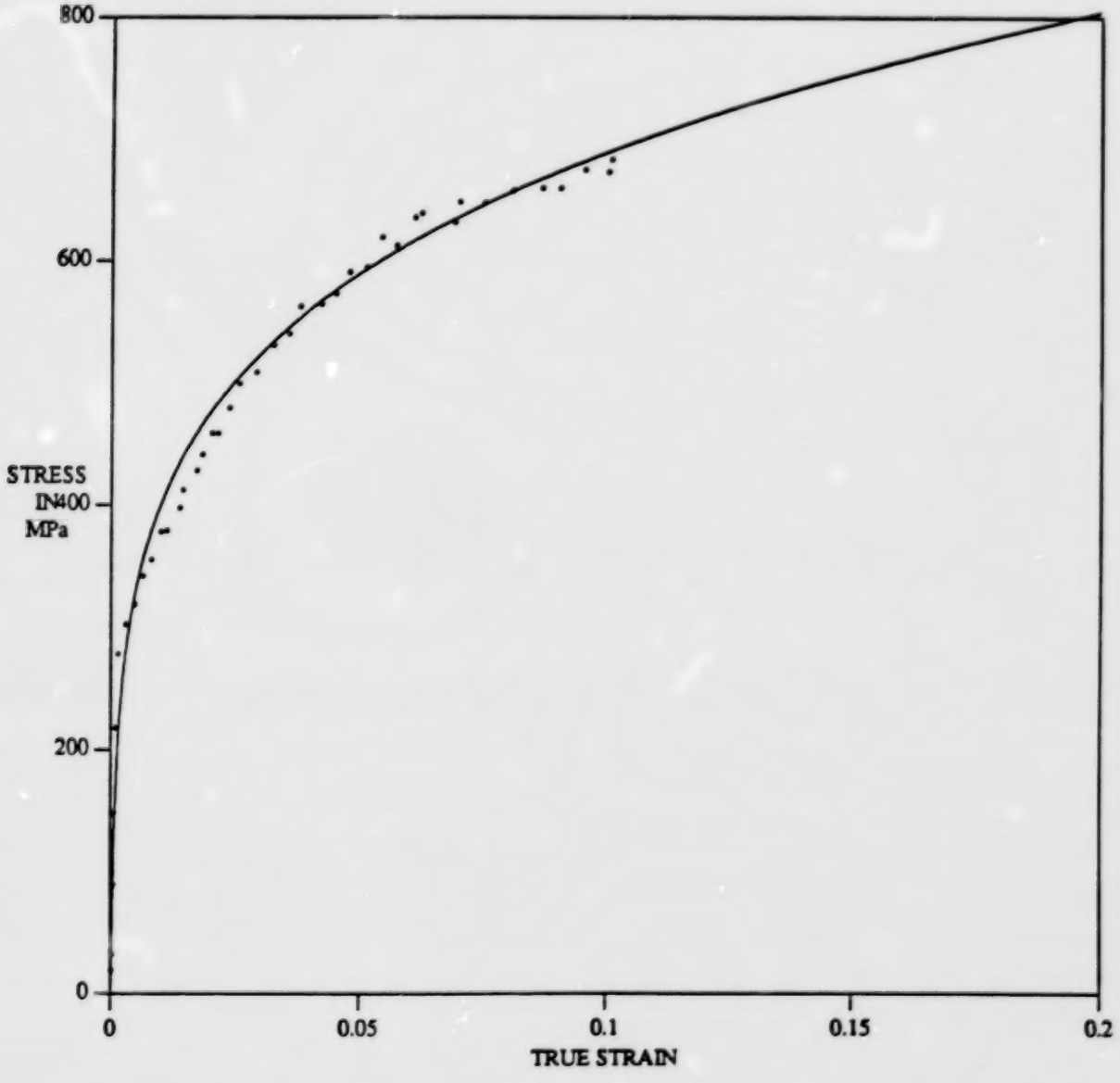

Figure B-10(b)

ZP15-4L (288 C)
TRUE STRESS versus TRUE STRAIN FOR ZP15 MATERIAL
LONGITUDINAL ORIENTATION SPECIMENS

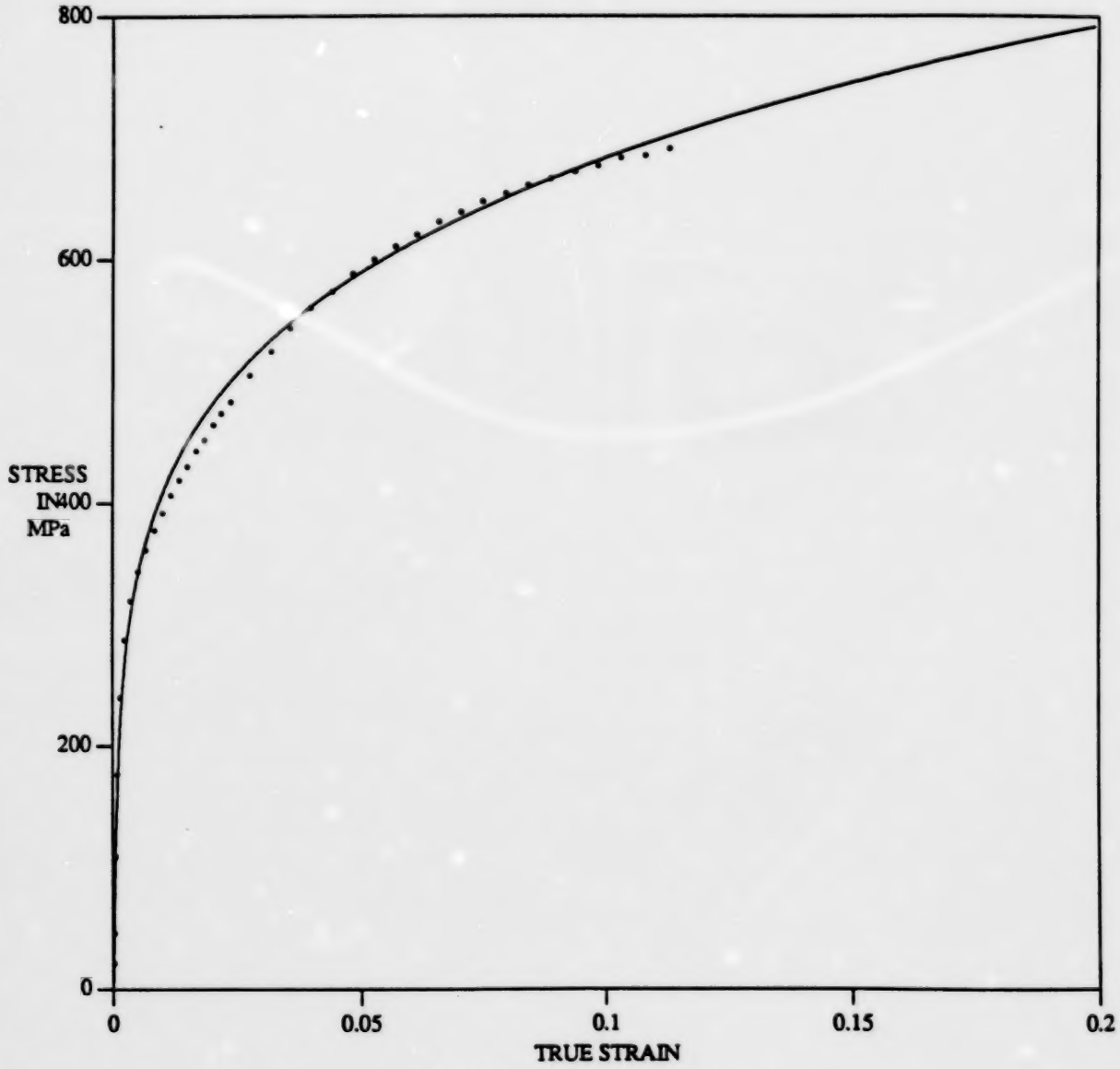

Figure B-10(c)

ZP15-1C (25 C)
TRUE STRESS versus TRUE STRAIN FOR ZP15 MATERIAL
CIRCUMFERENTIAL ORIENTATION SPECIMENS

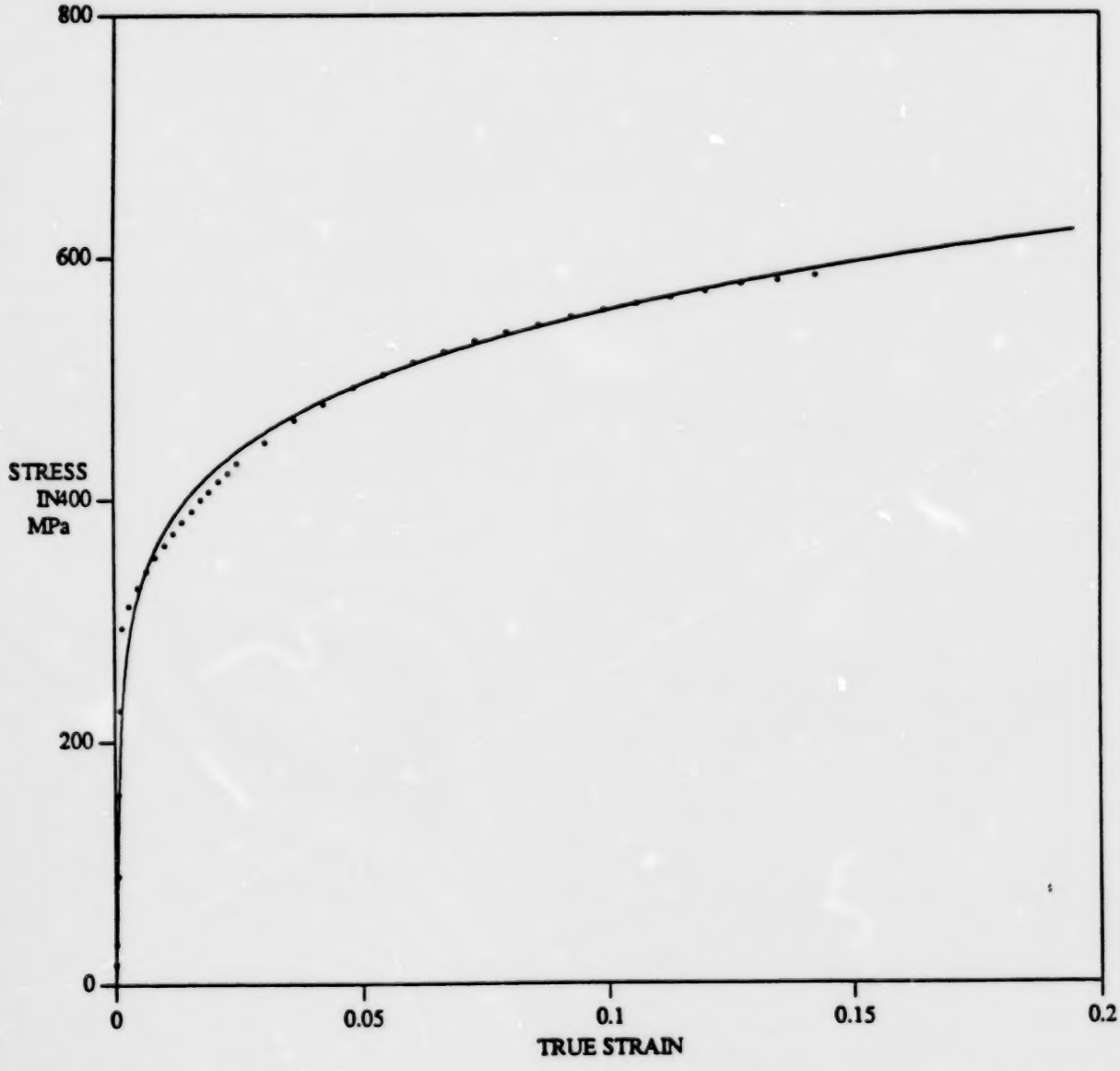

Figure B-10(d)

J-R CURVES FOR EPCS 10.0 mm THICKNESS ONLY

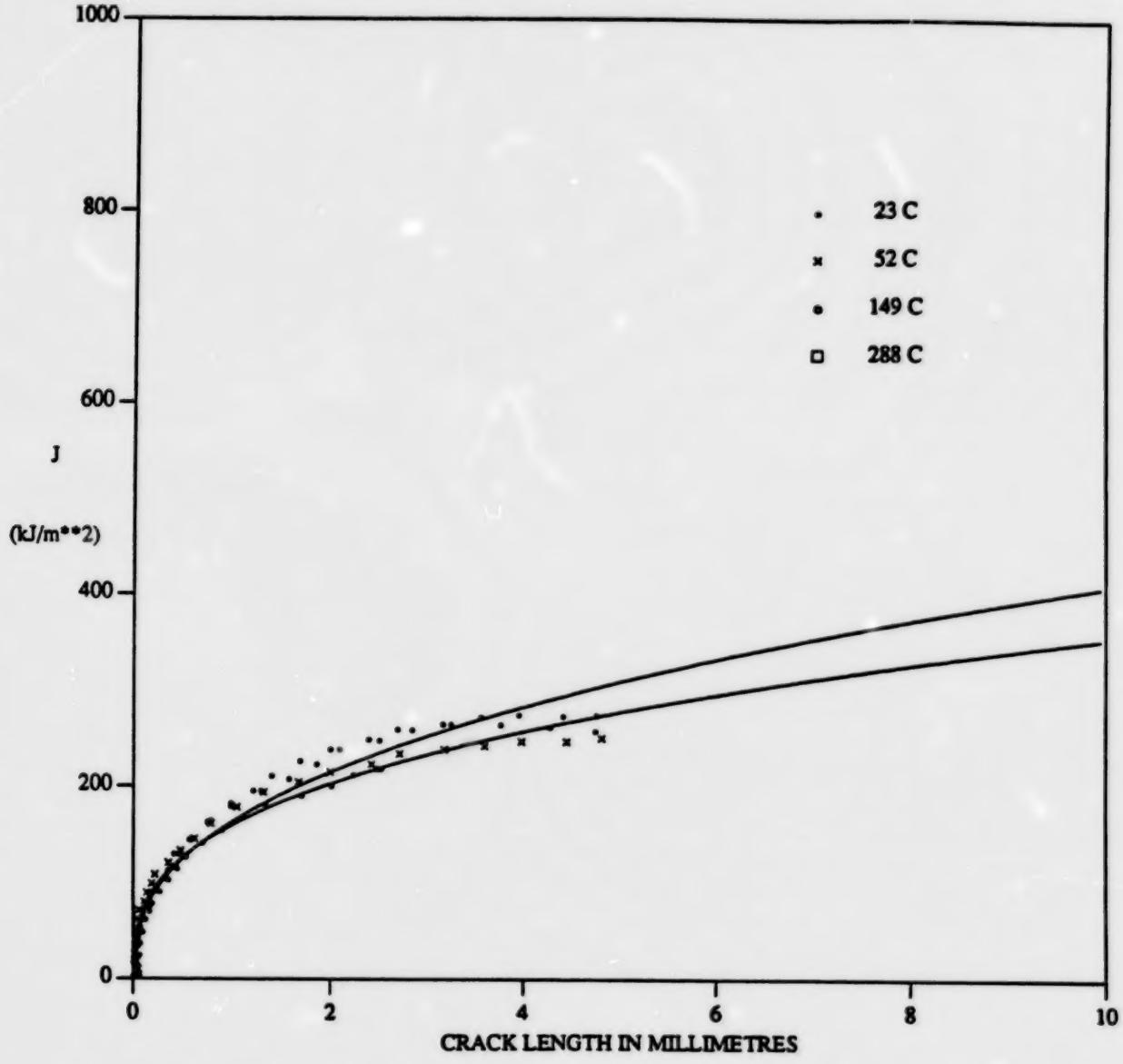

Figure B-11

Specimen Data For SA-106 Grade B Tests Specimens of Undefined Orientation From Lab Group 23							
Specimen ID	Thickness (mm)	Reduced Thickness (mm)	Temperature Degrees C	J_{IC} kJ/m**2	E GPa	σ_0 MPa	σ_{uts} MPa
epcs-1	10.0	8.0	52.0	116.1	204.2		
epcs-2	10.0	8.0	23.0	103.3	205.9		
epcs-3	10.0	8.0	23.0	105.0	205.9		
epcs-4	10.0	8.0	23.0	92.5	205.9		

Data for Figure B-11

J-R CURVES FOR 24-106b 10.0 mm THICKNESS ONLY

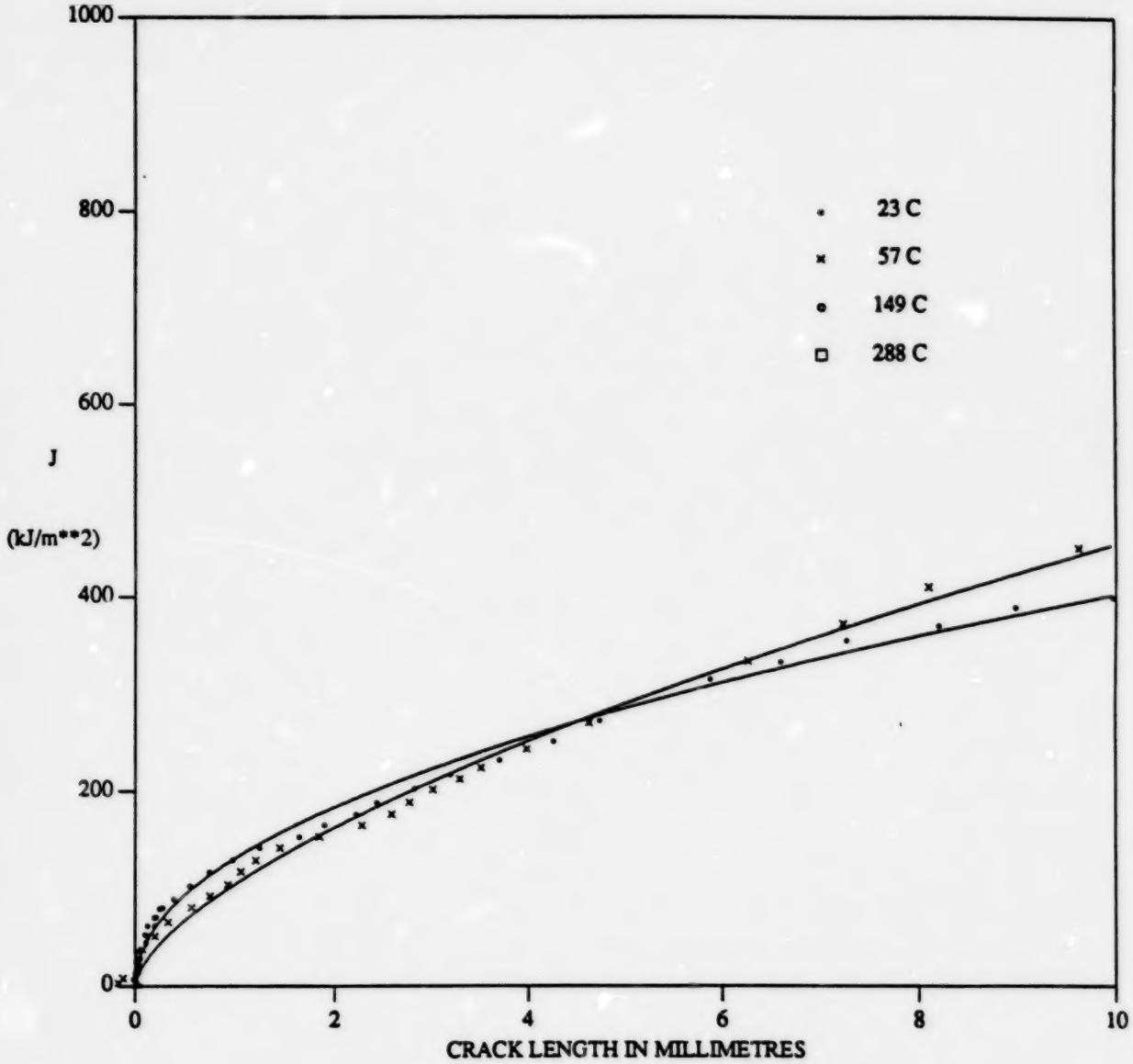

Figure B-12

Specimen Data For SA-106 Grade B Tests Specimens From Lab Group 24							
Specimen ID	Thickness (mm)	Reduced Thickness (mm)	Temperature Degrees C (mm)	J_{IC} kJ/m**2	E GPa	σ_0 MPa	σ_{uts} MPa
106B-F1T1	10.0	8.0	23	75.5	205.9		
106B-F1T2	10.0	8.0	23	82.2	205.9		
106B-F2T	10.0	8.0	57	51.3	204.0		

Data for Figure B-12

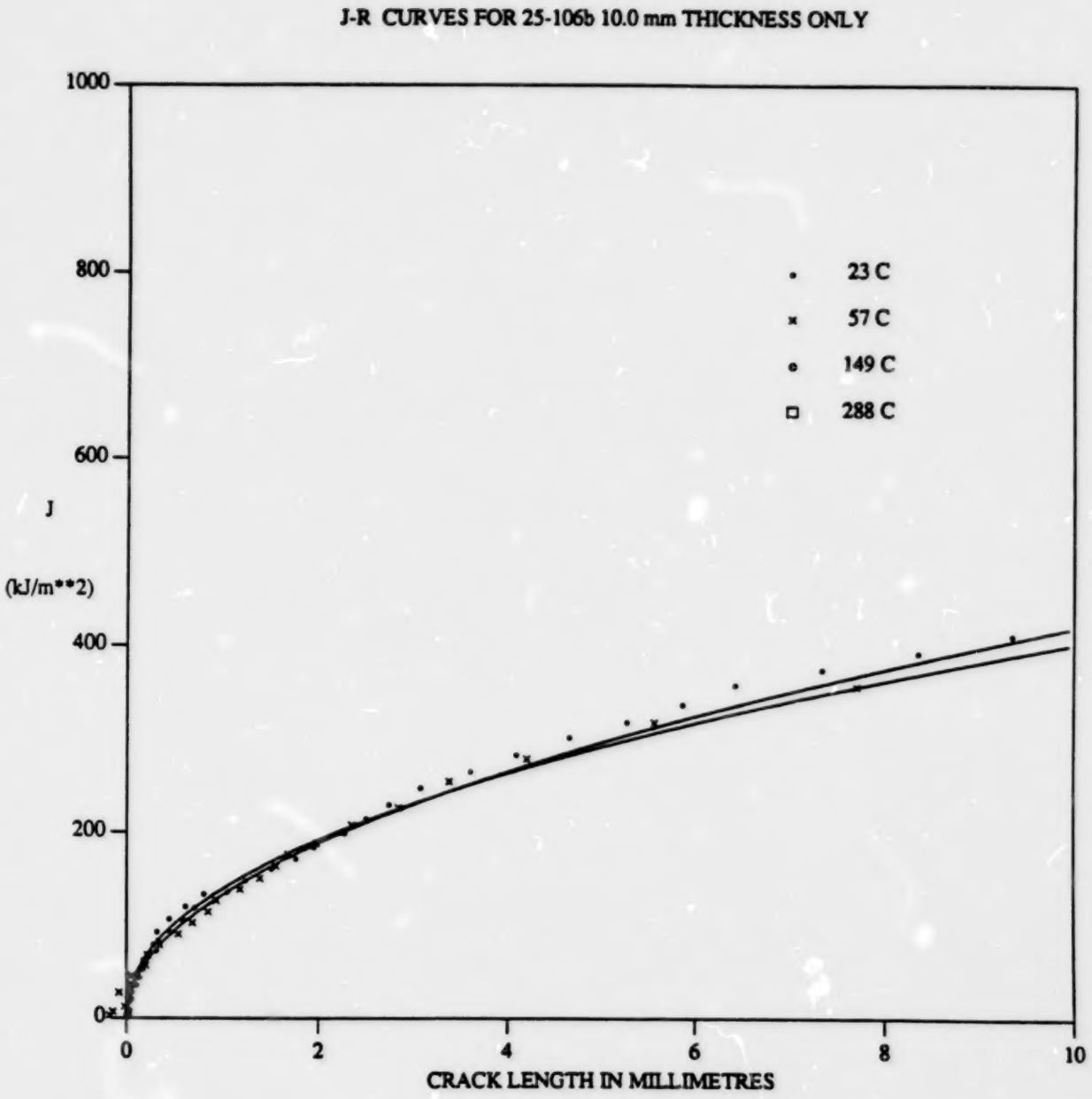
J-R CURVES FOR 25-106b 10.0 mm THICKNESS ONLY
1000
800
600
400
200
0
J
(kJ/m**2)
23 C
57 C
149 C
288 C
0
2
4
6
8
10
CRACK LENGTH IN MILLIMETRES

Figure B-13

Specimen Data For SA-106 Grade B Tests Specimens From Lab Group 25							
Specimen ID	Thickness (mm)	Reduced Thickness (mm)	Temperature Degrees C (mm)	J_{IC} kJ/m**2	E GPa	σ_0 MPa	σ_{uts} MPa
106B-FS1T1	10.0	8.0	23	76.9	205.9		
106B-FS1T2	10.0	8.0	23	70.0	205.9		
106B-FS2T	10.0	8.0	57	62.4	204.0		

Data for Figure B-13

L-C J-R CURVES FOR A106 SA-106 GRADE C 50.8 mm THICKNESS ONLY

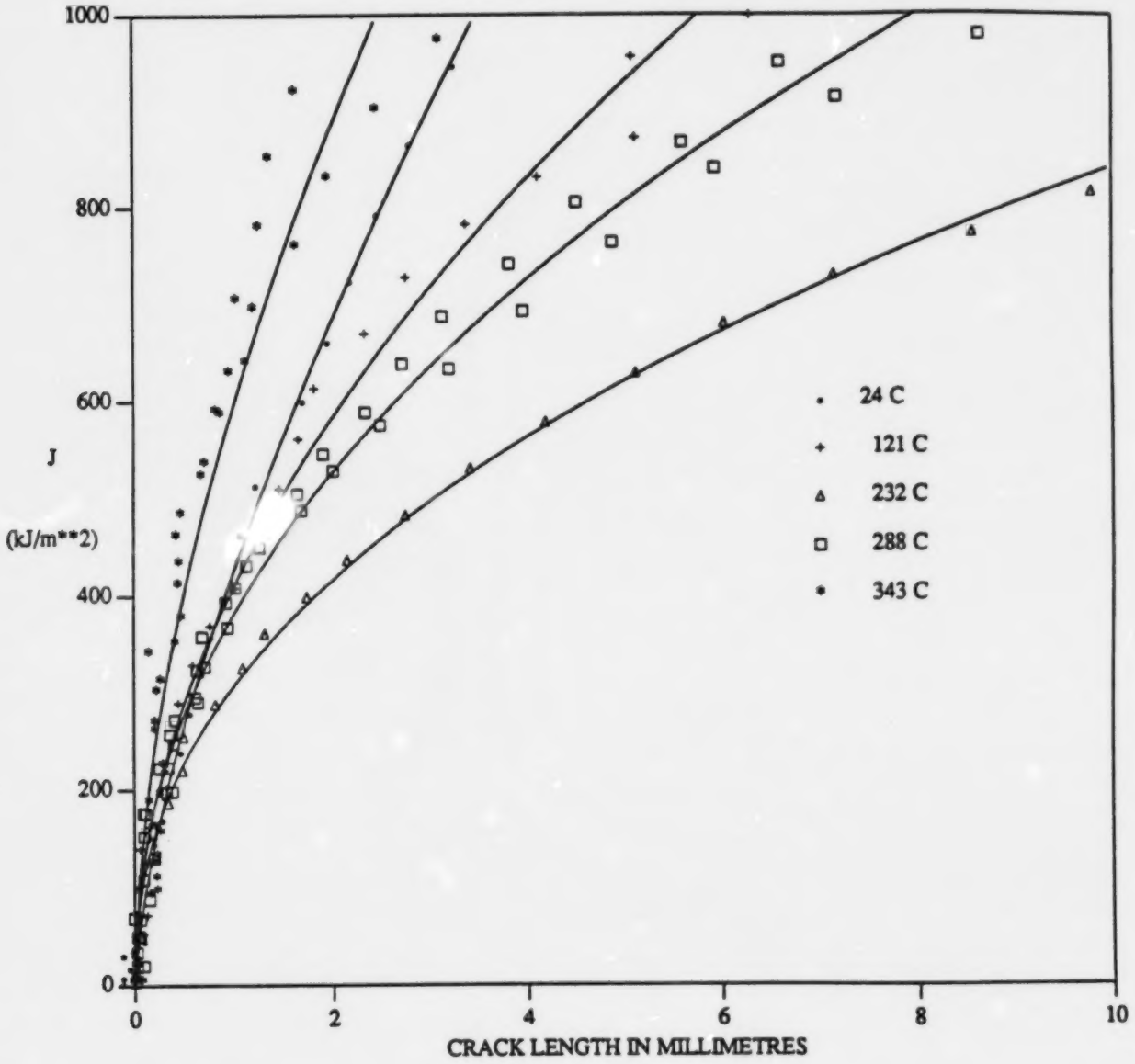

Figure B-14

Specimen Data For SA-106 Grade C Tests L-C Specimens From Lab Group 22							
Specimen ID	Thickness (mm)	Reduced Thickness (mm)	Temperature Degrees C	J_{IC} kJ/m**2	E GPa	σ_0 MPa	σ_{uts} MPa
a106-1lc	50.8	45.72	24	463.3	205.8	355.1	571.55
a106-2lc	50.8	45.72	121	445.4	200.3		
a106-3lc	50.8	45.72	232	435.1	194.0	282.0	588.1
a106-4lc	50.8	45.72	288	433.0	190.8		
a106-5lc	50.8	45.72	288	433.0	190.8		
a106-6lc	50.8	45.72	343	434.4	189.6	283.35	585.05
a106-7lc	50.8	45.72	343	434.4	189.6	283.35	585.05

Data for Figure B-14

J-R CURVES FOR F13 L-C ORIENTATION 9.0 mm THICKNESS ONLY

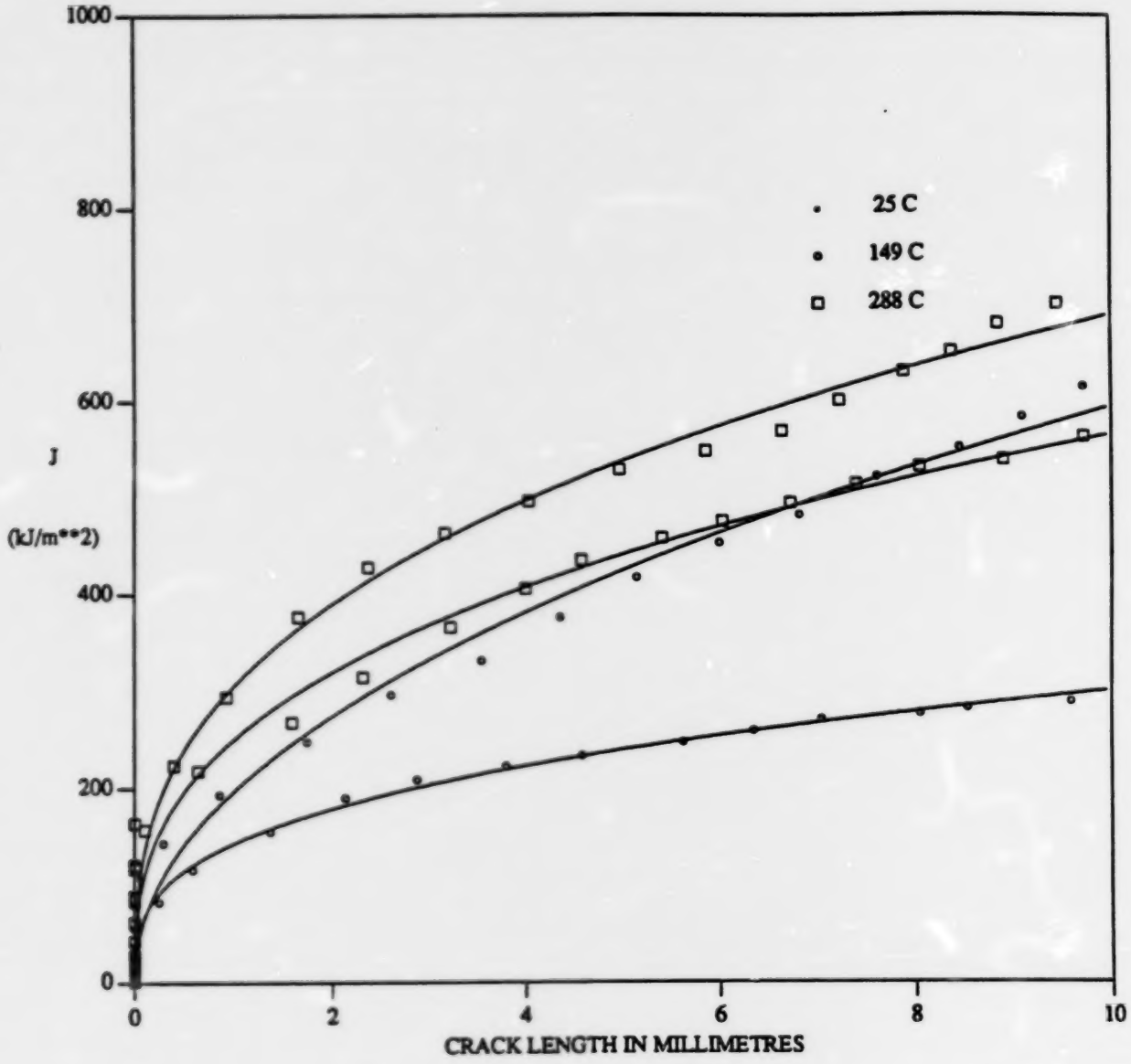

Figure B-15

Specimen Data For SA-106 Grade B Tests L-C Specimens From Lab Group 51							
Specimen ID	Thickness (mm)	Reduced Thickness (mm)	Temperature Degrees C	J_{IC} kJ/m**2	E GPa	σ_0 MPa	σ_{uts} MPa
f13-17	9.0	9.0	149	91.0	198.7	326.0	622.0
f13-18	9.0	8.0	149	137.0	198.7	326.0	622.0
f13-19	9.0	9.0	288	175.0	190.8	261.0	611.0
f13-20	9.0	8.0	288	138.0	190.8	261.0	611.0

Data for Figure B-15

J-R CURVES FOR F29 L-C ORIENTATION 21.0 mm THICKNESS ONLY

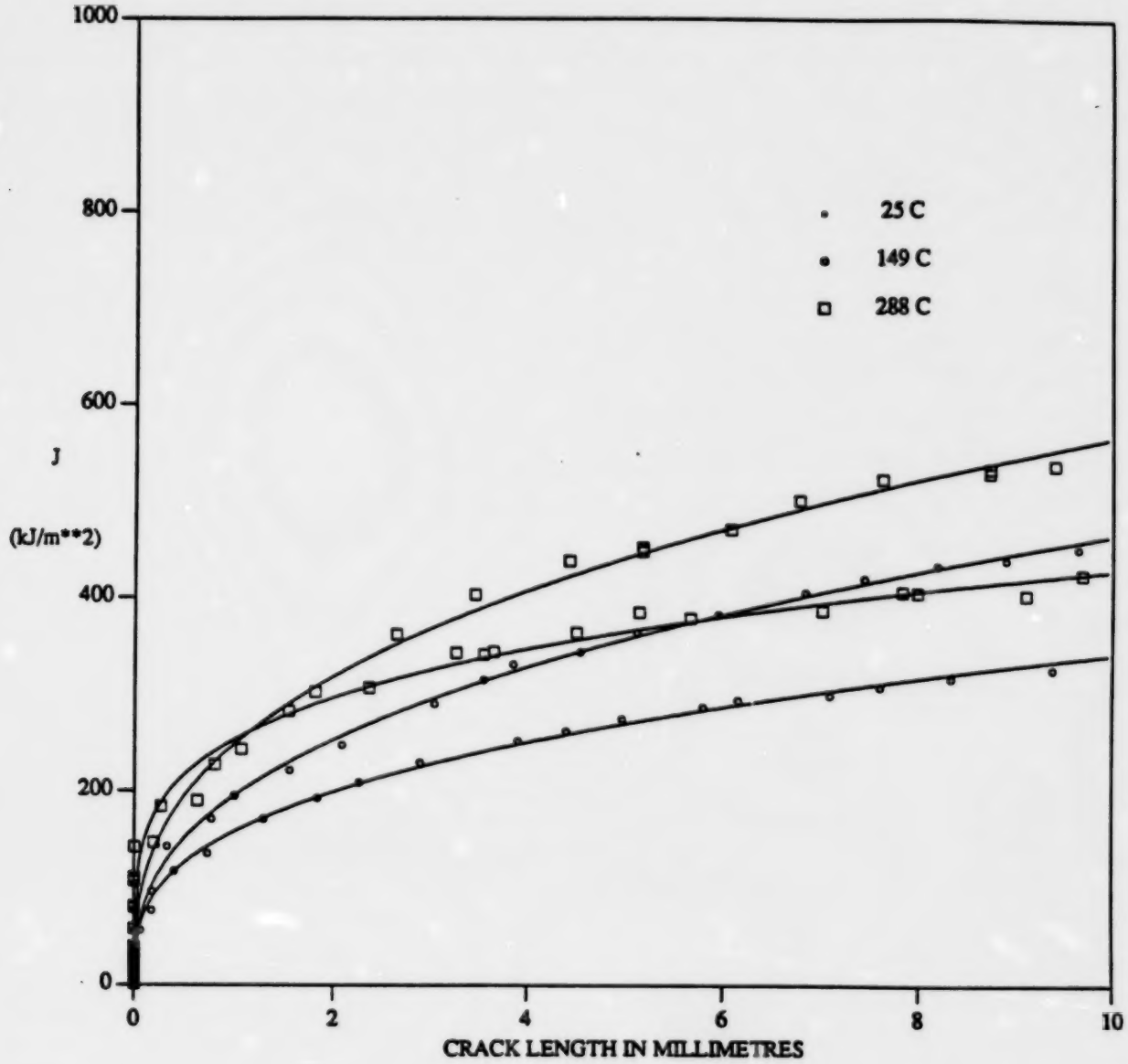

Figure B-16

Specimen Data For SA-106 Grade B Tests L-C Specimens From Lab Group 53							
Specimen ID	Thickness (mm)	Reduced Thickness (mm)	Temperature Degrees C	J_{IC} kJ/m**2	E GPa	σ_0 MPa	σ_{ult} MPa
f29-17	21.0	21.0	288	111.0	190.8	236.5	609.5
f29-18	21.0	17.0	288	149.0	190.8	236.5	609.5
f29-19	21.0	21.0	149	116.0	198.7	251.5	602.5
f29-20	21.0	17.0	149	52.0	198.7	251.5	602.5

Data for Figure B-16

J-R CURVES FOR F-45 L-C ORIENTATION 12.0 mm THICKNESS ONLY

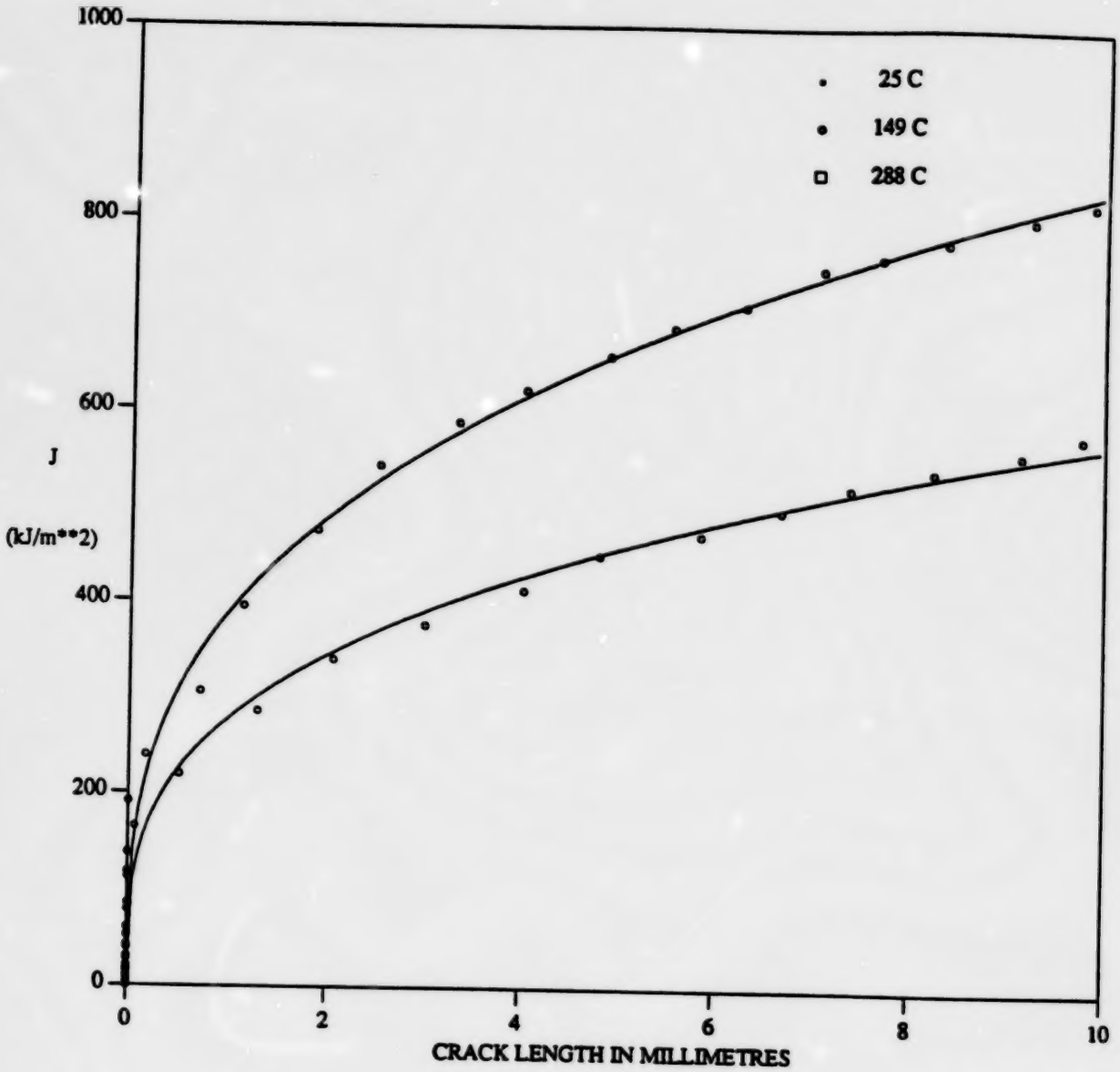

Figure B-17

Specimen Data For SA-106 Grade B Tests L-C Specimens From Lab Group 45							
Specimen ID	Thickness (mm)	Reduced Thickness (mm)	Temperature Degrees C	J_{IC} kJ/m**2	E GPa	σ_0 MPa	σ_{uts} MPa
f45-18	12.0	12.0	149	153.0	197.8	300.5	652
f45-20	12.0	12.0	149	203.0	197.8	300.5	652

Data for Figure B-17

Specimen Data For SA-106 Grade B Tests
J-R and Ramburg-Osgood Constants for Miscellaneous Data

Specimen ID	Temp. Deg. C	*J–R* Exponent	*J–R* Constant	Hardening Exponent	Alpha Constant	E GPa
epcs-1	52	0.347	159.40	NA	NA	204.2
epcs-2	23	0.400	162.86	"	"	205.9
epcs-3	"	"	"	"	"	"
epcs-4	"	"	"	"	"	"
106b-f1t1	23	0.488	130.92	NA	NA	205.9
106b-f1t2	"	"	"	"	"	"
106b-f2t	57	0.638	104.52	"	"	204.0
106b-fs1t1	23	0.495	139.47	NA	NA	205.9
106b-fs1t2	"	"	"	"	"	"
106b-fs2t	57	0.498	133.08	"	"	204.0
a106-1lc	24	0.682	426.31	NA	NA	205.8
a106-2lc	121	0.508	410.36	"	"	200.3
a106-3lc	232	0.436	307.97	"	"	194.0
a106-4lc	288	0.463	382.24	"	"	190.8
a106-5lc	"	"	"	"	"	"
a106-6lc	343	0.569	596.47	"	"	189.6
a106-7lc	"	"	"	"	"	"
f13-17	149	0.480	196.62	4.453	2.57	198.7
f13-18	"	0.322	143.19	"	"	"
f13-19	288	0.354	304.99	4.136	2.44	190.8
f13-20	"	0.354	250.06	"	"	"
f29-17	288	0.357	248.61	4.193	1.30	190.8
f29-18	"	0.227	253.50	"	"	"
f29-19	149	0.376	195.21	5.359	0.39	198.7
f29-20	"	0.334	158.13	"	"	"
f45-18	149	0.309	278.40	4.260	2.27	198.7
f45-20	"	0.330	388.87	"	"	"

Table B-3

F13-3L F13-4L (149 C)
TRUE STRESS versus TRUE STRAIN FOR F13 MATERIAL
LONGITUDINAL ORIENTATION SPECIMENS

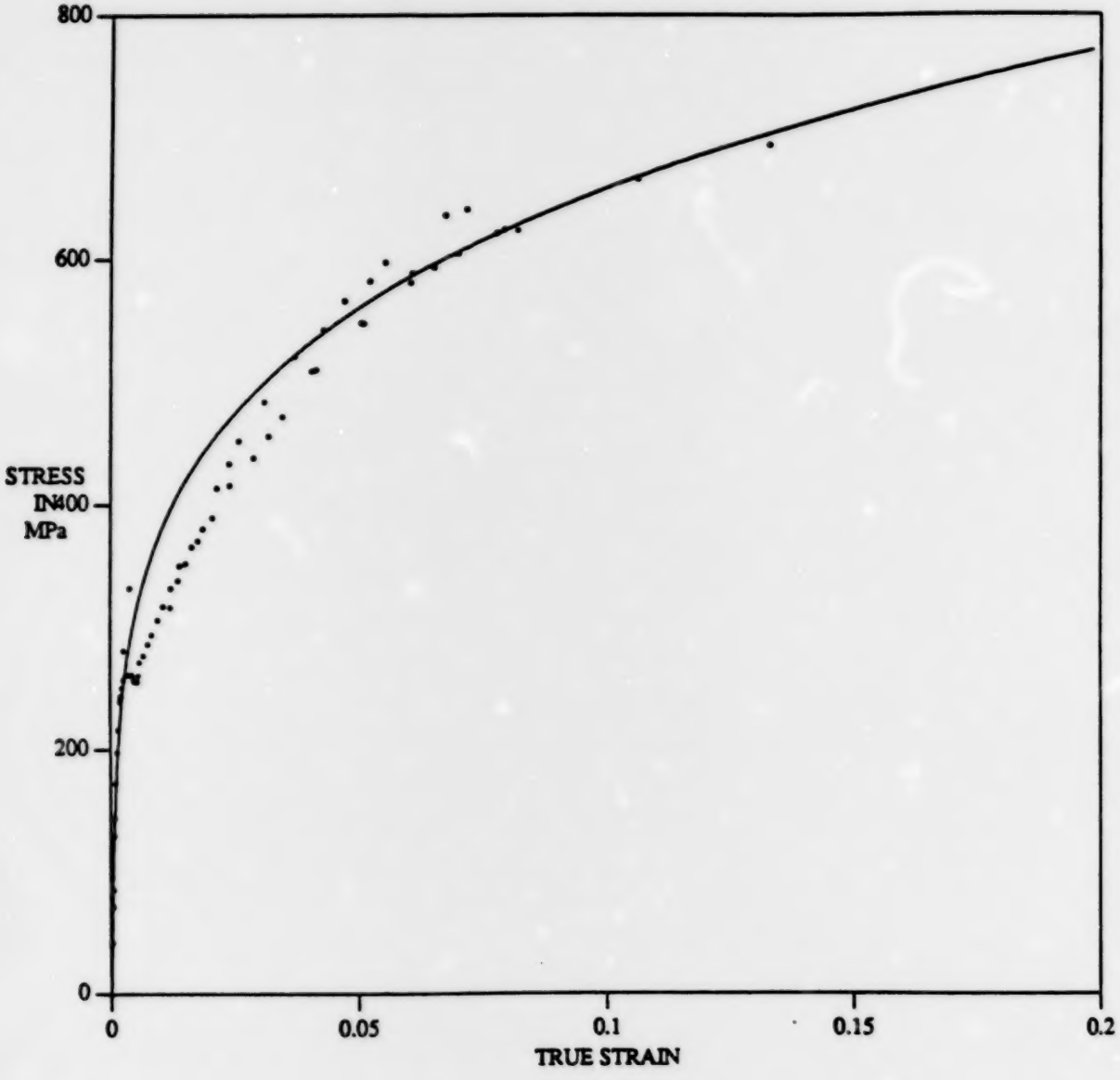

Figure B-18(a)

F13-5L F13-6L (288 C)
TRUE STRESS versus TRUE STRAIN FOR F13 MATERIAL
LONGITUDINAL ORIENTATION SPECIMENS

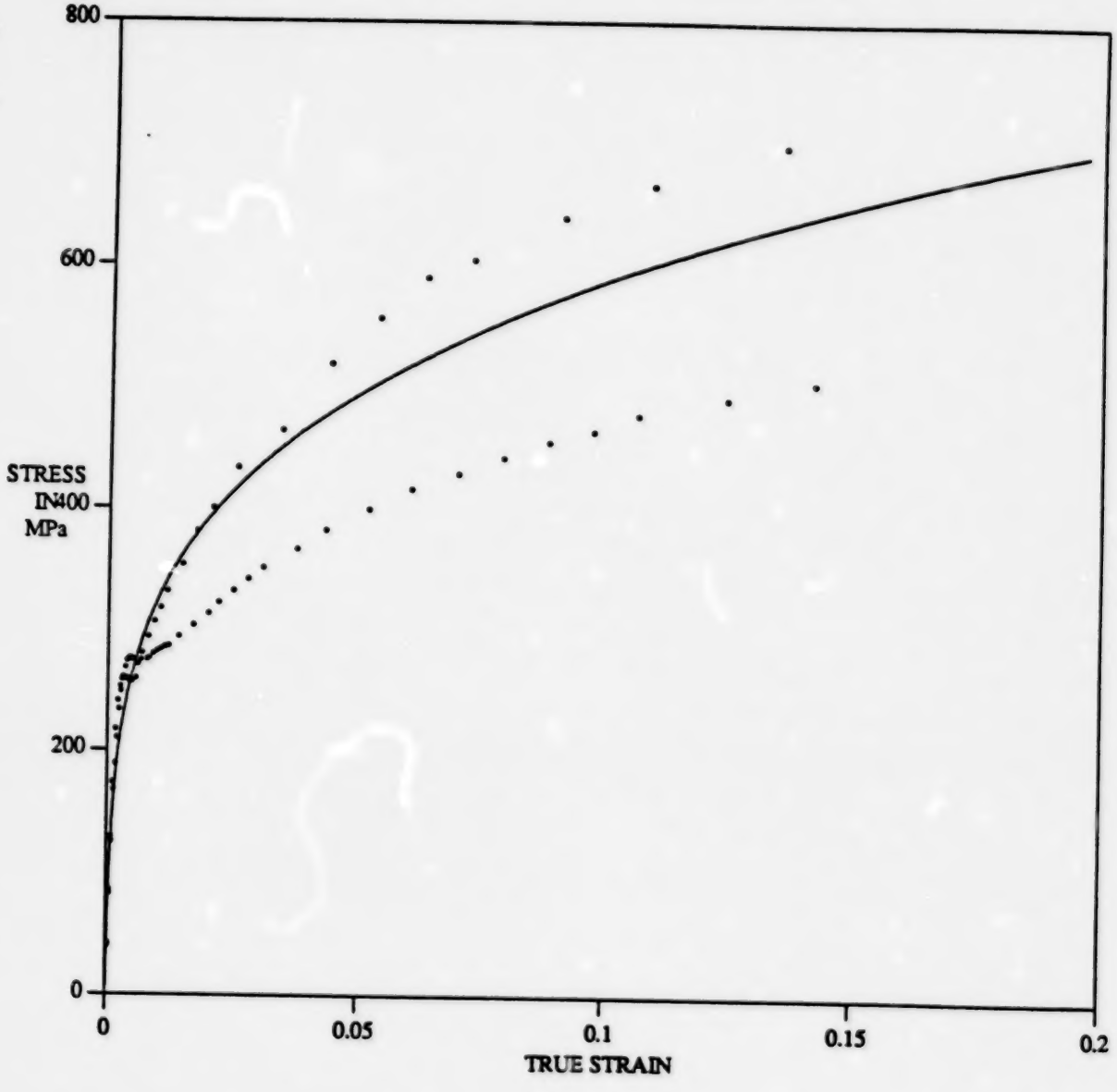

Figure B-18(b)

F29-3L F29-4L (149 C)
TRUE STRESS versus TRUE STRAIN FOR F29 MATERIAL
LONGITUDINAL ORIENTATION SPECIMENS

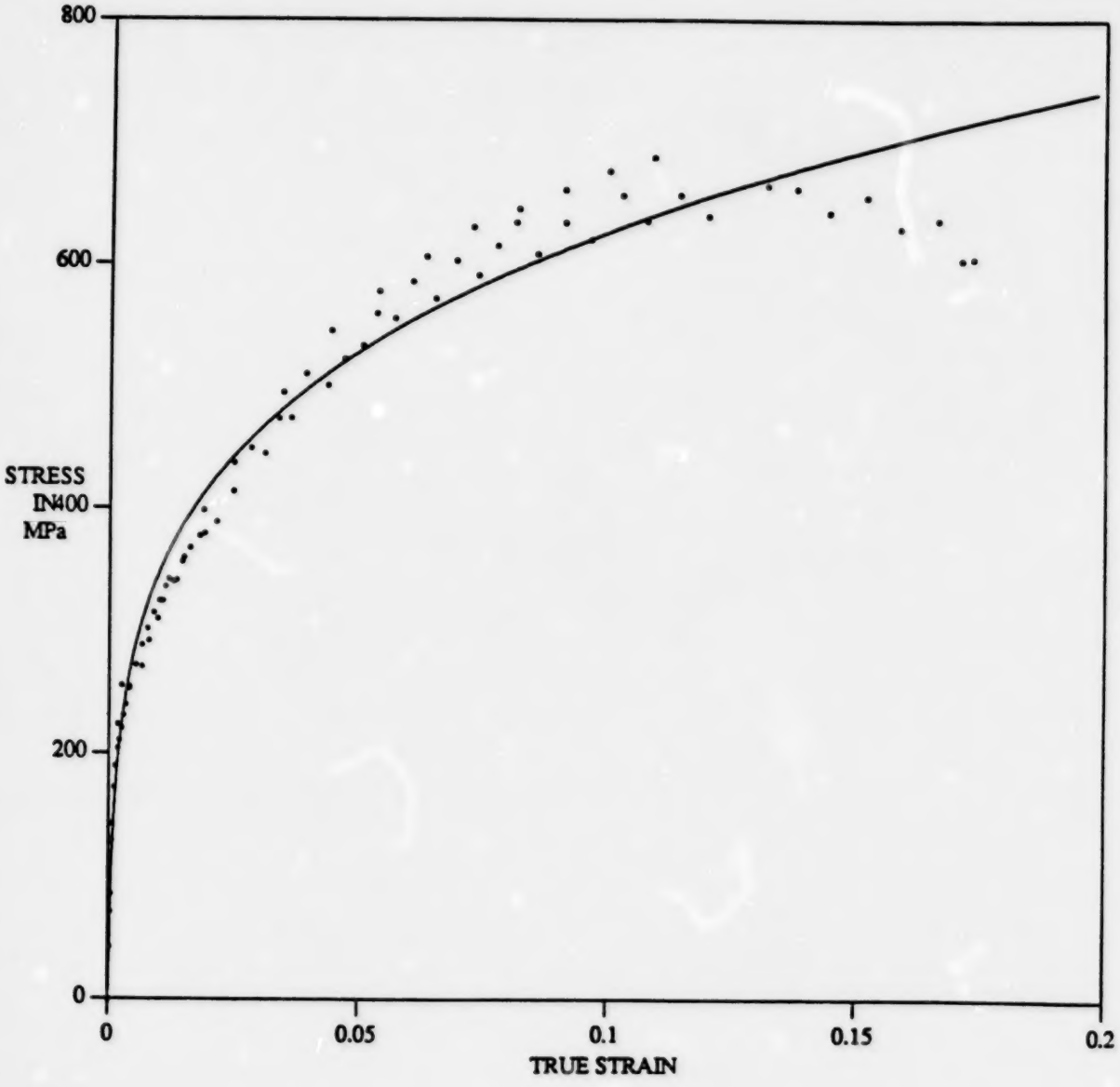

Figure B-19(a)

F29-5L F29-6L (288 C)
TRUE STRESS versus TRUE STRAIN FOR F29 MATERIAL
LONGITUDINAL ORIENTATION SPECIMENS

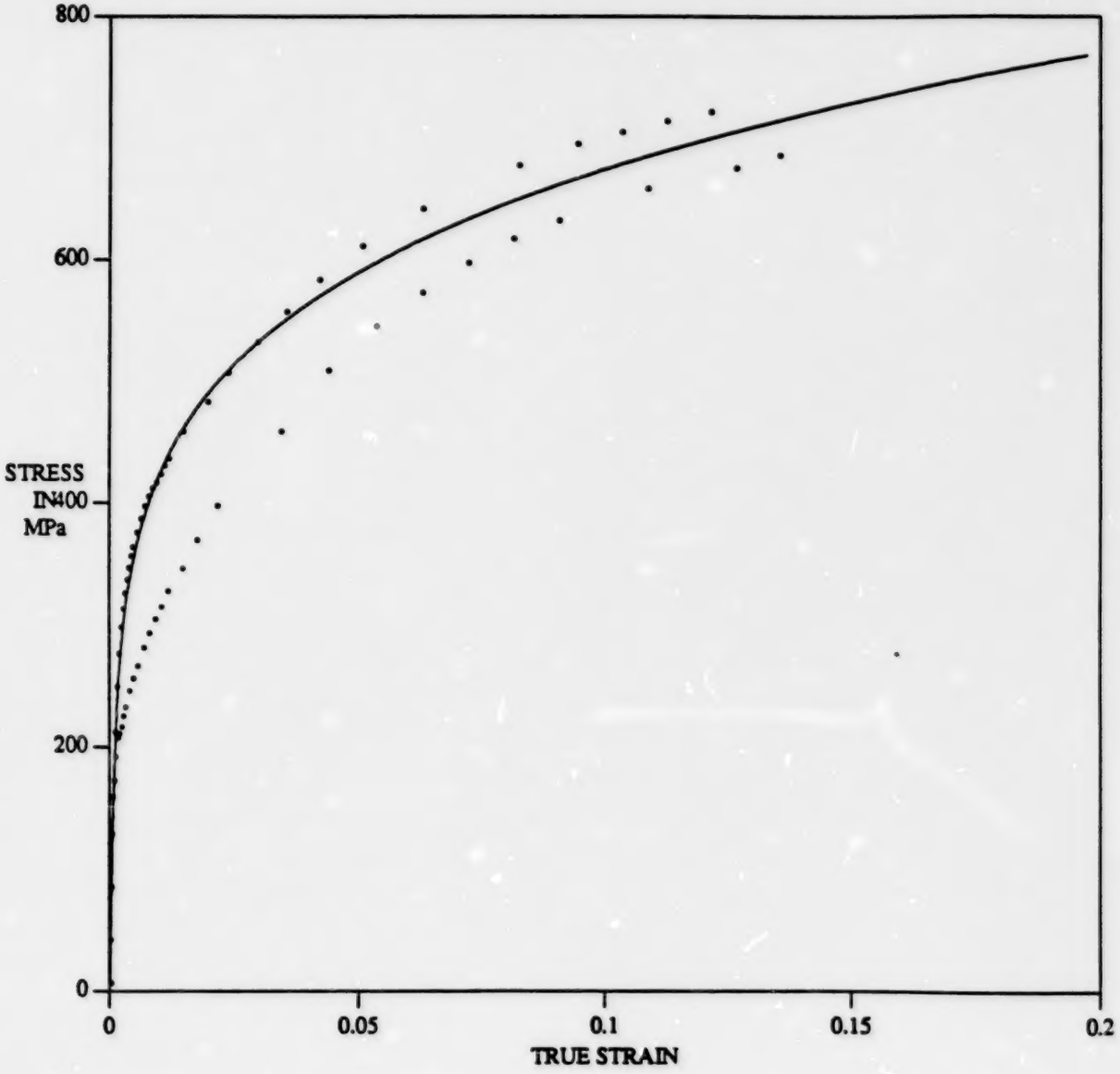

Figure B-19(b)

F45-3L F45-4L (149 C)
TRUE STRESS versus TRUE STRAIN FOR F45 MATERIAL
LONGITUDINAL ORIENTATION SPECIMENS

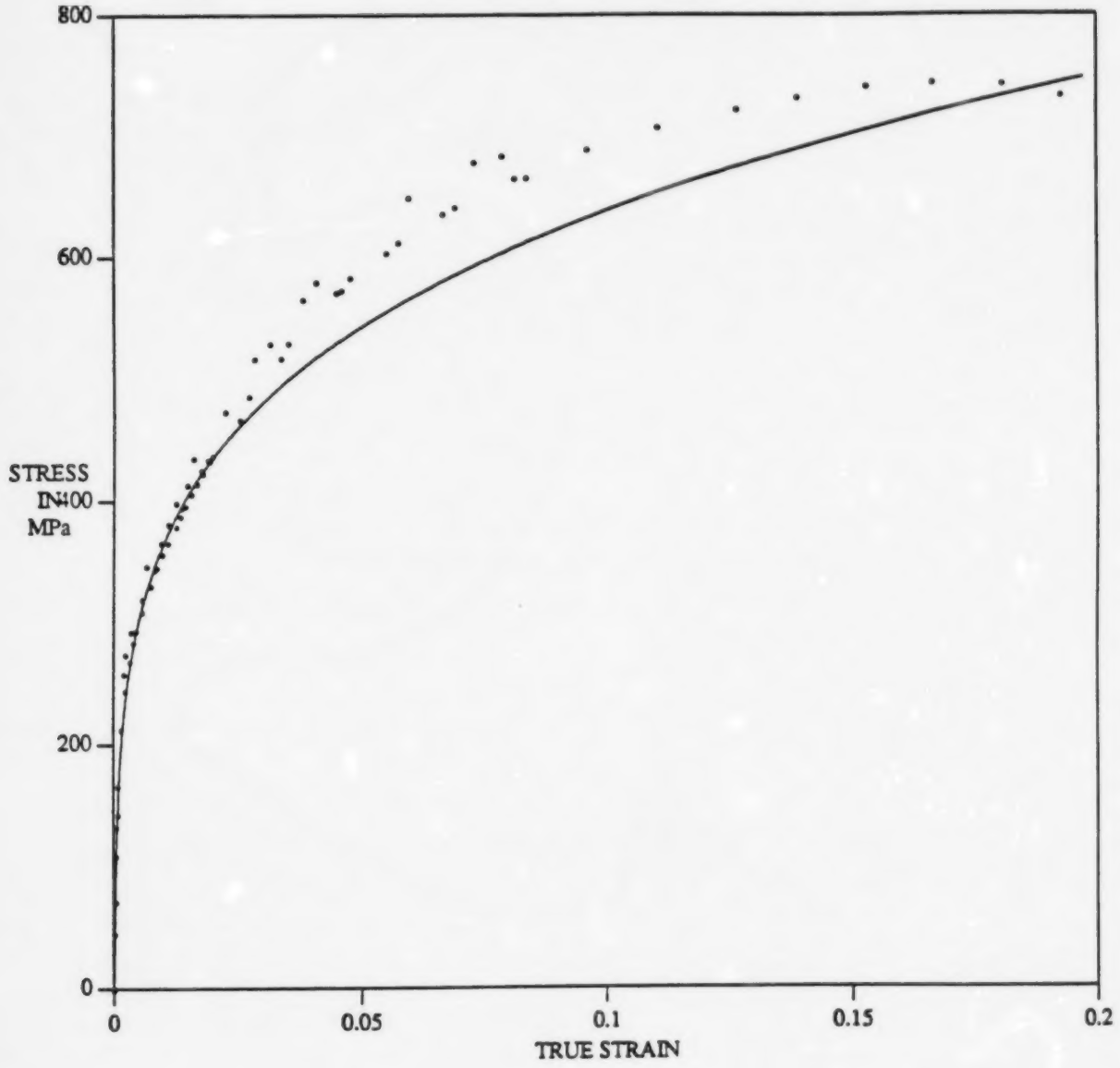

Figure B-20

APPENDIX C

TEST DATA FROM AECB INFO-0254-1

The experimental data obtained from the study "Crack Propagation in Tough Ductile Materials (Phase 1) AECB INFO-0254-1" are presented in this Appendix. It should be noted that this data was derived from load control tests on compact tension specimens of thickness 12.7 mm, 25.4 mm and 31.75 mm respectively. All tests were undertaken at approximately 23°C (room temperature) for both the *L–C* and *C–L* orientations.

The results are presented on the standardized format; the *J–R* curves are extrapolations based on the best fit obtained through the data points.

Summary

Figure C-1	University of Toronto tests	C-L	orientation	12.7 mm
Figure C-2	University of Toronto tests	L-C	orientation	12.7 mm
Figure C-3	University of Toronto tests	C-L	orientation	25.4 mm
Figure C-4	University of Toronto tests	L-C	orientation	25.4 mm
Figure C-5	University of Toronto tests	C-L	orientation	31.7 mm
Figure C-6	University of Toronto tests	L-C	orientation	31.7 mm

J-R CURVES FOR U of T TESTS C-L TYPE 12.7 mm THICKNESS ONLY

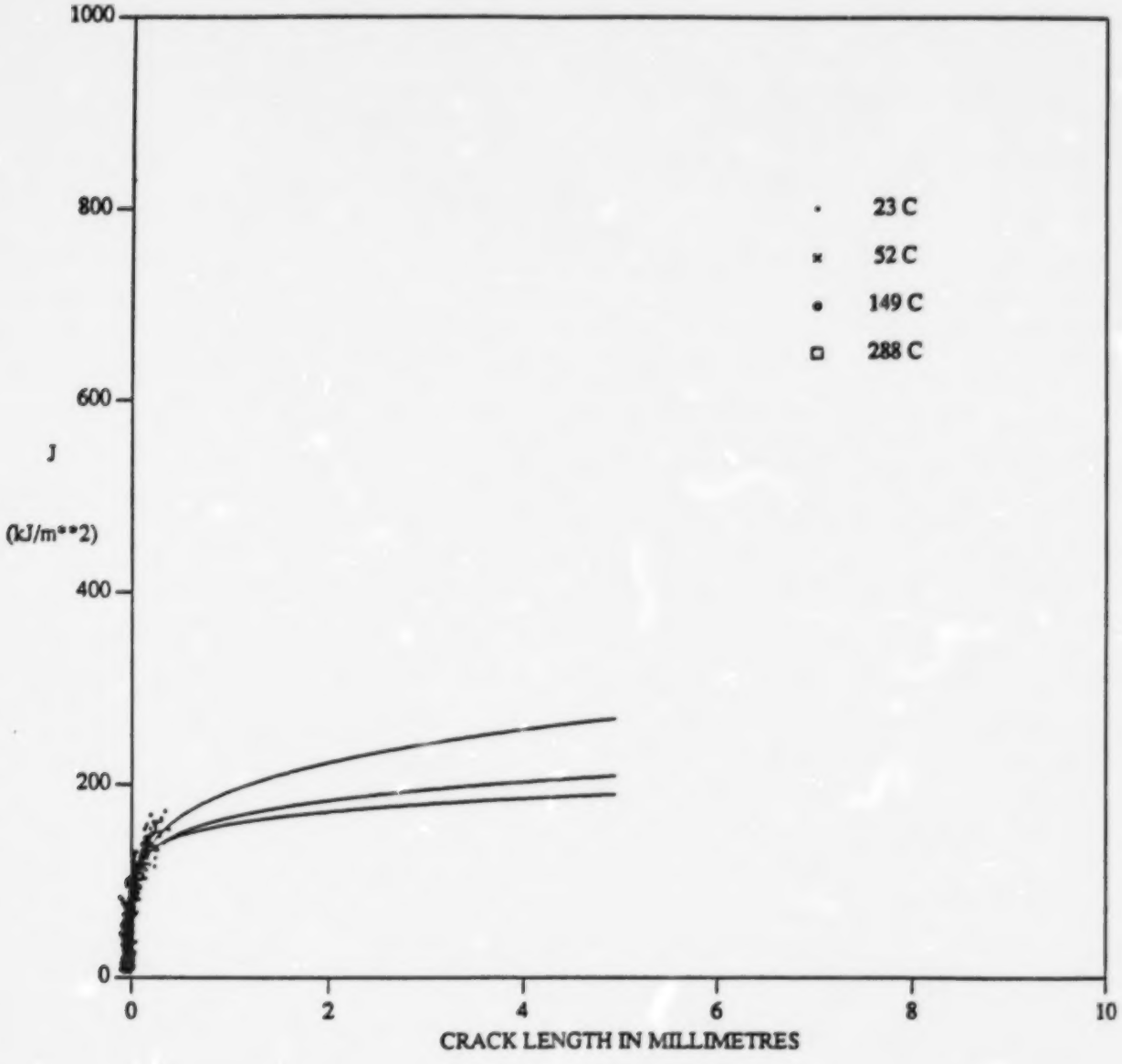

Figure C-1

Specimen Data For SA-106 Grade B Tests 12.7 mm C-L Specimens From U of T Tests							
Specimen ID	Thickness (mm)	Reduced Thickness (mm)	Temperature Degrees C	J_{IC} kJ/m**2	E GPa	σ_0 MPa	σ_{uts} MPa
ct05.ip1	12.7	10.16	23.0		210	288	600
ct05.ip2	12.7	10.16	23.0		210	288	600
ct05.ip3	12.7	10.16	23.0		210	288	600
ct05.ip4	12.7	10.16	23.0		210	288	600
ct05.ip5	12.7	10.16	23.0		210	288	600
ct05.cp1	12.7	10.16	23.0		210	288	600
ct05.cp2	12.7	10.16	23.0		210	288	600
ct05.cp3	12.7	10.16	23.0		210	288	600
ct05.cp4	12.7	10.16	23.0		210	288	600
ct05.cp5	12.7	10.16	23.0		210	288	600
ct05.op1	12.7	10.16	23.0		210	288	600
ct05.op2	12.7	10.16	23.0		210	288	600
ct05.op3	12.7	10.16	23.0		210	288	600
ct05.op4	12.7	10.16	23.0		210	288	600
ct05.op5	12.7	10.16	23.0		210	288	600

Data for Figure C-1

J-R CURVES FOR U of T TESTS L-C TYPE 12.7 mm THICKNESS ONLY

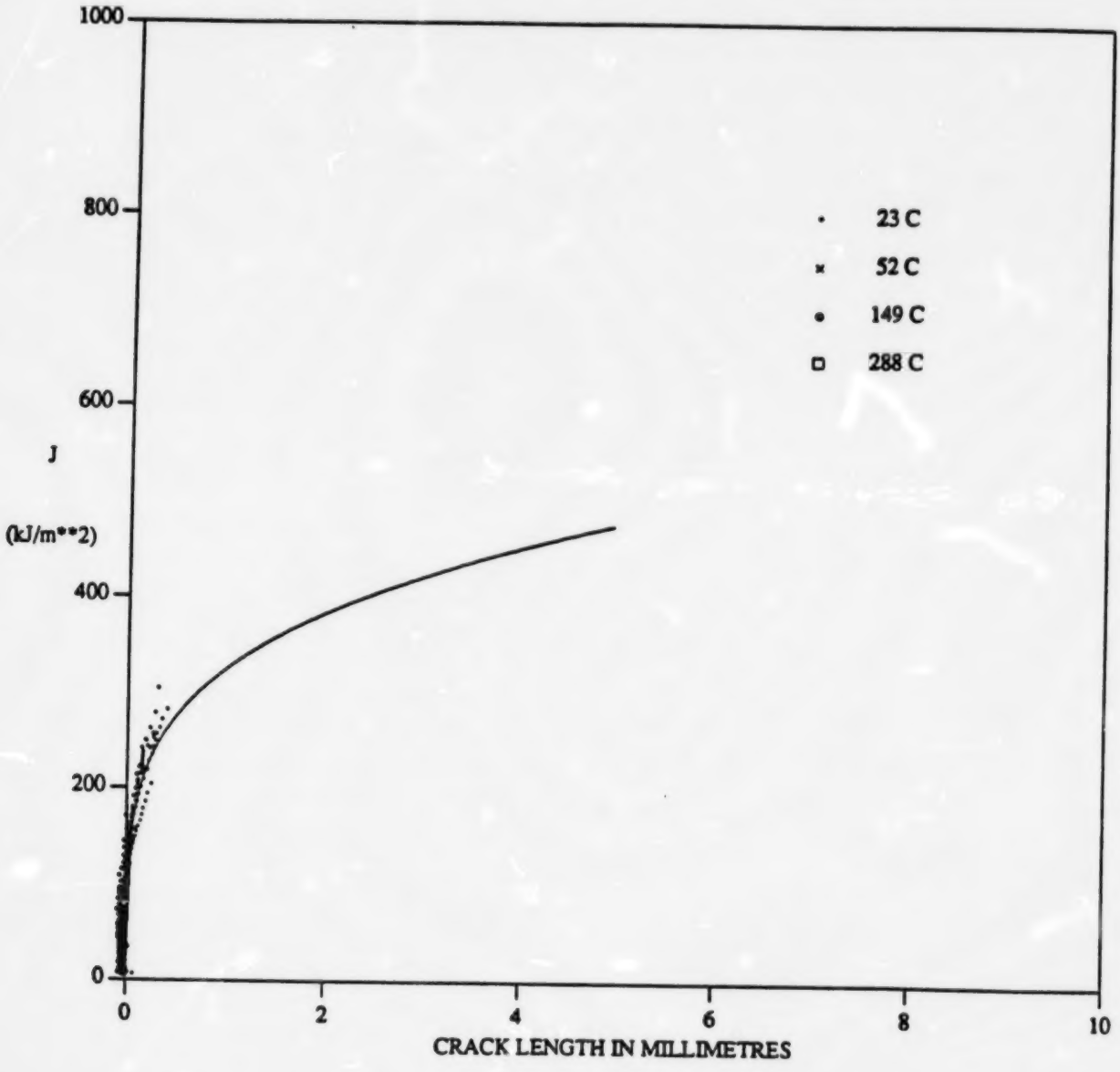

Figure C-2

Specimen Data For SA-106 Grade B Tests 12.7 mm L-C Specimens From U of T Tests							
Specimen ID	Thickness (mm)	Reduced Thickness (mm)	Temperature Degrees C	J_{IC} kJ/m**2	E GPa	σ_0 MPa	σ_{uts} MPa
ct05.b1	12.7	10.16	23.0		210	288	600
ct05.b2	12.7	10.16	23.0		210	288	600
ct05.b3	12.7	10.16	23.0		210	288	600
ct05.b4	12.7	10.16	23.0		210	288	600
ct05.b5	12.7	10.16	23.0		210	288	600
ct05.b6	12.7	10.16	23.0		210	288	600

Data for Figure C-2

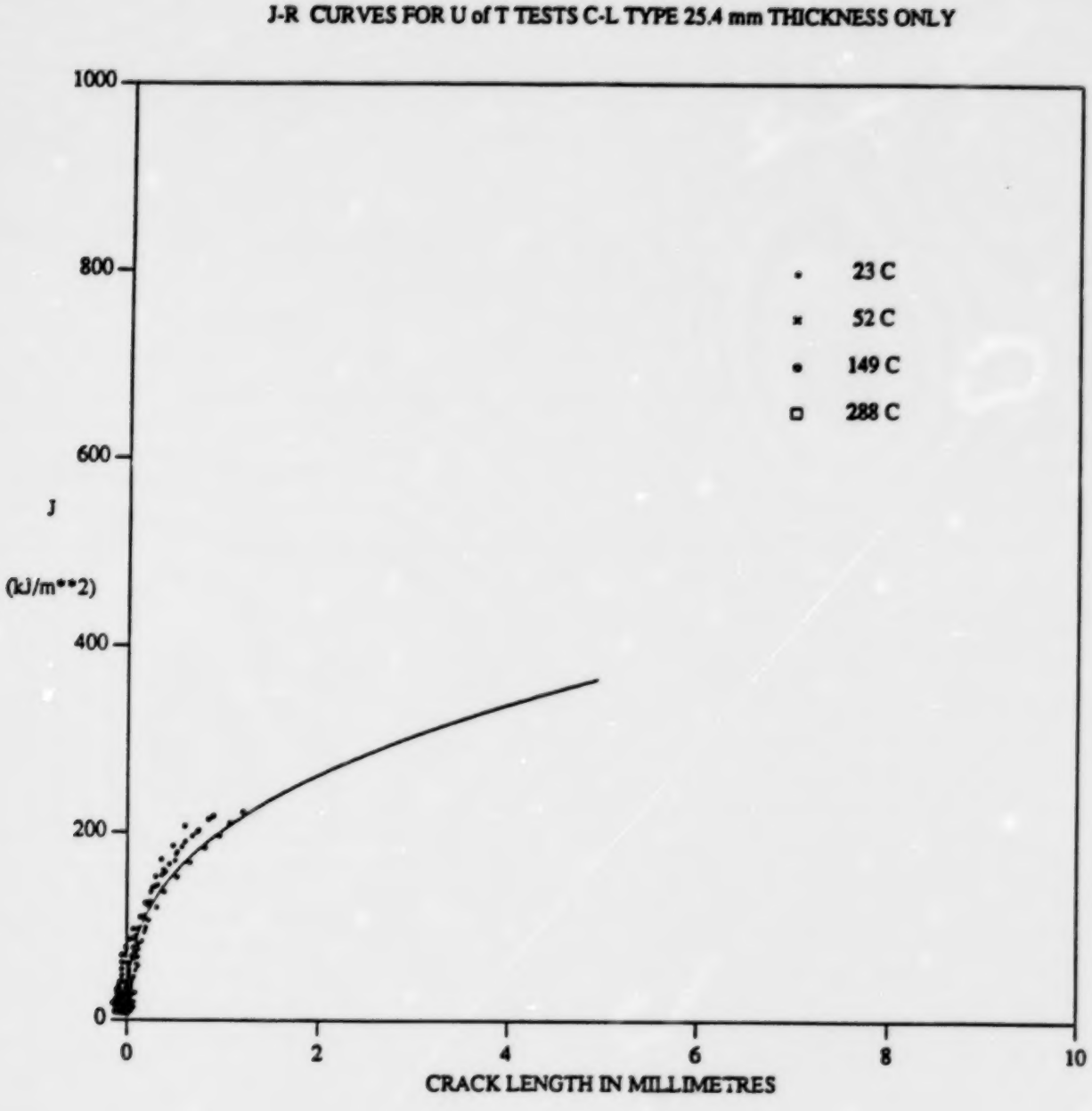
J-R CURVES FOR U of T TESTS C-L TYPE 25.4 mm THICKNESS ONLY
1000
800
600
400
200
0
J
(kJ/m**2)
23 C
52 C
149 C
288 C
0
2
4
6
8
10
CRACK LENGTH IN MILLIMETRES

Figure C-3

Specimen Data For SA-106 Grade B Tests 25.0 mm C-L Specimens From U of T Tests							
Specimen ID	Thickness (mm)	Reduced Thickness (mm)	Temperature Degrees C	J_{IC} kJ/m**2	E GPa	σ_0 MPa	σ_{uts} MPa
ct10.a1	25.4	20.32	23.0	113	210	288	600
ct10.a2	25.4	20.32	23.0	113	210	288	600
ct10.a3	25.4	20.32	23.0	113	210	288	600
ct10.a4	25.4	20.32	23.0	113	210	288	600
ct10.a5	25.4	20.32	23.0	113	210	288	600

Data for Figure C-3

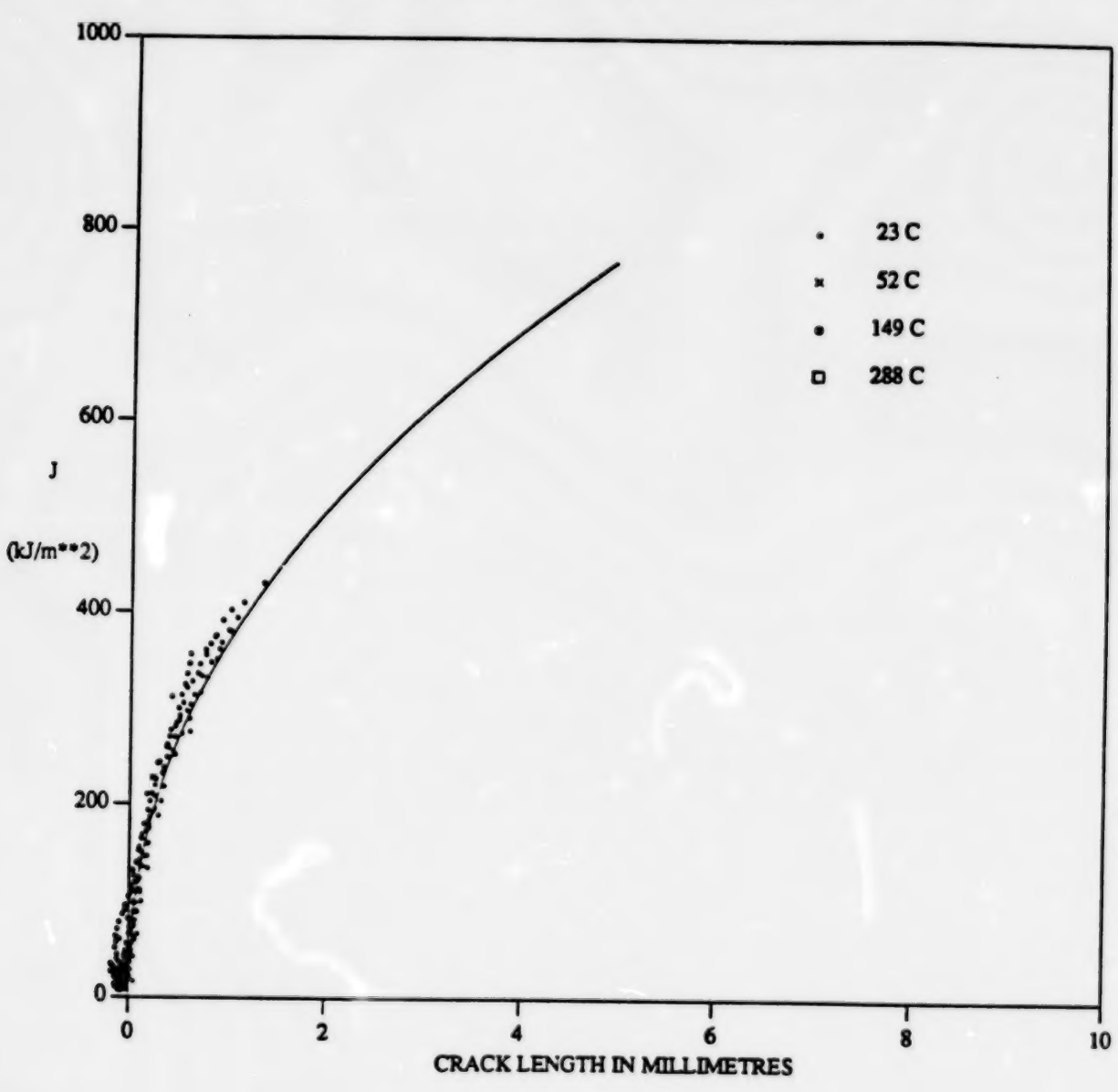
J-R CURVES FOR U of T TESTS L-C TYPE 25.4 mm THICKNESS ONLY
1000
800
600
400
200
0
J
(kJ/m**2)
23 C
52 C
149 C
288 C
0
2
4
6
8
10
CRACK LENGTH IN MILLIMETRES

Figure C-4

Specimen Data For SA-106 Grade B Tests 25.0 mm L-C Specimens From U of T Tests							
Specimen ID	Thickness (mm)	Reduced Thickness (mm)	Temperature Degrees C	J_{IC} kJ/m**2	E GPa	σ_0 MPa	σ_{uts} MPa
ct10.b1	25.4	20.32	23.0	280	210	288	600
ct10.b2	25.4	20.32	23.0	280	210	288	600
ct10.b4	25.4	20.32	23.0	280	210	288	600
ct10.b5	25.4	20.32	23.0	280	210	288	600
ct10.b6	25.4	20.32	23.0	280	210	288	600

Data for Figure C-4

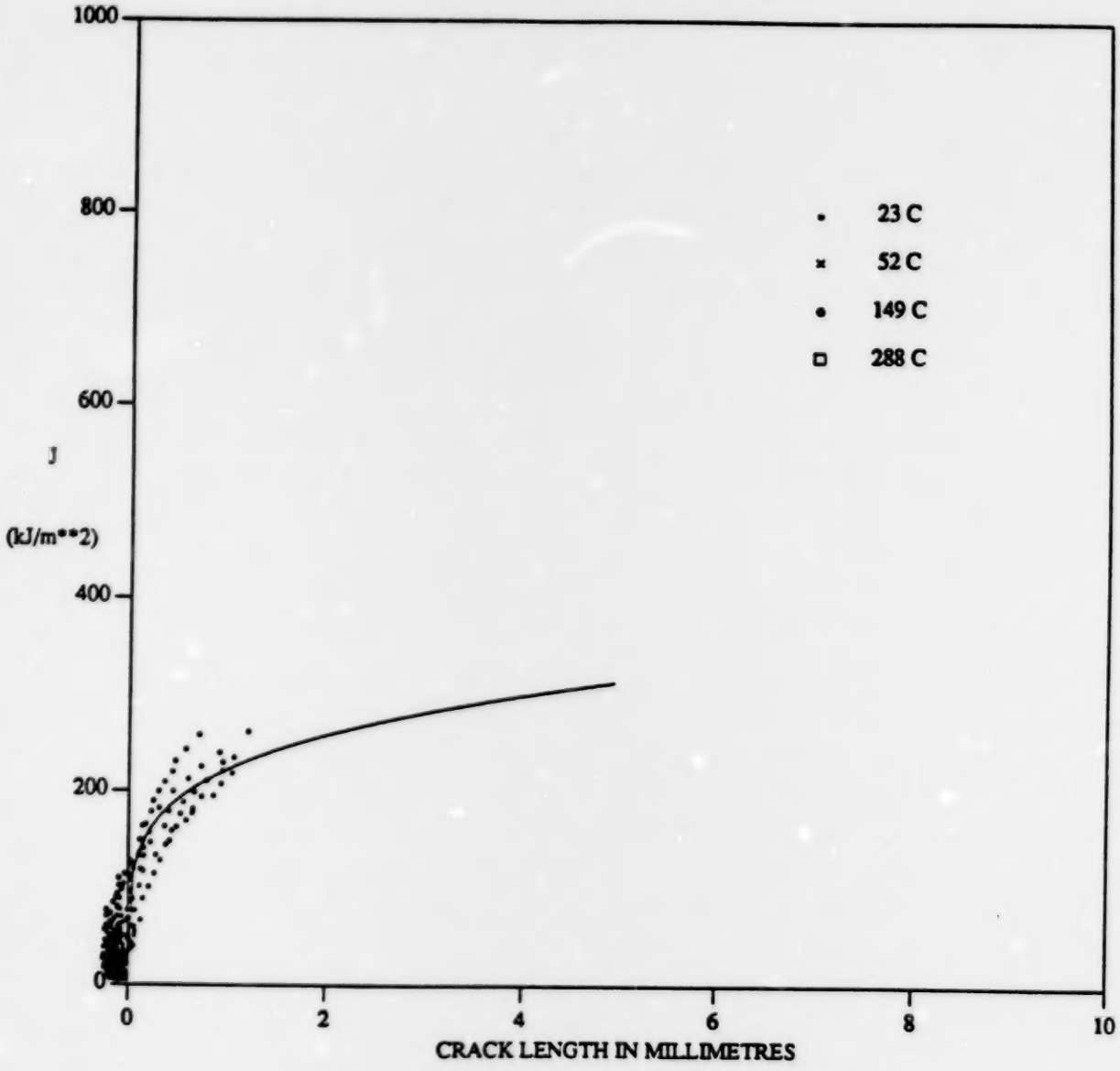
J-R CURVES FOR U of T TESTS C-L TYPE 31.75 mm THICKNESS ONLY
1000
800
600
400
200
0
J
(kJ/m**2)
23 C
52 C
149 C
288 C
0
2
4
6
8
10
CRACK LENGTH IN MILLIMETRES

Figure C-5

Specimen Data For SA-106 Grade B Tests 31.75 mm C-L Specimens From U of T Tests							
Specimen ID	Thickness (mm)	Reduced Thickness (mm)	Temperature Degrees C	J_{IC} kJ/m**2	E GPa	σ_0 MPa	σ_{us} MPa
ct15.a1	31.75	25.4	23.0	144	210	288	600
ct15.a2	31.75	25.4	23.0	144	210	288	600
ct15.a3	31.75	25.4	23.0	144	210	288	600
ct15.a4	31.75	25.4	23.0	144	210	288	600
ct15.a5	31.75	25.4	23.0	144	210	288	600
ct15.a6	31.75	25.4	23.0	144	210	288	600

Data for Figure C-5

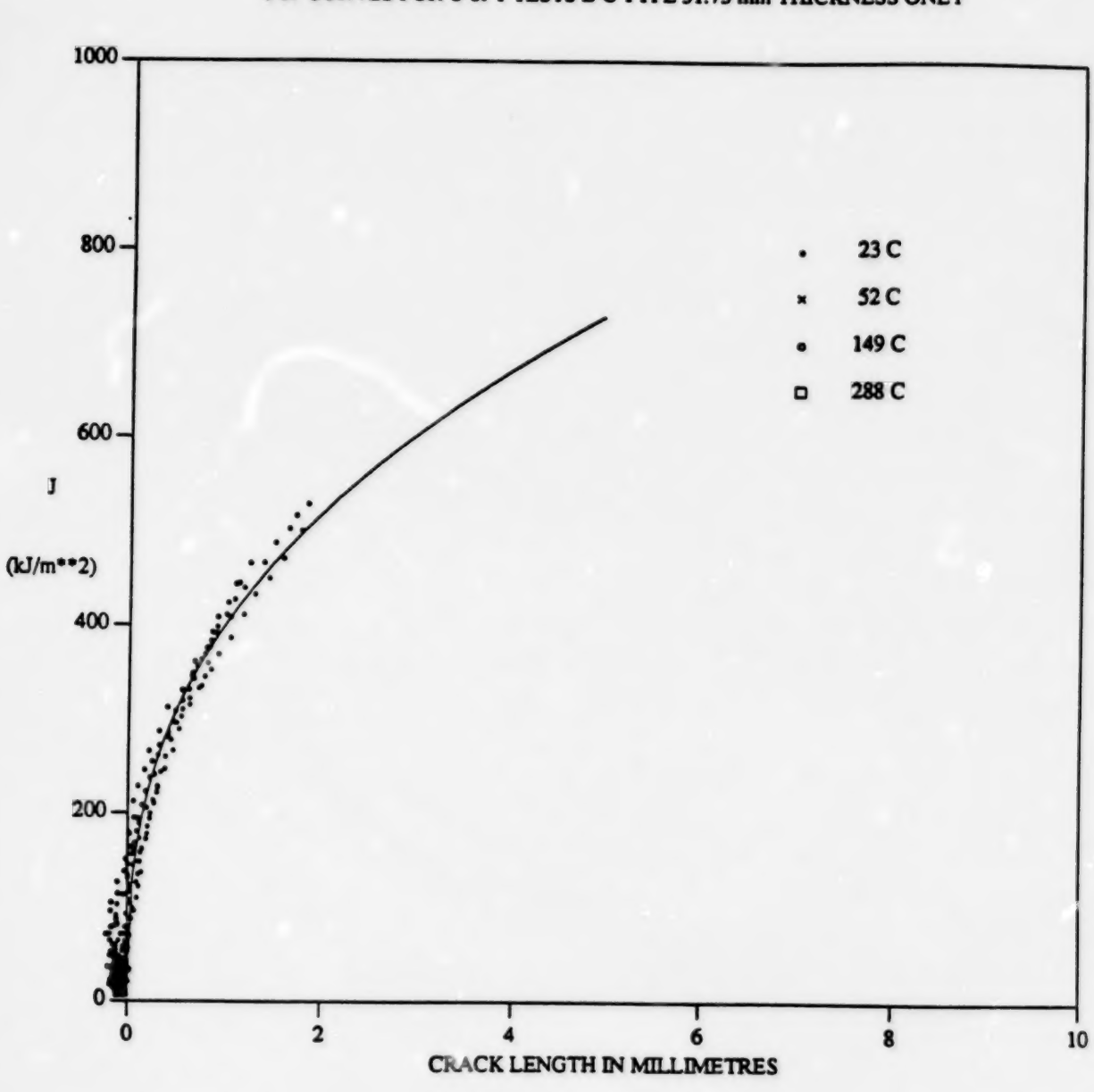
J-R CURVES FOR U of T TESTS L-C TYPE 31.75 mm THICKNESS ONLY
1000
800
600
400
200
0
J
(kJ/m**2)
23 C
52 C
149 C
288 C
0
2
4
6
8
10
CRACK LENGTH IN MILLIMETRES

Figure C-6

Specimen Data For SA-106 Grade B Tests 31.75 mm L-C Specimens From U of T Tests							
Specimen ID	Thickness (mm)	Reduced Thickness (mm)	Temperature Degrees C	J_{IC} kJ/m**2	E GPa	σ_0 MPa	σ_{uts} MPa
ct15.b1	31.75	25.4	23.0	219	210	288	600
ct15.b2	31.75	25.4	23.0	219	210	288	600
ct15.b3	31.75	25.4	23.0	219	210	288	600
ct15.b4	31.75	25.4	23.0	219	210	288	600
ct15.b5	31.75	25.4	23.0	219	210	288	600

Data for Figure C-6

APPENDIX D

ONTARIO HYDRO DATA

An additional set of data, provided from experimentation undertaken by Ontario Hydro, Canada has been assembled in this Appendix. Table D-1 provides a listing of the specimen identifications, subdivided into six groups, together with the J–R exponent and constant and the relevant Ramburg Osgoode constants. These constants were not determined from a best fit to the data, but were provided with the test data.

The J–R curves for similar type tests of approximately constant thickness have been grouped together to assess the influence of temperature and specimen orientation. These results are presented in Figures D-1 to D-6.

Summary

Figure D-1	Ontario Hydro	C-L	orientation	19.0 mm
Figure D-2	Ontario Hydro	L-C	orientation	19.0 mm
Figure D-3	Ontario Hydro	C-L	orientation	30.5 mm
Figure D-4	Ontario Hydro	L-C	orientation	30.5 mm
Figure D-5	Ontario Hydro	C-L	orientation	31.75 mm
Figure D-6	Ontario Hydro	L-C	orientation	31.75 mm

Specimen Data For SA-106 Grade B Tests

J-R and Ramburg-Osgood Constants for Ontario Hydro Data

Specimen ID	Temp. Deg. C	*J–R* Exponent	*J–R* Constant	Hardening Exponent	Alpha Constant	E GPa
j68	250	0.437	193.92	3.0104	3.1126	182.8
j69	"	"	"	"	"	"
j70						
j45	250	0.494	218.28	3.2507	3.5557	182.8
j46	"	"	"	"	"	"
j47	"	"	"	"	"	"
j63	20	0.546	180.37	4.0901	5.6549	192.3
j64	"	"	"	"	"	"
j65	250	0.427	116.7	3.5929	2.9779	182.8
j66	"	"	"	"	"	"
j67	"	"	"	"	"	"
j15	20	0.630	407.23	4.0007	5.617	192.3
j16	"	"	"	"	"	"
j17	250	0.556	215.51	3.8806	2.3106	182.8
j18	"	"	"	"	"	"
j19	"	"	"	"	"	"
td13	200	0.457	135.98	NA	NA	186.4
td14	"	"	"	"	"	"
j59	250	0.472	120.89	3.9698	3.0115	182.8
j60	"	"	"	"	"	"
j61	"	"	"	"	"	"
td15	"	"	"	"	"	"
td18	"	"	"	"	"	"
td16	300	0.453	131.92	NA	NA	178.5
td17	"	"	"	"	"	"
j1	250	0.442	259.28	5.2108	0.6345	182.8
j2	"	"	"	"	"	"
j3	"	"	"	"	"	"

Table D-1

C-L TYPE J-R CURVES FOR ONTARIO HYDRO TESTS OF 12 INCH DIAMETER NPS SCH 100 PARENT
SPECIMEN THICKNESS 19.0 mm

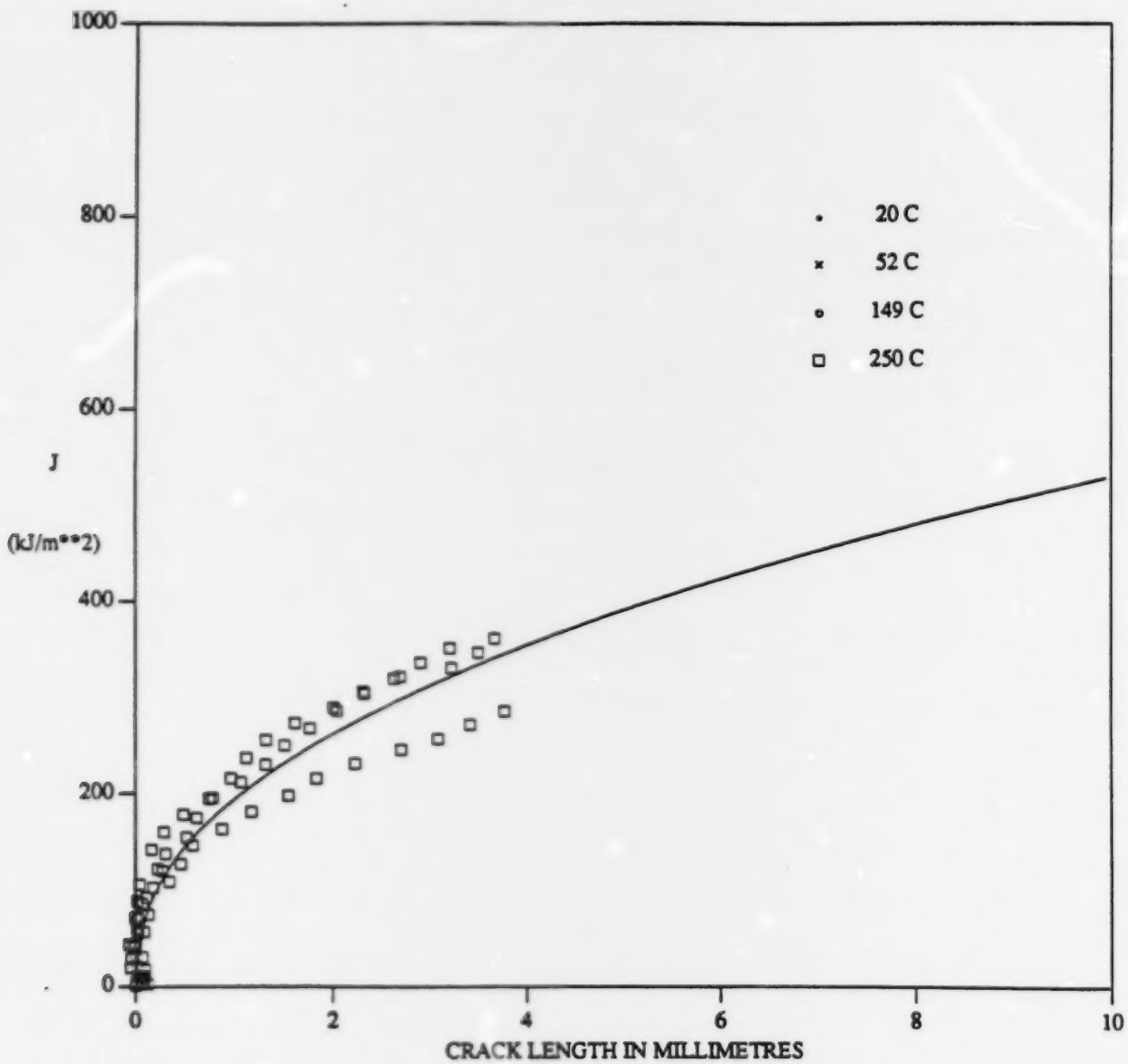

Figure D-1

Specimen Data For SA-106 Grade B Tests Ontario Hydro C-L Specimens From 12" NPS Sch 100 Pipe							
Specimen ID	Thickness (mm)	Reduced Thickness (mm)	Temperature Degrees C	J_{IC} kJ/m**2	E GPa	σ_0 MPa	σ_{MS} MPa
j68	19.05	15.16	250	102	182.8	218.0	554.9
j69	19.06	15.13	250	147	182.8	218.0	554.9
j70	19.06	15.12	250	133	182.8	218.0	554.9

Data for Figure D-1

L-C TYPE J-R CURVES FOR ONTARIO HYDRO TESTS OF 12 INCH DIAMETER NPS SCH 100 PARENT SPECIMEN THICKNESS 19.0 mm

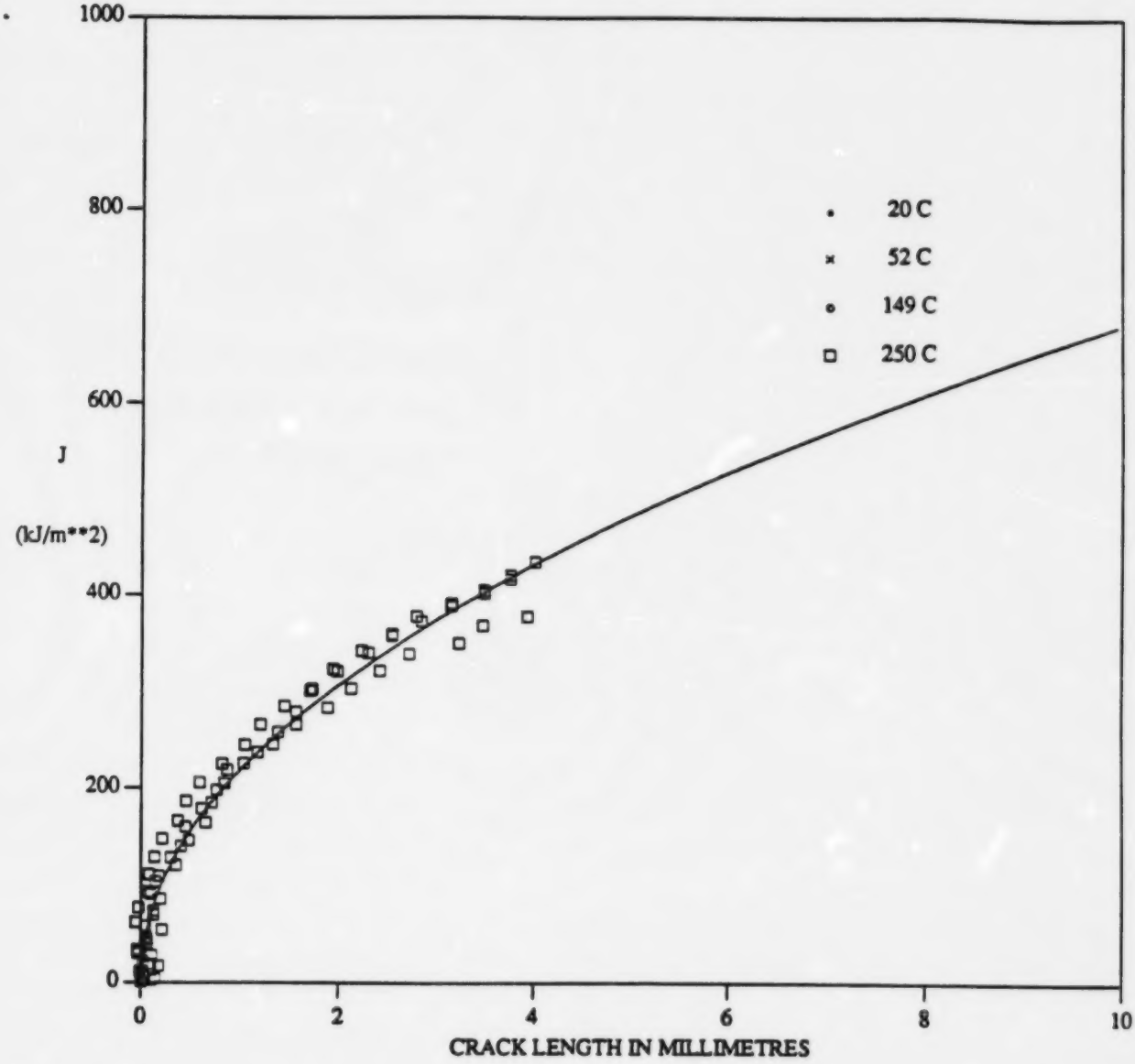

Figure D-2

Specimen Data For SA-106 Grade B Tests

Ontario Hydro L-C Specimens From 12" NPS Sch 100 Pipe

Specimen ID	Thickness (mm)	Reduced Thickness (mm)	Temperature Degrees C	J_{IC} kJ/m**2	E GPa	σ_0 MPa	σ_{uts} MPa
j45	19.0	15.20	250	131	182.8	267.3	559.3
j46	19.0	15.20	250	158	182.8	267.3	559.3
j47	19.0	15.20	250	112	182.8	267.3	559.3

Data for Figure D-2

C-L TYPE J-R CURVES FOR ONTARIO HYDRO TESTS OF 22 INCH DIAMETER NPS SCH 100 PARENT
SPECIMEN THICKNESS 30.5 mm

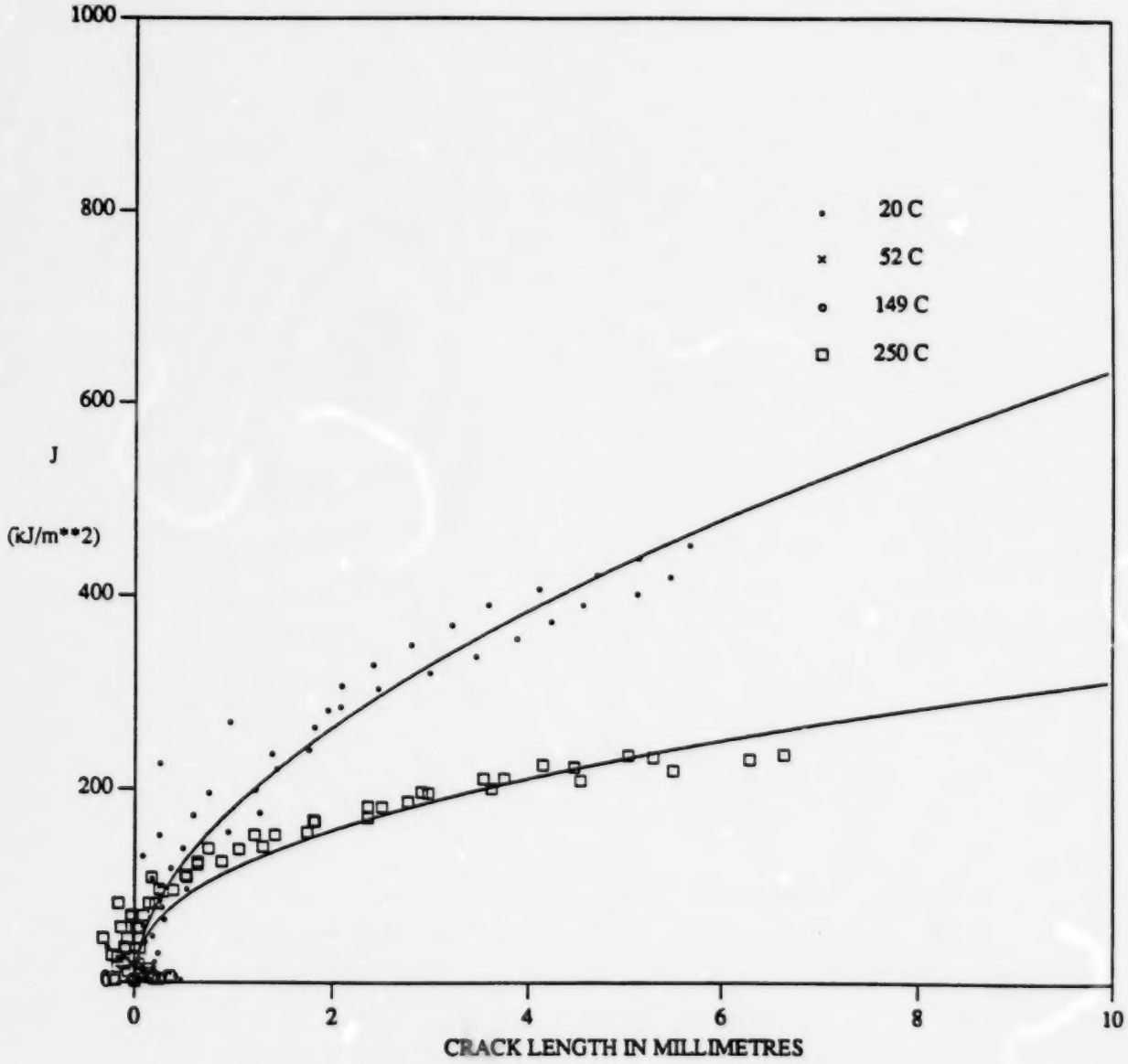

Figure D-3

Specimen Data For SA-106 Grade B Tests Ontario Hydro C-L Specimens From 22" NPS Sch 100 Pipe							
Specimen ID	Thickness (mm)	Reduced Thickness (mm)	Temperature Degrees C	J_{IC} kJ/m**2	E GPa	σ_0 MPa	σ_{uts} MPa
j63	31.5	25.76	20	190	192.3	324.0	529.5
j64	31.75	25.55	20	71	192.3	324.0	529.5
j65	31.60	25.62	250	111	182.8	224.0	506.1
j66	31.76	25.47	250	94	182.8	224.0	506.1
j67	31.77	25.38	250	86	182.8	224.0	506.1

Data for Figure D-3

L-C TYPE J-R CURVES FOR ONTARIO HYDRO TESTS OF 22 INCH DIAMETER NPS SCH 100 PARENT SPECIMEN THICKNESS 30.5 mm

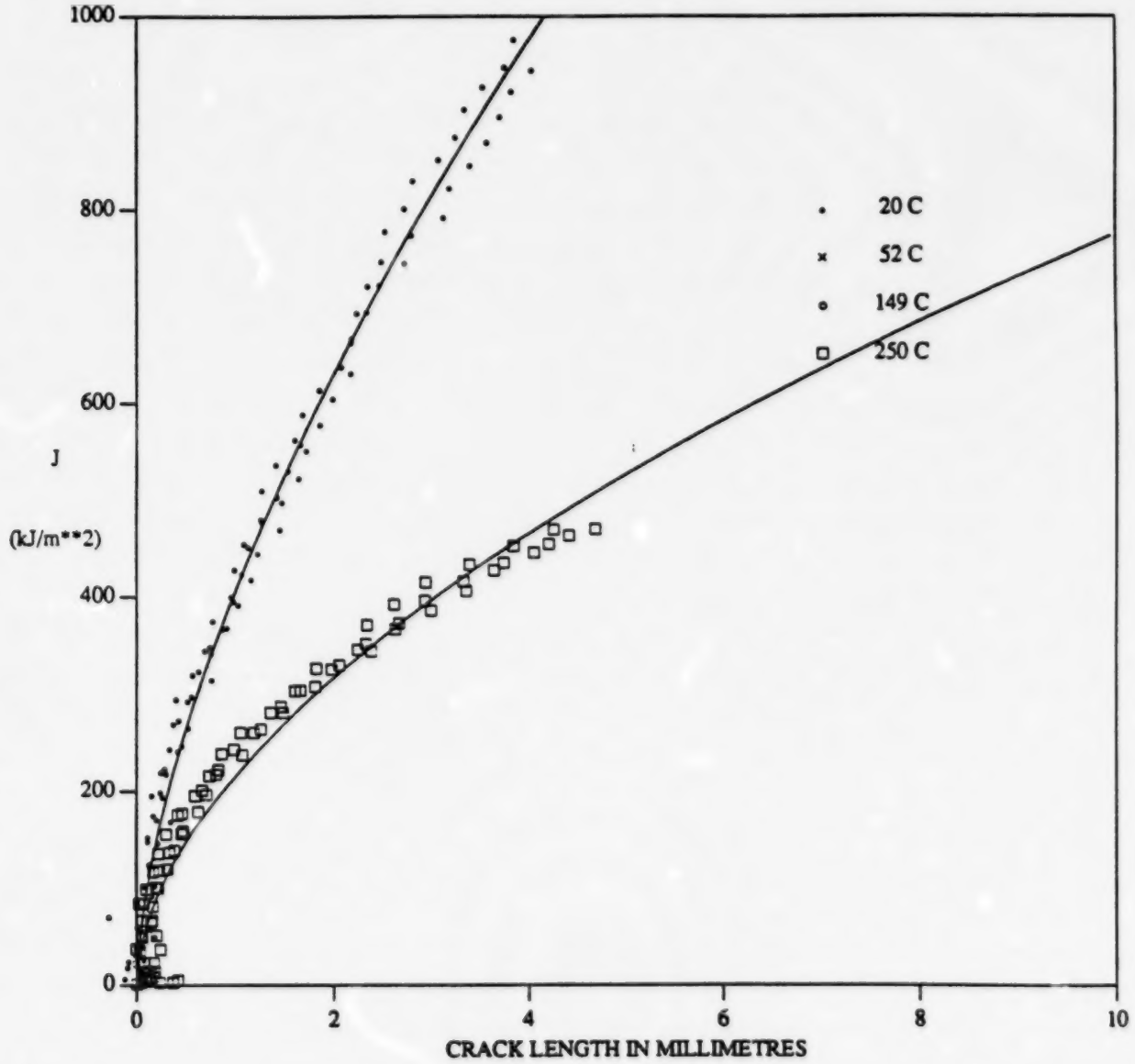

Figure D-4

Specimen Data For SA-106 Grade B Tests Ontario Hydro L-C Specimens From 22" NPS Sch 100 Pipe							
Specimen ID	Thickness (mm)	Reduced Thickness (mm)	Temperature Degrees C	J_{IC} kJ/m**2	E GPa	σ_0 MPa	σ_{uts} MPa
j15	30.5	24.58	20	219	192.3	320.3	532.6
j16	30.5	24.58	20	255	192.3	320.3	532.6
j17	30.5	24.58	250	131	182.8	220.7	508.5
j18	30.5	24.58	250	160	182.8	220.7	508.5
j19	30.5	24.58	250	138	182.8	220.7	508.5

Data for Figure D-4

C-L TYPE J-R CURVES FOR ONTARIO HYDRO TESTS OF 24 INCH DIAMETER NPS SCH 100 PARENT SPECIMEN THICKNESS 31.75 mm

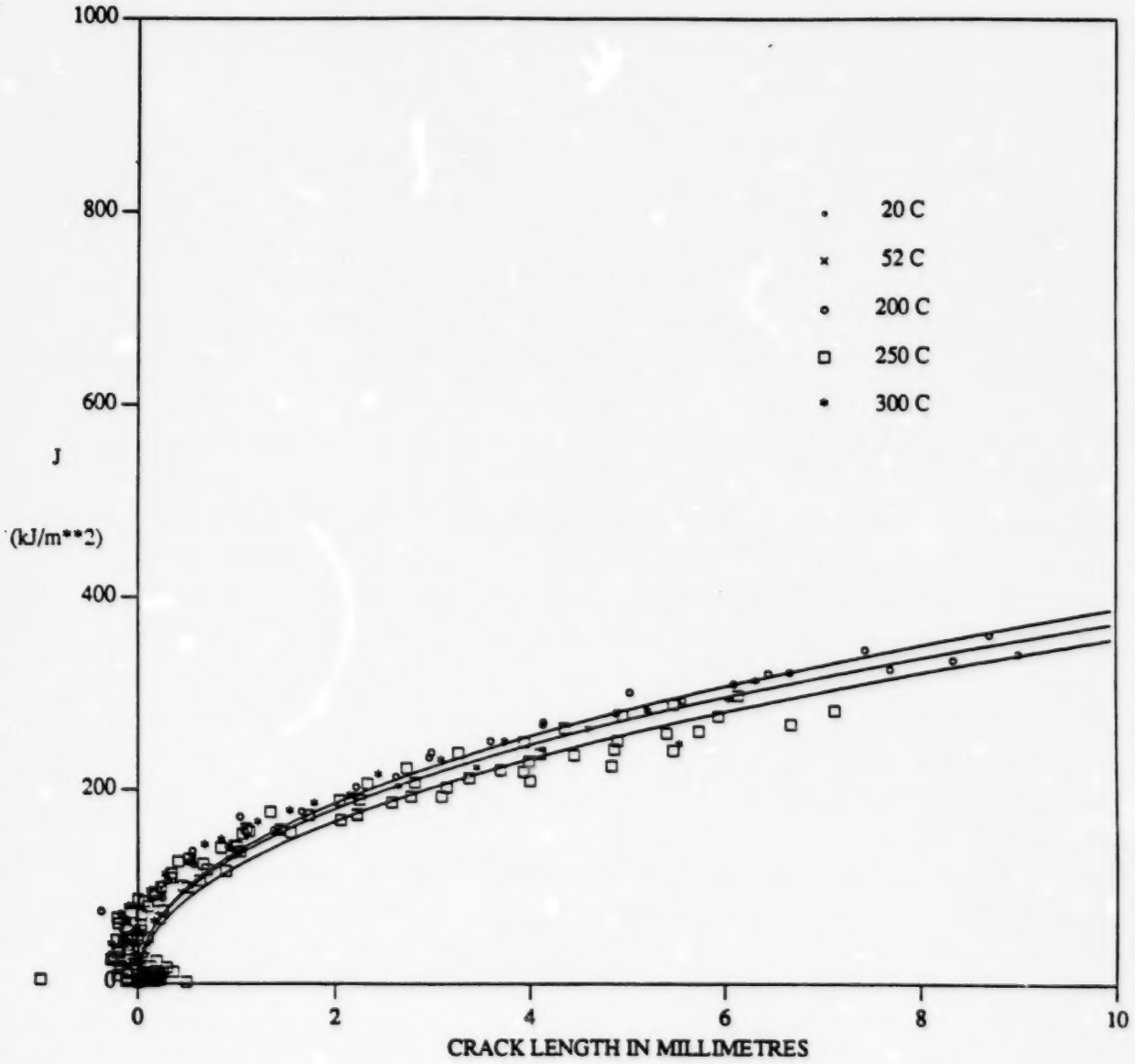

Figure D-5

Specimen Data For SA-106 Grade B Tests Ontario Hydro C-L Specimens From 24" NPS Sch 100 Pipe							
Specimen ID	Thickness (mm)	Reduced Thickness (mm)	Temperature Degrees C	J_{IC} kJ/m**2	E GPa	σ_0 MPa	σ_{uts} MPa
td13	31.77	25.32	200	113	186.4	248.5	482.0
td14	31.74	25.42	200	100	186.4	248.5	482.0
j59	31.8	25.44	250	81	182.8	268.3	525.5
j60	31.77	25.42	250	108	182.8	268.3	525.5
j61	31.77	25.42	250	100	182.8	268.3	525.5
td15	31.75	25.50	250	98	182.8	228.0	510.8
td18	31.76	25.34	250	79	182.8	228.0	510.8
td16	31.74	25.50	300	106	178.5	223.0	513.8
td17	31.75	25.40	300	104	178.5	223.0	513.8

Data for Figure D-5

L-C TYPE J-R CURVES FOR ONTARIO HYDRO TESTS OF 24 INCH DIAMETER NPS SCH 100 PARENT SPECIMEN THICKNESS 31.75 mm

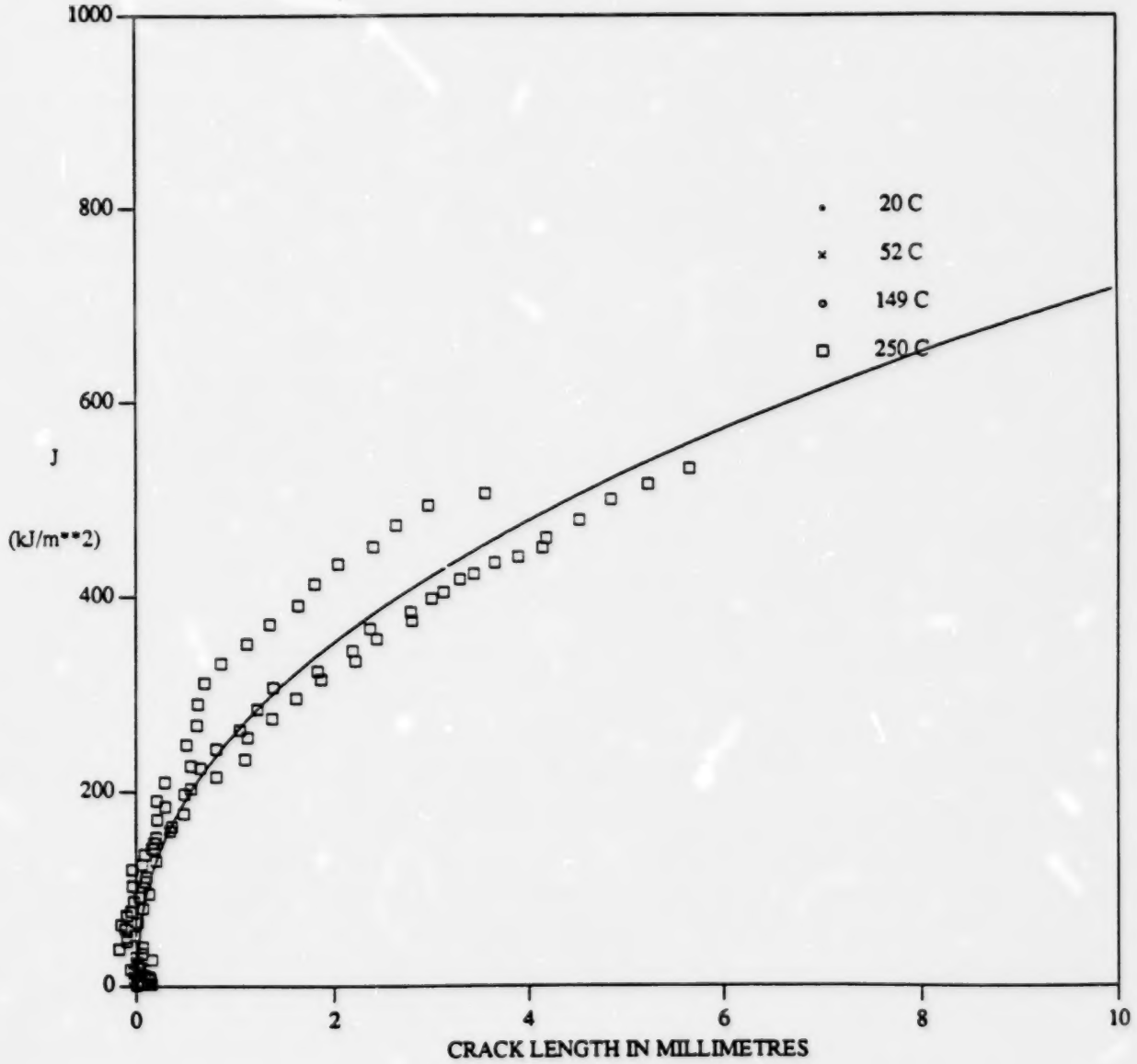

Figure D-6

Specimen Data For SA-106 Grade B Tests Ontario Hydro L-C Specimens From 24" NPS Sch 100 Pipe							
Specimen ID	Thickness (mm)	Reduced Thickness (mm)	Temperature Degrees C	J_{IC} kJ/m**2	E GPa	σ_0 MPa	σ_{uts} MPa
j1	31.75	25.46	250	185	182.8	228.0	510.8
j2	31.75	25.46	250	160	182.8	228.0	510.8
j3	31.75	25.46	250	265	182.8	228.0	510.8

Data for Figure D-6

ONTARIO HYDRO CL SPECIMENS (250 C)
TRUE STRESS versus TRUE STRAIN FOR 12 INCH NPS SCH 100 PIPE
CIRCUMFERENTIAL ORIENTATION SPECIMENS

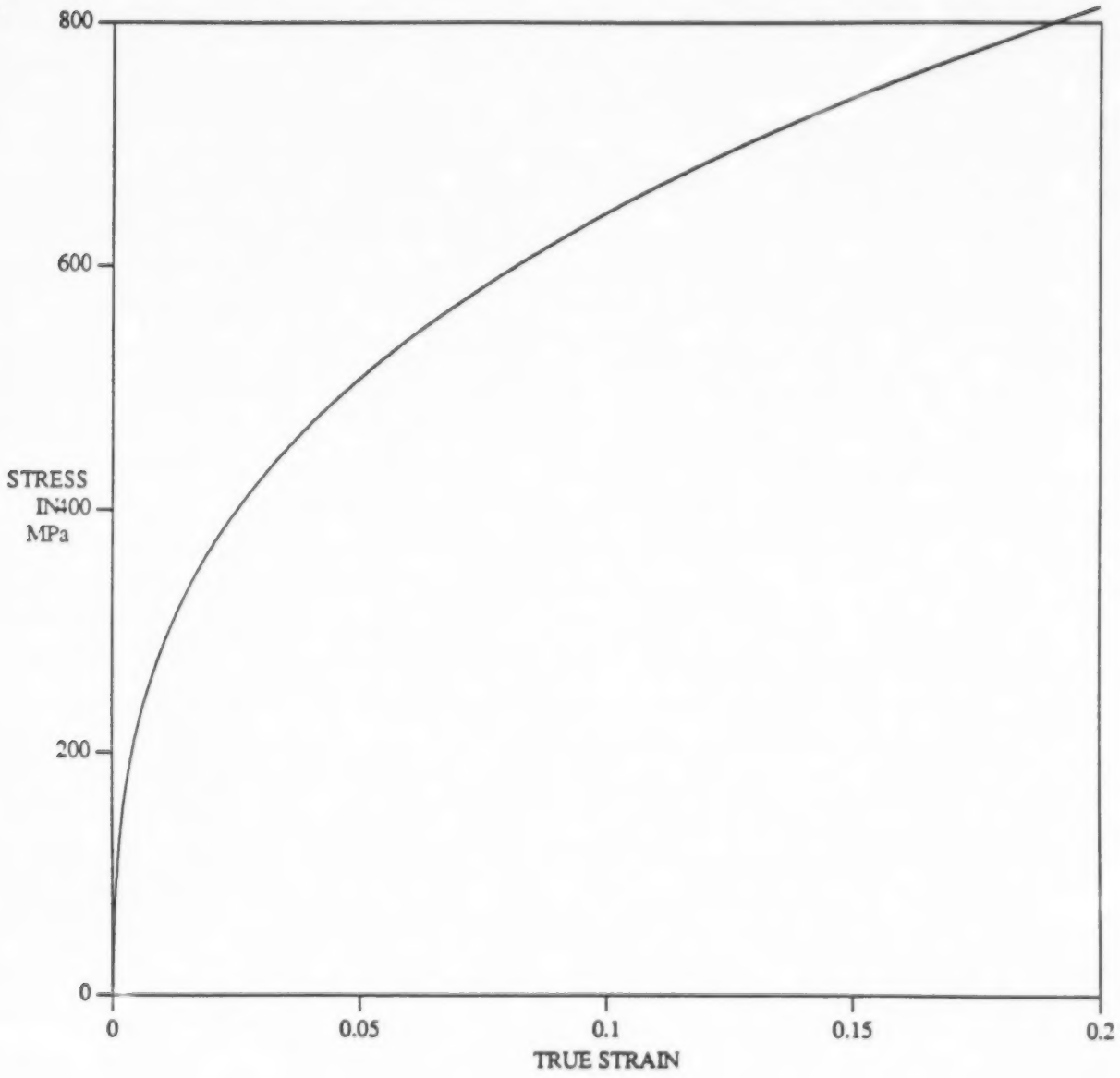

Figure D-7(a)

ONTARIO HYDRO LC SPECIMENS (20 C)
TRUE STRESS versus TRUE STRAIN FOR 22 INCH NPS SCH 100 PIPE
LONGITUDINAL ORIENTATION SPECIMENS

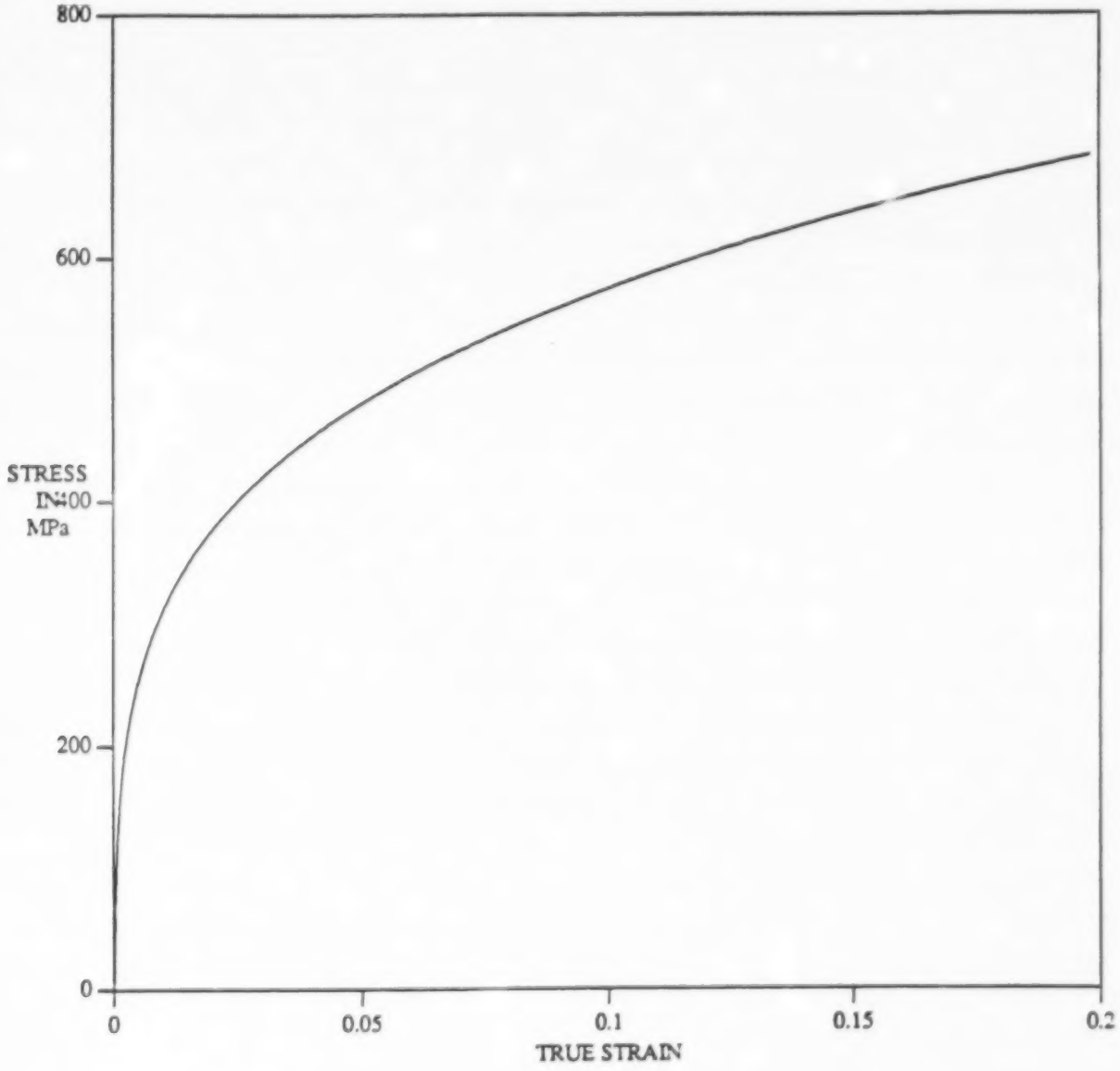

Figure D-8(a)

ONTARIO HYDRO LC SPECIMENS (250 C)
TRUE STRESS versus TRUE STRAIN FOR 22 INCH NPS SCH 100 PIPE
LONGITUDINAL ORIENTATION SPECIMENS

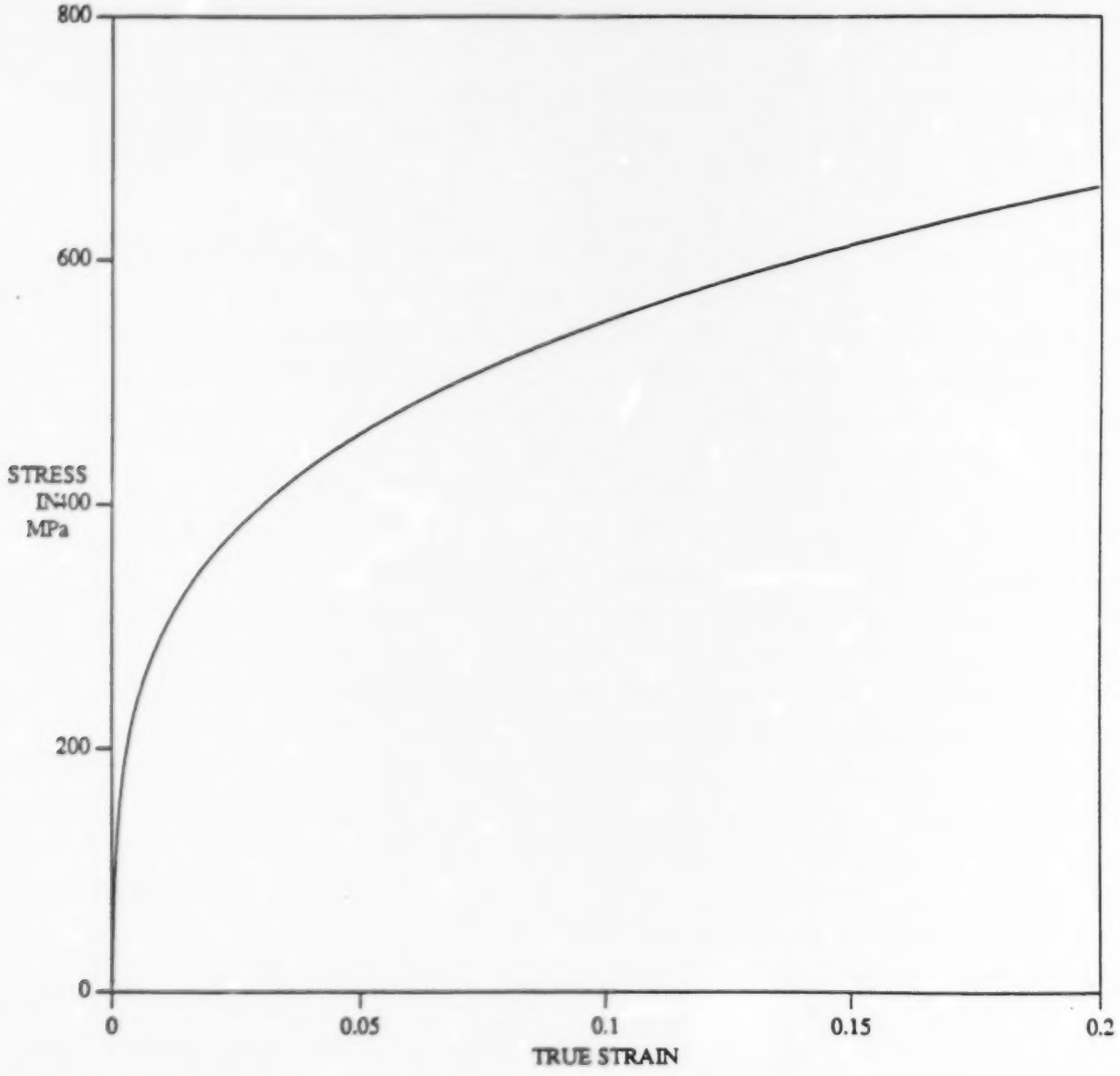

Figure D-8(b)

ONTARIO HYDRO CL SPECIMENS (250 C)
TRUE STRESS versus TRUE STRAIN FOR 24 INCH NPS SCH 100 PIPE
CIRCUMFERENTIAL ORIENTATION SPECIMENS

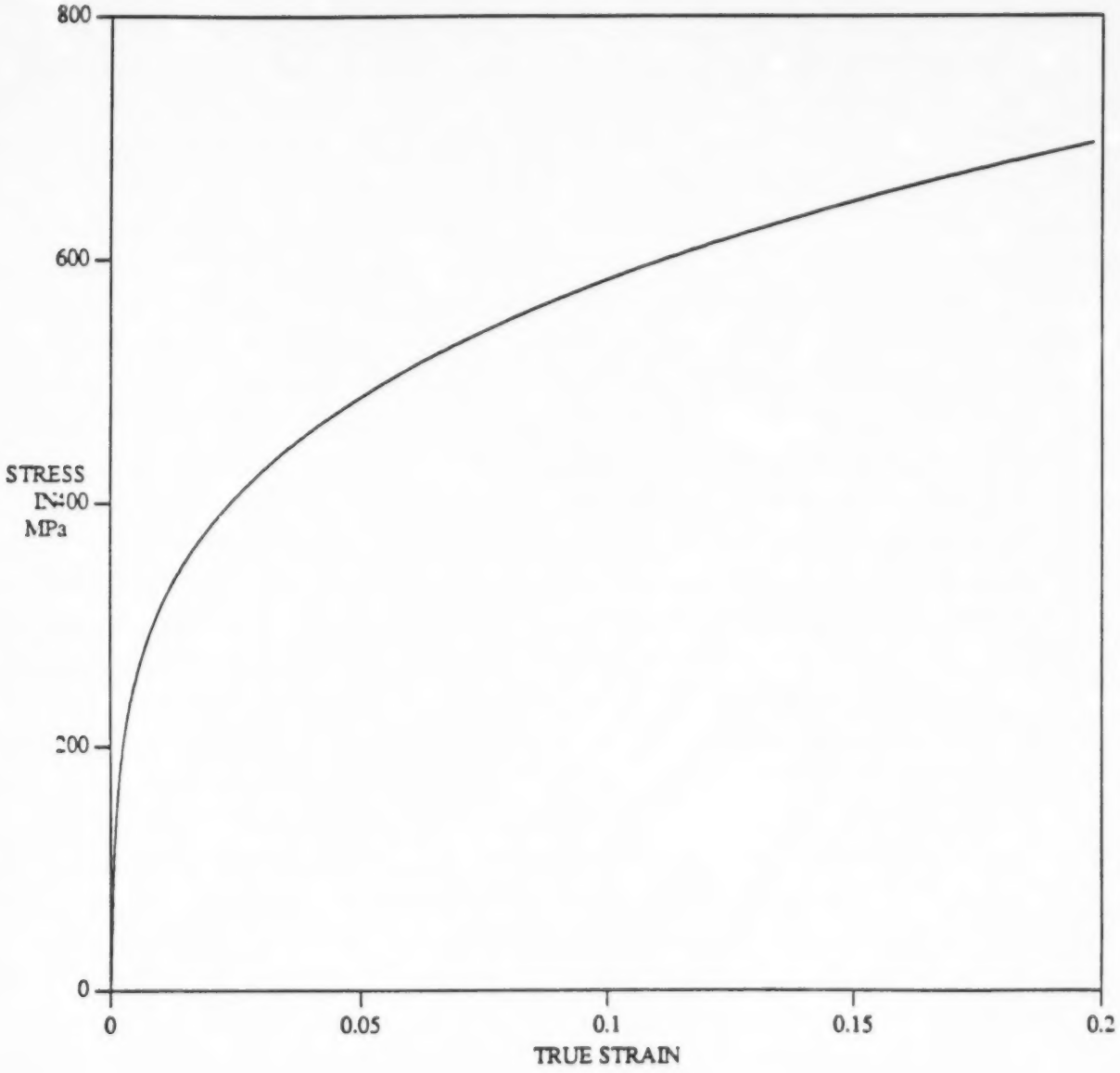

Figure D-9(a)

ONTARIO HYDRO LC SPECIMENS (250 C)
TRUE STRESS versus TRUE STRAIN FOR 24 INCH NPS SCH 100 PIPE
LONGITUDINAL ORIENTATION SPECIMENS

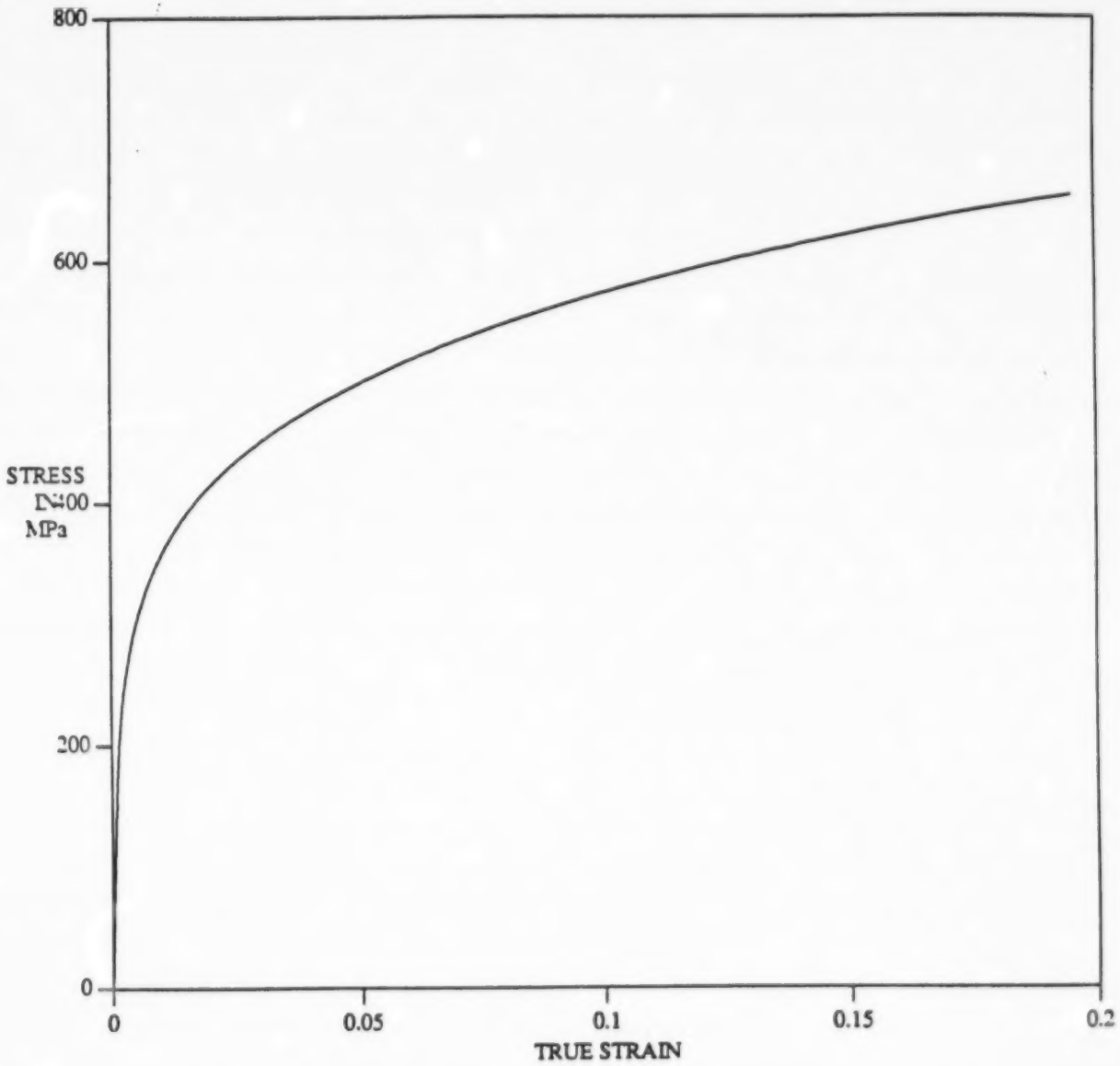

Figure D-9(b)

APPENDIX E

DEVELOPMENT OF SOFTWARE FOR ENGINEERING APPROACH TO ELASTO-PLASTIC ANALYSIS

The development of the software, hereafter referred to as CYL, is based on the Engineering Approach for elastic-plastic fracture analyses outlined in the EPRI documents NP-1931 and NP-3607. These documents present a handbook style catalogue of elastic and fully plastic solutions for evaluating the J-driving force for various cracked bodies. It has been shown [Refs. 4 and 5] that the elastic-plastic crack driving force solutions can be estimated as the arithmetic sum of the elastic and fully plastic solutions. Combining a knowledge of these driving force solutions with experimentally derived J-resistance curves, failure loads and the stable crack extension prior to failure can be evaluated.

J-integral versus crack growth resistance curves (J–R curves or J_R curves) are usually determined from experimentation. A J–R curve is a plot of measured J values on the coordinate axis versus the measured crack extension on the abscissa. The plot essentially defines the amount of crack extension that can be expected for a given crack driving energy, or the resistance to stable crack extension. That is, "the J–R curve characterizes the resistance of metallic materials to slow stable crack growth after initiation from a pre-existing fatigue crack or other sharp flaws." [Ref. 6]

CRACK DRIVING FORCE DIAGRAMS

"The J-integral crack driving force for a given flawed body can be obtained by superposing the elastic and fully plastic solutions" [Ref. 4]. As elastic solutions are applicable for very small plastic zones and fully plastic solutions are applicable where the plastic strains are large as compared to the elastic strains everywhere on the body, a simple summation of the plastic and elastic solutions yields a good approximation of the true elastic-plastic value of J.

Figure E-1 provides an illustration of this technique in which the material resistance curves are represented as heavy solid lines and the crack driving force curves as dotted or solid lines. By comparison of the crack driving force curves with the material resistance curve, one can determine the load at which the crack will become unstable and the amount of crack extension prior to instability. The instability point is determined by identifying that crack driving force curve which intersects the material resistance curve at a point where their tangents are parallel. The load used to produce this driving force curve is the instability load and the crack extension prior to instability is naturally the maximum stable crack extension. Thus, a diagram containing both the crack driving force curves and the crack growth resistance curve illustrates the complete history of deformation. From this diagram crack growth can be predicted.

To determine a crack driving force diagram the values of J are calculated for various values of crack length for a fixed load. Plotting J versus crack size, and J_R versus Δa provides a diagram with a series of constant load curves intersected by the J resistance curve for the material of interest.

It is assumed that the material behavior is characterized by the Ramburg-Osgood strain hardening equation:

$$\frac{\varepsilon}{\varepsilon_0} = \frac{\sigma}{\sigma_0} + \alpha \left[\frac{\sigma}{\sigma_0}\right]^n \qquad \text{E-1}$$

where

$$\varepsilon_0 = \frac{\sigma_0}{E}, \qquad \text{E-2}$$

and the constants α and n are determined from curve fitting to the lower bound of the true stress true strain curve.

Now J is reduced to a function of crack length and the strain hardening constants of the form,

$$J = J_e(a) + J_p(a, \alpha, n) \qquad \text{E-3}$$

CYL determines that load at which the driving force curve intersects the J–R curve such that the tangents to both curves at this point of intersection are parallel. The program then returns this load and the crack extension at instability.

THE CYL PROGRAM

The CYL program evaluates three specific flawed pipe configurations, namely

(a) Condition A: an internally pressurized cylinder with an internal axial crack, shown in Figure E-2(a),

(b) Condition B: a cylinder with an internal circumferential crack under remote tension, shown in Figure E-2(b), and

(c) Condition C: a through wall flaw in a cylinder under remote tension, as shown in Figure E-2(c).

(a) and (b) above are defined in EPRI NP-1931 RP-1237-1 [Ref. 4] whereas (c) is defined in EPRI NP-3607 RP-1237-1 [Ref. 5].

The CYL program will now be detailed in terms of its subroutines.

1. MAKEFILE

The MAKEFILE is not a subroutine of CYL, but serves as a simple method to recompile the program after any changes have been made. When changes have been made to but one subroutine only, that subroutine is recompiled and then linked to the rest of the program. Recompile is is accomplished by typing 'make'. It should be noted that the user has access to the source code and should feel free to modify it at any time if the output files of CYL are not in a form which is convenient.

The MAKEFILE has the following features/format:

```
FF=f77
FFLAGS=-O
SRC=main.f crack.f spegeom.f matprop.f loaddet.f minfind.f
  poly2.f poly3.f fuc1.f fuc2.f fuc3.f fuc4.f
OBJ=main.o crack.o spegeom.o matprop.o loaddet.o minfind.o
  poly2.o poly3.o fuc1.o fuc2.o fuc3.o fuc4.o
output: {OBJ}
      {FF} {FFLAGS} -o CYL {OBJ} -limsld
```

The names following SRC= are the names of the subroutines of CYL. The last line of the Makefile specifies that the executable code will be called CYL and that 'imsl' library routines are *called* in program.

2. MAIN.F

MAIN.F is the main program of CYL from which most subroutines are accessed. It declares the main variables of the program then provides default values for the required geometric and material properties of the pipe. A menu selection is generated and appears on the screen:

CYLINDER J-INTEGRAL ANALYSIS

1. Alter Material Properties
2. Alter Specimen Geometry
3. Axial crack under Internal Pressure
4. Radial crack under Remote Tension (Internal Pressure)
5. Through-wall under Remote Tension
6. Through-wall under Remote Bending*
7. Quit to UNIX

Enter Selection:

entering '1' calls subroutine matprop

entering '2' calls subroutine spegeom

entering '3 through 6' calls subroutine crack

entering '7' quits to UNIX

3. MATPROP.F

The MATPROP.F subroutine allows the user to change the material properties of the pipe. A selection screen is presented:

MATERIAL PROPERTIES MENU

1. yield stress (Pa) xxxxx
2. elastic modulus (Pa) xxxxx
3. hardening exponent xxxxx
4. alpha material constant xxxxx
5. Quit to Main Menu

Enter Number Selection :

where xxxxx represents the appropriate value for the given material constant.

If the user chooses to alter any of the material properties, the new value is displayed in the appropriate line. If a new value of the strain hardening exponent n is chosen the program also calls the subroutine *spegeom*.

---

* excluded at present.

4. SPEGEOM.F

The solution for the J–driving force curves requires the determination of the values for the dimensionless parameters F and h_1. The following represents a typical solution for J–driving force curves, that of an internally pressurized cylinder with an axial crack. Figure E-2(a) describes a long, thin walled cylinder with an internal radius R_i and an outer radius R_o, containing an internal crack oriented on a radial axial plane. The crack depth is a. A uniform pressure acts on the inside of the cylinder and on the crack face. The body is assumed to be in plane strain, where b is the wall thickness and c is the uncracked ligament. K_I is given by,

$$K_I = \frac{2pR_o^2(\pi a)^{0.5}}{R_o^2 - R_i^2} \times F(a/b,\, b/R_o) \qquad \text{E-4}$$

where

$F(a/b,\, b/R_o)$ is a dimensionless geometry parameter, the value of which is obtained from a two dimensional curve fit of data from V. Kumar et. al. [Ref. 4].

Now the elastic component of J can be determined from,

$$J_{(el)} = \frac{K_I^2}{E'} \qquad \text{E-5}$$

and

$$J_{(pl)} = \alpha\sigma_o\varepsilon_o c(a/b)\, h_1(a/b,\, n,\, R_i/R_o)\, (p/p_o)^{n+1} \qquad \text{E-6}$$

where

$h_1(a/b, n, R_i/R_o)$ is a dimensionless parameter dependent on geometry and the strain hardening exponent n

p_o is the limit pressure for this geometry in the perfectly plastic case ($n=\infty$). A lower bound value is given by,

$$p_o = \frac{2}{(3)^{0.5}} \frac{c\,\sigma_o}{R_c} . \qquad \text{E-7}$$

where

$R_c = R_i + a$, the radial distance from the center of the cylinder to the tip of the crack, and,

$$J = J_{(el)} + J_{(pl)} . \qquad \text{E-8}$$

The values of F and h_1 are determined in subroutine *spegeom* by fitting polynomials to the data tabulated in References [4] and [5]. These tables are given on pages 4-10 to 4-13 and 6-27 to 6-34 in References [4] and [5] respectively. The parameter F is a function of the thickness over the inner radius of the cylinder (b/R_i) and crack length over original ligament length (a/b). In the first section of *spegeom*, F is calculated for the input thickness to radius ratio at four values of (a/b) for the four geometries of flawed

pipe. Each of the equations is a polynomial fit for a vertical columns of one of the tables of F data (for example Table 4-1 in Reference [4]). Once the value of F has been determined at each value of a/b, a polynomial is fitted through these points yielding F as a function of a/b. Once this function has been determined, J_{el} can be calculated for any crack length. This polynomial is fitted using subroutine *poly* 3, a third order polynomial fit routine.

The values of h_1 are calculated in a similar manner. However, since the data table for h_1 is three dimensional, three polynomials must be fitted to determined h_1 as a function of a/b. In the second section of *spegeom*, equations are provided to calculate h_1 for given values of b/R_i and a/b at any value of the strain hardening exponent n. Using the input value of n to solve these equations reduces the data table from three to two dimensions. That is, a table of values for h_1 is produced with three vertical columns for values of b/R_i and four rows for values of a/b.

By fitting second order polynomials (using subroutine *poly* 2) to the columns of this table and then solving these polynomials for the input value of b/R_i, the second dimension is eliminated from the table. The data table for each of the flawed pipe geometries is now one dimensional, with four values of h_1 given at four values of a/b. By fitting a third order polynomial to this reduced data set using the subroutine *poly* 3, h_1 is given as a function of a/b only.

These functions of F and h_1 for the four flawed cylinder cases examined are used in *function calls fuc* 1 *fuc* 2 *fuc* 3 *fuc* 4 to calculate the value of the J–driving force curve at the required load and crack length.

5. CRACK.F

Subroutine CRACK.F is called if the operator requests a solution for the failure load of a given flawed cylinder case. Entering 3 through 6 on the main menu will call this subroutine. *Crack* follows the following sequence:

1) The program prompts a series of questions to gather information on the J–R properties of the material:

   Enter specimen number -- to help catalogue files

   Enter J-R curve constant -- The constant for a power law fit to J–R data with J in kN/m^2 and Δa in *mm*.

   Enter J-R curve exponent -- The exponent for the power law fit described above.

   Enter KIC -- The value of K_{IC} from tables or calculated from the expression $K_{IC} = (J_{IC} * E)^{1/2}$.
2) The program prompts the user for the initial value of the crack length as a function of the total ligament.
3) The program calculates the load for first yield and the load required for an LEFM type failure of the geometry being considered.
4) The program calls subroutine *loaddet* which determines the J–driving curve which meets the required condition of the unique intersection point.
5) The program writes to a file called '*load*':
   a) initial crack length as a function of the total ligament
   b) load for EPFM failure divided by the load for first yield
   c) LEFM failure load divided by the load for first yield
   d) initial crack length
   e) crack length at failure
   f) elastic component of J at failure

g) plastic component of J at failure

7) Three curves are generated and written to files named - axial1 ... axial3, or radial1 ... radial3, or tension1 ... tension3, or bending1 ... bending3. The first curve is a J–driving force curve for a load of 0.9*(the critical load), the second is for the critical load and the third is for a load of 1.1*(the critical load). A J–resistance curve is generated and written to a file labeled '*resistance*'.

8) The program prompts the user to try another value of (a/b). If 'y' is answered the program returns to step 3); if 'n' is answered the program returns to the main menu.

6. LOADDET.F

This subroutine determines the critical load for EPFM failure of the chosen pipe geometry. *Loaddet* initially "guesses" the critical load. A curve representing the J–driving force curve minus the J–R curve is generated for values of crack length between the initial (a/b) and (a/b)-0.75. The minimum of this curve is determined by subroutine *minfind*. If the minimum of this curve is negative, the load estimate is incremented. If the minimum is positive, the load estimate is decreased. When the value of the minimum is sufficiently close to zero, *loaddet* returns the critical load value to the subroutine *crack*.

7. MINFIND.F

This subroutine determines the minimum of the curve defined in *loaddet*.

8. POLY2.F and POLY3.f

The subroutines *poly* 2 and *poly* 3 force a polynomial of second and third order respectively through points provided by subroutine *spegeom* and returns the coefficients of these curves to that subroutine.

9. FUC1.F FUC2.F FUC3.F FUC4.F

These functions calculate the values of the J–driving and J–resistance curves and the value of their difference at a given value of crack length.

The equations used in these functions are found in References [4] and [5] on:

fuc 1 -- reference [4] pages 4-2 to 4-4
fuc 2 -- reference [4] pages 4-4 to 4-7
fuc 3 -- reference [5] pages 6-7 to 6-11
fuc 4 -- reference [5] pages 6-11 to 6-14

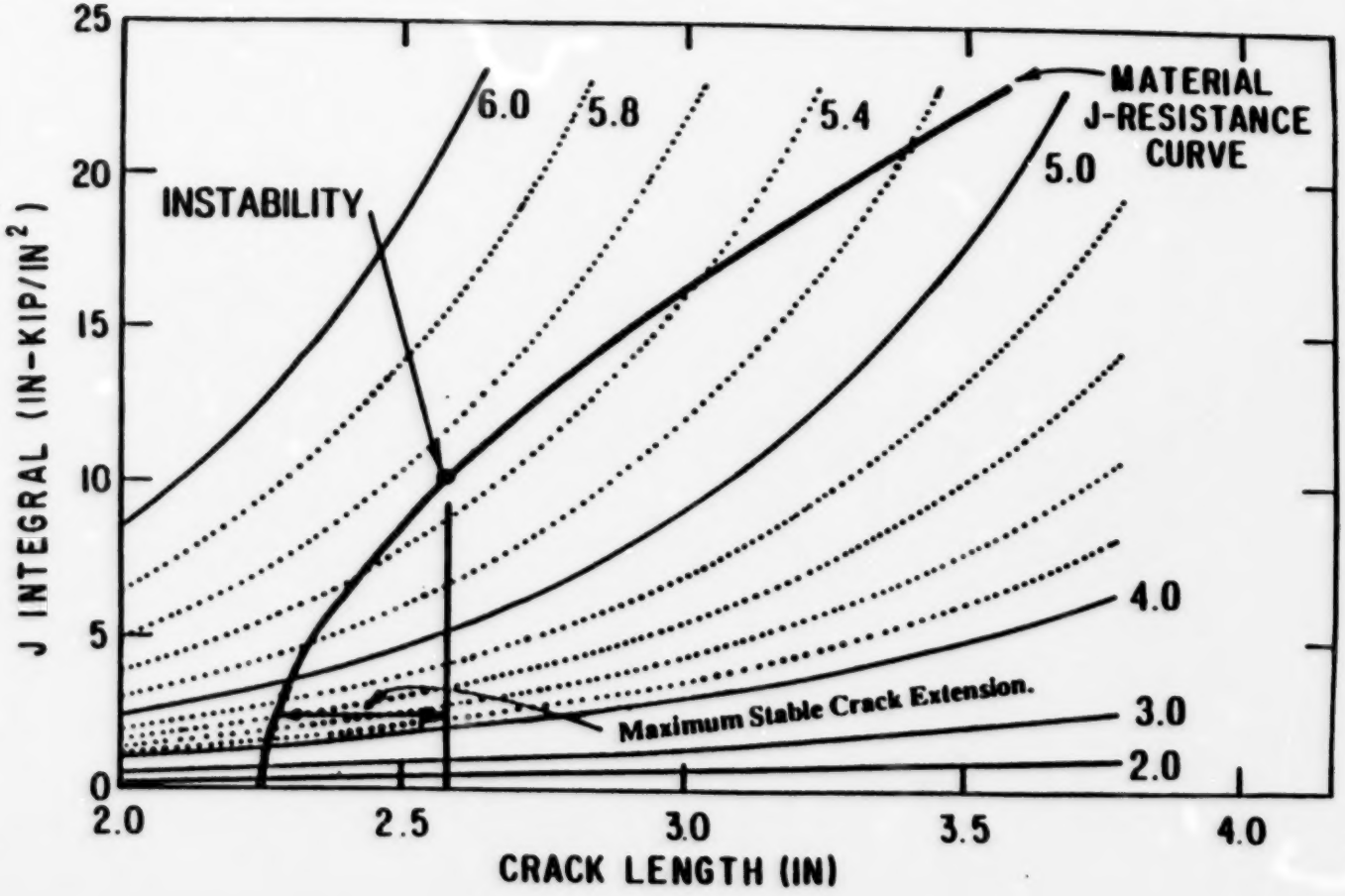

Figure E-1: An Example from the Literature of a J-R Curve Showing the Maximum Attained Load and Maximum Stable Crack Extension.

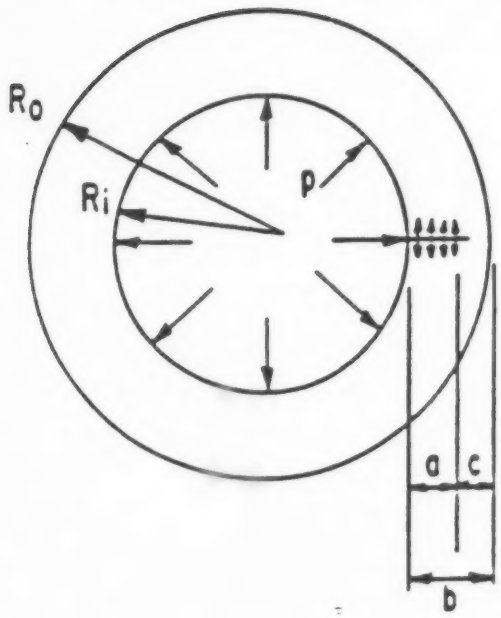

Axially cracked cylinder under internal pressure

CONDITION A

Internally pressurized cylinder with an axial crack. Internal pressure also acts on the crack face.

The pressure reported in the figures is the internal pressure. This pressure value is divided by the yield strength of the material to obtain the co-ordinate axis.

Figure E-2(a)

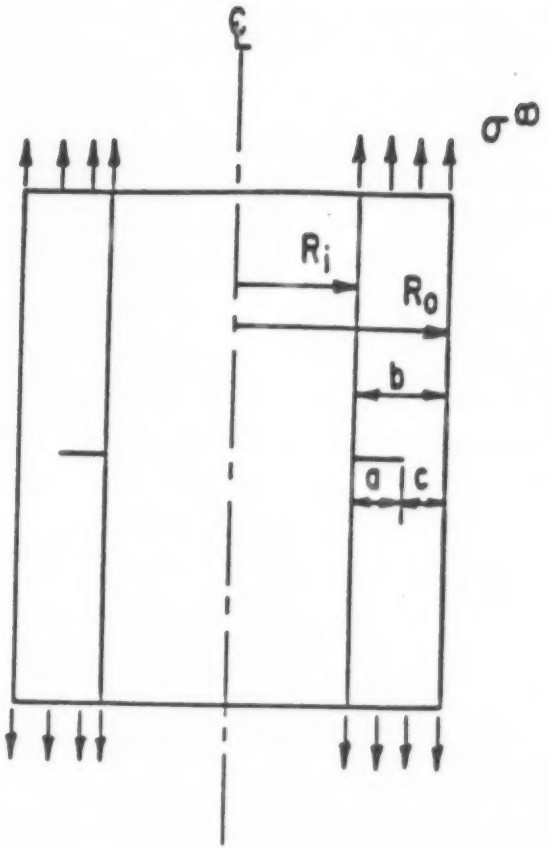

Circumferentially cracked cylinder in tension

CONDITION B

Cylinder with an internal circumferential crack under remote tension. The tensile load can be resolved into a uniform tensile stress field, σ^∞

$$\sigma^\infty = P/\pi\ (R_o^2 - R_i^2)$$

The reported load in the figures is the remote load in Newtons. This load is divided by the yield strength of the material to obtain the co-ordinate axis.

Figure E-2(b)

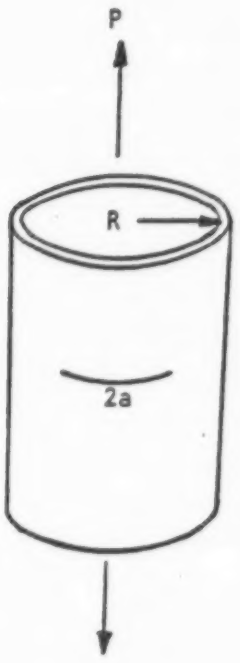

CONDITION C

Through wall flaw in a cylinder under remote tension.

The load reported in the figures is the remote load in Newtons.

The load is divided by the yield strength of the material to obtain the co-ordinate axis.

R = mean radius
2a = 2γR
2b = 2πR

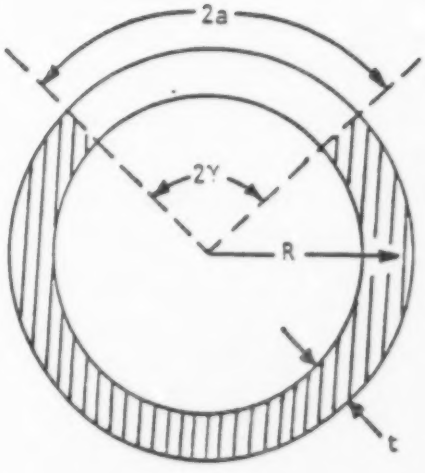

Figure E-2(c)